

(12) INTERNATIONAL APPLICATION PUBLISHED UNDER THE PATENT COOPERATION TREATY (PCT)

(19) World Intellectual Property Organization
International Bureau



(43) International Publication Date
24 December 2003 (24.12.2003)

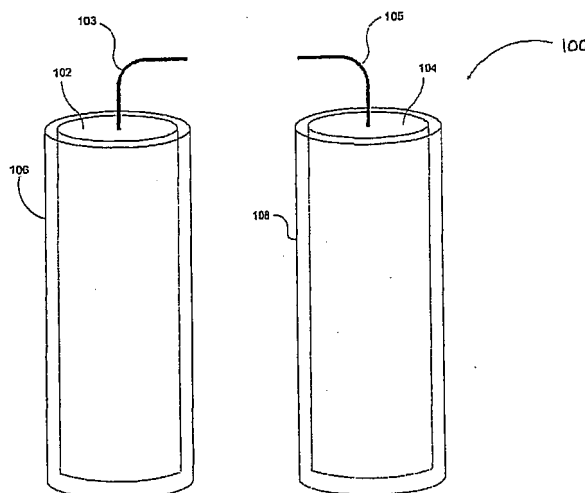
PCT

(10) International Publication Number
WO 03/106966 A2

- (51) International Patent Classification⁷: G01N
- (21) International Application Number: PCT/US03/13806
- (22) International Filing Date: 2 May 2003 (02.05.2003)
- (25) Filing Language: English
- (26) Publication Language: English
- (30) Priority Data:
60/377,886 2 May 2002 (02.05.2002) US
10/427,113 1 May 2003 (01.05.2003) US
- (71) Applicant: THERASENSE, INC. [US/US]; 1360 South Loop Road, Alameda, CA 94502 (US).
- (72) Inventors: HELLER, Adam; 4711 Spicewood Springs Road, #271, Austin, TX 78705 (US). MANO, Nicholas; 2804 Rio Grande, #201, Austin, TX 7805-3659 (US). KIM, Hyug-Han; 4701 Staggerbush Road, #1517, Austin, TX 78749 (US). ZHANG, Yongchao; 2501 Lake Austin Blvd., #E102, Austin, TX 78703 (US). MAO, Fei; 34379 Benedick Lane, Fremont, CA 94555 (US). CHEN, Ting; 2501 Lake Austin Blvd., #D102, Austin, TX 78703 (US). BARTON, Scott, C.; 5703 Bull Creek Road, Austin, TX 78756 (US).
- (74) Agents: DE RUNTZ, K., Alison et al.; Parsons Hsue & de Runtz LLP, 655 Montgomery Street, Suite 1800, San Francisco, CA 94111 (US).
- (81) Designated States (*national*): AE, AG, AL, AM, AT, AU, AZ, BA, BB, BG, BR, BY, BZ, CA, CH, CN, CO, CR, CU, CZ, DE, DK, DM, DZ, EC, EE, ES, FI, GB, GD, GE, GH, GM, HR, HU, ID, IL, IN, IS, JP, KE, KG, KP, KR, KZ, LC, LK, LR, LS, LT, LU, LV, MA, MD, MG, MK, MN, MW, MX, MZ, NI, NO, NZ, OM, PH, PL, PT, RO, RU, SC, SD, SE, SG, SK, SL, TJ, TM, TN, TR, TT, TZ, UA, UG, UZ, VC, VN, YU, ZA, ZM, ZW.
- (84) Designated States (*regional*): ARIPO patent (GH, GM, KE, LS, MW, MZ, SD, SL, SZ, TZ, UG, ZM, ZW), Eurasian patent (AM, AZ, BY, KG, KZ, MD, RU, TJ, TM), European patent (AT, BE, BG, CH, CY, CZ, DE, DK, EE, ES, FI, FR, GB, GR, HU, IE, IT, LU, MC, NL, PT, RO, SE, SI, SK, TR), OAPI patent (BF, BJ, CF, CG, CI, CM, GA, GN, GQ, GW, ML, MR, NE, SN, TD, TG).
- Published:**
— without international search report and to be republished upon receipt of that report

[Continued on next page]

(54) Title: MINIATURE BIOLOGICAL FUEL CELL THAT IS OPERATIONAL UNDER PHYSIOLOGICAL CONDITIONS, AND ASSOCIATED DEVICES AND METHODS



(57) Abstract: A fuel cell is provided with an anode and a cathode. The anode is in electrical communication with an anode enzyme and the cathode is in electrical communication with a cathode enzyme. The anode enzyme is preferably an oxidase or a dehydrogenase. The cathode enzyme is a copper-containing enzyme, such as a lacasse, an ascorbate oxidase, a ceruloplasmin, or a bilirubin oxidase. Preferably, the cathode enzyme is operable under physiological conditions. Redox polymers serve to wire the anode enzyme to the anode and the cathode enzyme to the cathode. The fuel cell can be very small in size because it does not require a membrane, seal, or case. The fuel cell can be used in connection with a biological system, such as a human, as it may operate at physiological conditions. By virtue of its size and operability at physiological conditions, the fuel cell is of particular interest for applications calling for a power source implanted in a human body, such as a variety of medical applications.

WO 03/106966 A2



For two-letter codes and other abbreviations, refer to the "Guidance Notes on Codes and Abbreviations" appearing at the beginning of each regular issue of the PCT Gazette.

**MINIATURE BIOLOGICAL FUEL CELL THAT IS OPERATIONAL
UNDER PHYSIOLOGICAL CONDITIONS,
AND ASSOCIATED DEVICES AND METHODS**

5

Field of the Invention

[0001] This invention relates to electrochemical cells, and in particular, miniature biological fuel cells. More particularly, the invention relates to biological fuel cells that may be used as power sources residing within a biological system, such as an animal or a plant.

10

Background of the Invention

[0002] Packages comprising autonomous electronic and electromechanical systems that are implanted in the body of animals, such as sensors and their associated electronic circuits that function to amplify the sensor signals and transmit them to a nearby receiver, require a power source. Today, these packages are powered externally by batteries. The smallest batteries are, however, much larger than the implantable sensors and their associated signal amplifier circuits. For this reason, the size of autonomous packages that include a sensor, an amplifier-transmitter, and a power source are generally defined by the battery. Batteries cannot be made as small as the sensors or amplifiers because the batteries require cases and seals, the miniaturization of which is difficult and prohibitively expensive.

15

20

[0003] Known fuel cells are also much larger than available sensors because they require a case and a seal, and usually also a membrane, which is difficult to miniaturize and seal. By way of illustration, in a conventional fuel cell, usually a membrane separates the cathode and anode compartments of the cell so as to separate electrooxidized reactant of the anodic reaction and electroreduced reactant of the cathodic reaction. If these reactants were not separated, they could react with one another, thereby reducing the power and the efficiency of the cell. As the miniaturization and sealing of membranes present difficult manufacturing issues, conventional fuel cells are generally much larger than is desirable for certain

25

30

applications.

[0004] Biological fuel cells, also known as biofuel cells, have received much attention in past years. Herein, the term "biological fuel cell" or "biofuel cell" refers to an electrochemical cell having performance attributes that permit its use as a power source for an implanted device in a biological system, such as an animal, including a human, or a plant. Biological fuel cells generate electrical energy using components found in biological systems, such as sugars, alcohols, carboxylic acids, carbohydrates, starches, cellulose, and oxygen. Such devices are generally disclosed and discussed in United States Patent Nos. 6,294,281 and 6,531,239. Miniature biofuel cells having oxygen electroreducing cathodes and glucose electrooxidizing anodes are of current interest because such cells may power future autonomous electronic and electromechanical systems implanted in a biological system, and particularly, the human body.

[0005] Numerous biofuel cells have been described in the past fifty years. However, only a few of these biofuel cells could be operated under physiological conditions, which are the conditions relevant to operation in the body of animal. Physiological conditions include, for instance, a pH of about 7.2 to 7.4, a temperature of near 37°C, and a chloride concentration of about 0.14 M. The power density of known biofuel cells is small, the typical currents per square centimeter of electrode area being less than 1 mA/cm², and usually less than 100 µA/cm².

[0006] Furthermore, known biofuel cells having higher power densities require ion-conducting separation membranes, such as Nafion™ membranes. These membranes are required because components of the catalysts of the anode and cathode reactions are often dissolved or reversibly adsorbed on the electrodes. Most of these known biofuel cells comprise two different dissolved or absorbed enzymes, one in the anode compartment, and the other in the cathode compartment. The most efficient of these cells also comprise diffusional redox mediators dissolved in their respective compartments. These mediators carry electrons between the electrodes and the dissolved enzymes. Because these fuel cells have limited power densities and unstable dissolved enzymes, and require membranes that are difficult to miniaturize, they have not been produced in dimensions smaller than 1 mm in length, width, or

height.

[0007] As the electronic circuits and sensors used in implantable devices have become miniaturized, autonomous sensor-amplifier-transmitter devices of millimeter and sub-millimeter dimensions can be built. For example, signal amplifier circuits and sensors with footprints less under 1 mm^2 can be produced. The size reduction in these implantable devices is severely limited, however, by battery size and/or cost. For example, smaller batteries, such as lithium batteries of sub-millimeter dimensions, are prohibitively expensive to manufacture. Therefore, reduction in the size of implantable medical devices depends on the availability of power sources that can be miniaturized to dimensions comparable to the implantable devices themselves, and on the cost of such power sources. These factors are important, for example, in the development of autonomous medical sensors and associated transmitters, or of receivers and associated actuators.

[0008] Accordingly, the development of a miniaturized power source is desirable. Further, the development of a power source, having millimeter to sub-millimeter dimensions, is desirable. Still further, the development of a power source that can function under physiological conditions is desirable.

Summary of the Invention

[0009] The present invention is directed to power sources, or fuel cells, of reduced physical dimensions. The power source of the present invention is a fuel cell that, unlike other fuel cells, can operate without a membrane. As a membrane can be eliminated as a component of the fuel cell, the dimensions of the cell can be reduced. For example, according to one aspect of the invention, the power source can have a footprint less than or equal to approximately 3 mm^2 , and generally less than or equal to 1 mm^2 , such as down to about 0.1 mm^2 . This reduced size compares well with the size of conventional methanol-air or hydrogen-oxygen fuel cells, which is on the order of 10 mm^2 or more, and is of great advantage for a variety of applications, such as applications calling for the implantation of fuel cells in biological systems.

[0010] A membrane is rendered unnecessary in the inventive fuel cells by virtue of two special electrocatalysts, one of which is immobilized on the surface of the anode,

the other of which is immobilized on the surface of the cathode. Generally, immobilization refers to the direct or indirect, entrapment of an electrocatalyst on an electrode surface or chemical binding, such as covalent, ionic, or coordinative binding, of an electrocatalyst on an electrode surface. The anode electrocatalyst is a poor catalyst for oxygen reduction and the cathode electrocatalyst is a poor catalyst for oxidation of the fuel of the cell, such as glucose. In other words, the anode electrocatalyst is so selective for the fuel of the cell, that oxygen is not rapidly electroreduced at the anode, even though the anode is poised at a potential that is much more reducing than the potential of the cathode, where oxygen is reduced. Further, the cathode electrocatalyst is so selective for oxygen, that the fuel of the cell is not rapidly electrooxidized at the cathode, even though the cathode is poised at a potential that is much more oxidizing than the potential of the anode, where the cell fuel is electrooxidized. As a result, the current loss associated with the oxidation of the cell fuel at the cathode, and the current loss associated with the reduction of oxygen at anode, are both small.

[0011] Thus, in the cell of the present invention, the rate of fuel oxidation, such as glucose oxidation, at the wired cathode, or the cathode that is in electrical communication with the immobilized cathode enzyme, such as bilirubin oxidase, is much slower than the rate of oxygen electroreduction, such that no membrane is required. This aspect differentiates the inventive fuel cell from the known methanol-air fuel cell, which requires a membrane. Further, in the cell of the present invention, the rate of oxygen electroreduction at the wired anode, or the anode that is in electrical communication with the immobilized anode enzyme, is much slower than the rate of fuel electrooxidation, such as glucose oxidation, such that no membrane is required. This aspect differentiates the inventive fuel cell from the known hydrogen-oxygen fuel cell, in which oxygen is rapidly reduced at the hydrogen anode and a membrane is required. In summary, the fuel cell of the present invention can operate with the anode and the cathode in the same compartment, in the presence of both oxygen and the fuel of the cell, such as glucose.

[0012] Not only can the fuel cell operate without cumbersome components, such as membranes, seals and cases, it can do so effectively. For example, according to one aspect of the invention, the fuel cell of the present invention can produce a current

density of from about 0.1 to about 10 mA/cm², which compares well with the lower current densities associated with conventional fuel cells, such as methanol-air and hydrogen-oxygen fuel cells. In addition, the effective fuel cell of the present invention can be manufactured relatively inexpensively, such as on the order of about 10¢ per cell, which compares favorably with the manufacturing costs of conventional cells, such as methanol-air and hydrogen-oxygen fuel cells, which are on the order of more, and often considerably more, than \$100. The very low cost of the inventive fuel cells is a particular advantage with respect to applications that call for fuel cells having a short life span, such as disposable fuel cells used in biological systems for medical purposes, which may be in use for only a week, or even less.

[0013] According to another aspect of the invention, the fuel cell comprises a miniature biofuel cell capable of operating under physiological conditions, or generally, a temperature of about 37°C, a pH of 7.2 to 7.4, and a NaCl concentration of about 0.14 M (although physiological temperatures may be up to about 37.5°C and physiological NaCl concentrations may be up to about 0.15M, for example). This aspect differentiates the inventive biofuel cell from conventional methanol-air and hydrogen-oxygen fuel cells, which operate at non-physiological conditions of neutral pH and relatively high temperature, such as 70°C to 120°C. As such, the biofuel cell of the present invention may be used within a biological system, such as a body of an animal. For example, according to a particular aspect of the invention, the biofuel cell electrooxidizes oxidizable components of a body fluid within an animal, particularly glucose or lactate components, and electroreduces oxygen within that fluid. Power is generated in the biofuel cell via the electrooxidation of glucose or lactate in the fluid, coupled with the electroreduction of oxygen in the same fluid. Advantageously, this biofuel cell is small, effective, powerful, and easy and inexpensive to manufacture.

[0014] These and other aspects, features and advantages of the present invention are described in the drawings and the description of the invention set forth below, or will be apparent or appreciated upon consideration thereof.

Brief Description of the Drawings

[0015] FIG. 1 is a cross-sectional view of components of a biological fuel cell, according to an embodiment of the invention.

[0016] FIG. 2 is a schematic illustration of electron transfer in the electrocatalytic oxidation of glucose and in the electrocatalytic reduction of oxygen that occur in a biological fuel cell, according to an embodiment of the invention.

5 [0017] FIGS. 3A to 3E are illustrations of various configurations of an anode and a cathode used in a biological fuel cell, according to various embodiments of the invention.

[0018] FIG. 4 is a representation of the molecular structure of a redox polymer that can be used as an electrical coupler or "wire" in an anode electrocatalyst layer, according to an embodiment of the invention.

10 [0019] FIG. 5 is a representation of the molecular structure of a redox polymer that can be used as an electrical coupler or "wire" in an anode electrocatalyst layer, according to an embodiment of the invention.

[0020] FIG. 6 is a representation of the molecular structure of a redox polymer that can be used as an electrical coupler or "wire" in a cathode electrocatalyst layer, according to an embodiment of the invention.

[0021] FIG. 7 is a representation of the molecular structure of a redox polymer that can be used as an electrical coupler or "wire" in a cathode electrocatalyst layer, according to an embodiment of the invention.

20 [0022] FIG. 8 is a scanning electron microscope image of a composite electrode, which shows the crosslinking of a redox polymer-enzyme adduct on carbon fibers, according to an embodiment of the invention.

[0023] FIG. 9 is a schematic illustration of an analyte-monitoring device, shown in cross-section, where dashed lines represent electrical coupling of components of the device, and dotted lines represent communicative couplings between components of the device and between the device and a remote device, according to an embodiment of the invention.

25 [0024] FIG. 10 is a schematic illustration of an analyte-monitoring and/or treatment device, shown in cross-section, where dashed lines represent electrical coupling of components of the device and a dotted line represents a communicative coupling

between components of the device, according to an embodiment of the invention.

[0025] FIG. 11 is a schematic, block-diagram illustration of an autonomous, analyte-monitoring and treatment device, which includes a drug delivery system, according to an embodiment of the invention.

5 [0026] FIG. 12A is a graph of current density ($\mu\text{A}/\text{cm}^2$) versus cell potential (V), which shows the polarization of an anode (in bold line) and of a cathode (in fine line) in a biological fuel cell, as described in Experimental Example 3.

[0027] FIG. 12B is a graph of power density ($\mu\text{W}/\text{mm}^2$) versus cell potential (V) at 25°C (in fine line) and at 37°C (in bold line) in a biological fuel cell, as described in
10 Experimental Example 3.

[0028] FIG. 13A is a graph of power output (power density in $\mu\text{W}/\text{mm}^2$) versus cell potential (V) in air (bold line) and under oxygen (fine line) in a biological fuel cell, as described in Experimental Example 3.

[0029] FIG. 13B is a graph of power density ($\mu\text{W}/\text{mm}^2$) versus glucose concentration (mM) in air (closed circle) and under oxygen (open circle) in a biological fuel cell
15 operating at 0.52 V, as described in Experimental Example 3.

[0030] FIG. 14 is a graph of power density ($\mu\text{W}/\text{mm}^2$) versus temperature (°C) in a biological fuel cell operating at 0.52 V, as described in Experimental Example 3.

[0031] FIG. 15A is a graph of power density ($\mu\text{W}/\text{mm}^2$) versus pH in a biological fuel
20 cell operating at 0.52 V, as described in Experimental Example 3.

[0032] FIG. 15B is a graph of residual power density (%) versus chloride concentration in a biological fuel cell operating at 0.52 V, as described in Experimental Example 3.

[0033] FIG. 16A shows photographs of a whole and a sliced grape with implanted
25 fibers and associated electrical contacts, as described in Experimental Example 3. Lines are drawn to show the position of the 7- μm -diameter fibers, as they were barely visible.

[0034] FIG. 16B is a graph of power output (power density in $\mu\text{W}/\text{mm}^2$) versus cell

potential (V) of the biological fuel cell associated with FIG. 16A above, where the cathode fiber is implanted near the skin of the grape (bold line) and near the center of the grape (fine line), as described in Experimental Example 3.

5 [0035] FIG. 17 is a schematic illustration of redox potentials (vs Ag/AgCl at pH 7.2) of enzymes and associated "wiring" redox polymers in a biological fuel cell, as described in Experimental Example 3.

Detailed Description of Embodiments

10 [0036] The present invention is generally directed to a biological fuel cell and more particularly directed to a biological fuel cell of reduced physical dimensions that can be used under physiological conditions. A biological fuel cell that is miniaturized according to the present invention may be used in connection with various devices, including autonomous electronic, electromechanical and microfluidic medical implants, such as sensors, transmitters, receivers, and actuators, and the like. Such devices may be reduced in size by virtue of being powered by a miniaturized
15 biological fuel cell.

[0037] The biological fuel cell of the invention may comprise, consist essentially of, or consist of an anode and an anode enzyme in electrical communication and a cathode and a cathode enzyme in electrical communication. That is, the biological fuel cell may be based on two primary electrical connections. One electrical
20 connection is between an anode of the biological fuel cell and a catalyzing enzyme for the oxidation of oxidizable components of a biological fluid, such as glucose or lactate. For example, glucose may be electrooxidized by the catalyzing enzyme via this first electrical connection. The other electrical connection is between a cathode of the biological fuel cell and a catalyzing enzyme, such as a copper-containing enzyme,
25 for the reduction of oxygen. For example, oxygen may be electroreduced by the catalyzing enzyme, bilirubin oxidase (often referenced herein as BOD), via this second electrical connection.

[0038] The implantable biological fuel cell of the invention has a footprint smaller than 3 mm², preferably smaller than 1 mm², and most preferably less than or equal to
30 about 0.3 mm², such as down to about 0.1 mm². The volume of the cell is on the order

of about 1 mm³ or less. The biological fuel cell can be used, for example, to power an implanted miniature sensor, or sensor/transmitter, such as a sensor of blood flow or pressure, pH, oxygen, carbon dioxide, electrolyte(s), lactate, pyruvate, glucose, creatine phosphate, creatine, creatinine, or the like. The biological fuel cell can be integrated with the sensor or other electronic device on a chip, such as an organic or a silicon-based integrated circuit, to facilitate integration and manufacture of a sensor or other device that will carry its own power source. In a preferred embodiment, none of the components of the cell is dissolved or leached at appreciable levels, *in vivo*, such that the components do not diffuse away from the working electrodes during the operation of the cell.

The Biological Fuel Cell

[0039] The biological fuel cell of the invention typically uses compounds available in a variety of biological systems as fuel. Generally, the cell operates in association with a biological fluid, such as blood in an animal, including a human, or sap in a plant, for example. By way of example, a biological fuel cell may be configured for implantation within a biological system, such as an animal, to operate an electrical device, such as a glucose sensor, a pacemaker, a stimulator for nerve growth, a stimulator for relief of chronic pain, a stimulator for regrowth of bone or other tissue, a drug-release valve or microvalve, a fluid-flow control valve, such as a valve in a duct or in the urinary tract, or the like. When the fuel cell is implanted in a blood vessel of an animal, biological fluid may be pumped through the fuel cell by the heart of the animal, thereby obviating any need for a mechanical pump. Further by way of example, a biological fuel cell may be configured for providing electricity from a biological system, such as a plant, including a tree, or a component of a plant, such as a plant residue or fruit, or the like, which electricity may be used to operate a device that is external to the cell or to the system in which the cell resides.

[0040] Typically, the cell operates in association with a biological fluid of an animal, such as blood, subcutaneous interstitial fluid, fluid between cells in various tissues, fluid in the peritoneum, fluid near the spinal cord, or the like. Since the biofuel cells are generally used within an animal when the animal is alive, components of the biological fluid that fuel the biofuel cell are replenished. These replenishable components serve as oxidizable fuel for the operation of the biological fuel cell, and

include, without limitation, glucose, lactate, and pyruvate. Merely by way of example, other exemplary components include sugars, alcohols, carboxylic acids, carbohydrates, starches, and cellulose. Through the biofuel cell, these components are oxidized by dissolved or complexed oxygen, which is usually supplied by the blood in which it is mostly hemoglobin-bound. In other fluids, the oxygen may be more or less associated with or bound to myoglobin.

[0041] FIG. 1 illustrates components of a biological fuel cell 100, according to an embodiment of the invention. Biological fuel cell 100 is intended for use within a biological system, which provides electrolyte (as shown in FIG. 2) for the cell. The cell 100 includes two electrodes, an anode 102 and a cathode 104, which are separated to avoid electrical shorting. The separation of anode 102 from cathode 104 can be accomplished using one or more spacers (not shown). The spacers are often permeable, porous, microporous, and/or fibrous. Alternatively, the spacers can have gaps to allow fluid to flow through them. In alternate embodiments, the spacers can comprise ion-selective membranes. Suitable materials for spacers include, but are not limited to, polyamides (e.g., nylon), polyesters (e.g., DacronTM), a cation-exchange membrane (e.g., a NafionTM membrane), an anion-exchange membrane, porous polyolefins, polyimides, polyethers, and polyurethanes.

[0042] In accordance with the embodiment shown, anode 102 and cathode 104 are formed from two carbon fibers. The carbon fibers can vary in size, but generally have a diameter that ranges from about 2 μm to about 50 μm , and a length that ranges from about 10 μm to about 10 cm. In one embodiment of the invention, the carbon fibers used in anode 102 and cathode 104 have a diameter of about 7 μm and a length of about 2cm. Anode 102 and cathode 104 can also have electrical connections 103 and 105 that couple biological fuel cell 100 to an electrical device, such as a sensor, an amplifier, a storage device, such as a capacitive storage element or battery, or some other electronic circuit or device. The carbon fibers that form anode 102 and cathode 104 can be coated with thin films of electrocatalyst layers 106 and 108, as shown in FIG. 1. Although clearly shown in FIG. 1, electrocatalyst layers 106 and 108 will generally be much too thin to be distinguishable from the carbon fibers.

[0043] Anode electrocatalyst layer 106 is formed on at least a portion of anode 102.

Generally, anode electrocatalyst layer 106 will coat the majority of the surface of anode 102. Anode electrocatalyst layer 106 typically comprises an anode redox polymer and an anode enzyme. Examples of enzymes that can be used in anode electrocatalyst layer 106 are oxidases and dehydrogenases of glucose, lactate and pyruvate, as exemplified by glucose oxidase (GOx), lactate oxidase (LOx), and pyruvate oxidase.

[0044] Cathode electrocatalyst layer 108 is formed on at least a portion of cathode 104. Generally, cathode electrocatalyst layer 108 will coat the majority of the surface of cathode 104. Cathode electrocatalyst layer 108 typically comprises a cathode redox polymer and a cathode enzyme. Preferred cathode enzymes comprise four copper ions in each of their functional units. An example of a cathode enzyme that can be used in cathode electrocatalyst layer 108 is bilirubin oxidase (BOD).

[0045] For purposes of this specification, GOx will often be used herein to reference an enzyme that can be used in anode electrocatalyst layer 106, while BOD will often be used herein to reference an enzyme that can be used in cathode electrocatalyst layer 108. It should be noted that these are merely examples of these enzymes, which examples should not be construed as a limitation as to enzymes that can be used with this invention.

[0046] Electrocatalyst layers 106 and 108 electrically couple their respective enzymes to anode 102 and cathode 104 through their respective redox polymer components, which are crosslinked, electron-conducting structures. More than one redox polymer and/or more than one enzyme can be used in each electrocatalyst layer 106 and 108. The electrical coupling provided by the redox polymers is often referred to herein as "wiring" or "wires" or the like. In water, the redox polymers swell, but do not dissolve, to form electron-conducting hydrogels. When the redox polymers and enzymes are sufficiently crosslinked, the hydrogels can be tough, and can have leather-like strength and other mechanical properties. As the electrocatalyst layers 106 and 108 form hydrogels that immobilize the anode enzymes on the anode 102 and the cathode enzymes on the cathode 104, respectively, a membrane for separating the anode reactants and the cathode reactants is not required in biological fuel cell 100. This is a major advantage, in terms of manufacturability and cost reduction, for example, of biofuel fuel cell 100.

[0047] In particularly preferred modes of the invention, chemistry that essentially immobilizes or binds the enzymes on anode 102 and the cathode 104 of fuel cell 100 is employed such that an ion- or electrode-separating membrane can be eliminated as a component of the cell. Thus, biological fuel cell 100 may be, and preferably is, a
5 membrane-free or single-compartment cell. As used herein, "membrane-free" or "single-compartment" cell refers to a cell 100 in which the anode 102 and the cathode of the cell, and the immobilized enzymes associated therewith, are not separated by a membrane or partition, although other portions of the cell may be so separated.

[0048] The biological fuel cell 100 may comprise anode 102, having disposed thereon
10 an anode enzyme, and cathode 104, having disposed thereon a cathode enzyme, at least a portion of the anode and cathode enzymes being substantially immobilized on anode 102 and cathode 104. For a physiological biofuel cell 100, substantial immobilization refers to a lack of dissolution of the enzyme over a 24-hour period at 37 °C in a pH 7.2 aqueous buffer solution that contains 0.14 M NaCl and 20 mM
15 phosphate ions added to their sodium salts. Those skilled in the art will appreciate that the proportion of the enzyme that must be bound to the electrode (directly or indirectly, but in any case, in adequate proximity to the electrode surface to permit the movement of electrons as the electrochemical reaction proceeds), will be determined by the desired or necessary performance properties of the cell. Overall, the amount of
20 enzyme that may not be fully bound to the electrode will be limited by the need to avoid, in a particular cell design, interference with the performance of the membrane-free or single-compartment cell due to the shuttling of reactive species between the electrodes.

[0049] The enzyme in each electrocatalyst layer 106 and 108 typically catalyzes an
25 electrochemical reaction of an anode reductant or a cathode oxidant, respectively. The anode reductant and cathode oxidant are provided by the biological system and comprise the fuel source for biological fuel cell 100. Examples of the most common anode reductants used in biological fuel cell 100 include glucose, lactate, and pyruvate. The cathode oxidant primarily comprises oxygen present in the biological
30 system, found as dissolved molecular oxygen, or as hemoglobin- or myoglobin-bound oxygen. Biological fuel cell 100 can also include other enzymes that break down more complex molecules, for example, carbohydrates, such as starches (for example,

glycogen) or celluloses, into simpler components, such as sugars (for example, glucose), alcohols, or carboxylic acids, thereby allowing these more complex molecules to be used as a fuel source as well.

5 [0050] During the operation of biological fuel cell 100, the anode reductant is electrooxidized at anode electrocatalyst layer 106 and the cathode oxidant is electroreduced at cathode electrocatalyst layer 108. The anode redox polymer passes electrons, or a current, between the anode reductant and anode 102, while the cathode redox polymer passes electrons, or a current, between the cathode oxidant and cathode 104. The electrical power of biological fuel cell 100 is generated from the overall
10 oxidation of the anode reductant by the cathode oxidant. In a biological system, for example, the electrical power can be generated by the overall oxidation of glucose, lactate, or pyruvate by dissolved oxygen delivered as hemoglobin-bound oxygen (HbO_2), which is in rapid equilibrium with dissolved oxygen passing through the oxygen-permeable membranes of red blood cells. Biological fuel cell 100 facilitates
15 this oxidation reaction, and uses the resulting flow of electrons to produce an electrical current that can power an implanted electrical device.

[0051] In biological fuel cell 100, the source of an electron current can be glucose, as it delivers a pair of electrons to anode electrocatalyst layer 106. Such a cell is schematically depicted in FIG. 2. The electrons then travel via anode 102 to an
20 external electrical device or an internal electrical device, such as an implanted device, that is powered by biological fuel cell 100. The electrons power the electrical device and then travel to cathode 104, where they are transmitted via cathode electrocatalyst layer 108 to oxygen (i.e., the cathode oxidant is electroreduced).

[0052] In general, for each of electrocatalyst layers 106 and 108, it is preferred that
25 the redox polymer and the enzyme are oppositely charged polyelectrolytes. In one embodiment of the invention, an enzyme used for the electrooxidation of glucose can be GOx wired to anode 102, and an enzyme for the electroreduction of oxygen can be BOD wired to cathode 104. The reaction centers of the two enzymes are electrically wired to anode 102 and cathode 104 via electron-conducting hydrogels, or redox
30 polymers that have swelled in water. As the enzyme GOx is a polyanion at neutral pH, a polycationic redox polymer is most effective as to its wiring. In the operation of the cell, via its wiring, electrons are collected from glucose-reduced GOx at anode

protons from the biological system to form a water molecule 312.

[0054] The physical dimensions of biological fuel cell 100, as well as its operational parameters (e.g., output power and voltage) are, at least in part, a function of the components that form biological fuel cell 100. Merely by way of example, the open-circuit voltage of biological fuel cell 100 can range from about 0.1 volts to about 1.2 volts, and typically, from about 0.2 volts to about 0.9 volts. The voltage at the maximum power point can range from about 0.2 to about 0.8 volts, for example. The volumetric output power density of biological fuel cell 100 can range from about 0.5 mW/cm³ to about 5 W/cm³, for example, although a higher or a lower volumetric output power density is certainly possible. The gravimetric output power density can range from about 5 mW/g to about 5 W/g, for example, although a higher or a lower gravimetric output power density is certainly possible.

[0055] The output power density can depend on the flow of fluid through biological fuel cell 100, particularly if the dimensions of the electrodes are large, such as greater than about 0.1 mm. Generally, increasing the rate of this flow of fluid increases the output power density of cells having larger electrodes. By way of example, when the electrodes of the cell 100 are made with carbon cloth discs having a diameter of about 4 mm, the power, or output power density, increases substantially with flow. On the other hand, the power output density is nearly independent of the flow of fluid through the cell 100, or may even decrease slightly with this flow, when the dimensions of the electrodes are small, such as less than about 0.1 mm, less than preferred dimensions of about 0.05 mm, and less than most-preferred dimensions of about 0.02 mm. Thus, when biological fuel cell 100 is formed from two carbon-fiber electrodes, having a diameter of about 7 μ m, and a length of about 2 cm, the power, or output power density, is nearly independent of fluid flow through the cell.

[0056] The output power density, and therefore the size of an implanted biological fuel cell 100, can be limited by electrode kinetics, ohmic resistance, and/or mass transport. When the electrode kinetics is fast and the biological fuel cell 100 is small enough for the ohmic resistance of the electrolytic solution to be low, the power density is determined by the mass transport of the reactants to the electrodes. When mass transport is rapid, such as via rapidly flowing blood, the power density is determined by the electrode kinetics. The mass-transport-limited current density

increases upon raising the concentration of the reactants or upon increasing the flow rate of the biological fluid. Because the concentrations of glucose (about 4 to about 7 mM in the blood of non-diabetic people) and HbO₂ (about 5 mM in venous and about 8 mM in arterial blood at normal hematocrit) are defined in blood and in other tissues of the human body, the power density is controlled by the flow rate of the biological fluid when the turnover of the anode or cathode electrocatalyst is fast enough to electrooxidize or electroreduce the entire influx of reactant. If, however, one of the dimensions of the electrodes is small enough, then as discussed above, the power density can be made nearly independent of flow.

10 [0057] In an embodiment of the invention, anode 102 and cathode 104, as well as all other components of biological cell 100, are preferably coated such that they are bio-inert. This is to prevent protein fouling or an immune reaction, for example. By way of example, in one embodiment of the invention, the components of biological fuel cell 100 can be coated with a thin coating that is highly permeable to the reactants.

15 This coating can comprise a photo-crosslinked, bioinert, 18-kD poly(ethylene glycol) diacrylate, formed of a solution containing a photoinitiator, 2,2-dimethoxy-2-phenyl-acetophenone. An appropriate coating can be applied in a variety of ways. For example, aqueous precursor monomer and pre-polymer (a low molecular weight polymer) solutions can be dip-coated on fibers or other structures. Alternatively, these

20 solutions can be spun on the rotating components by a process similar to that of spinning photoresists on silicon wafers in the manufacture of integrated circuits. In this latter process, the components being coated are rotated at a defined angular velocity while the solution is applied. The thickness of the film is defined by the angular velocity and the viscosity of the solution. After water evaporates from the

25 deposited films, the films are photo-polymerized via exposure to ultraviolet radiation, for example, from a 150 W mercury lamp disposed 30 cm away from the film.

[0058] Miniaturization of biological fuel cell 100 is possible because the cell does not have corroding or corrosive components, and because the cell reactants react much faster at their respective electrodes than at their respective counter electrodes. (See,

30 for example, Mano *et al.*, *A Miniature Biofuel Cell Operating in a Physiological Buffer*, J. Am. Chem. Soc. 2002, 124, 12962-12963.) In other words, miniaturization is made possible by the absence of reaction of glucose at cathode 104 and the very

slow reaction of O₂ at anode 102, which, as the two electrocatalysts are immobilized on their respective electrodes, eliminates the need for a compartment-separating membrane. As a result, biological fuel cell 100 does not require any of the three components that are generally the most difficult to miniaturize, namely, the case, the seal, and the compartment-separating membrane. Further, as a result of the high selectivity of the electrodes, the surfaces of the electrodes need not be clean, as is required in conventional methanol-air and hydrogen-oxygen fuel cells, and the cleanliness of the cell's fuel and the fuel cell itself is irrelevant.

[0059] Thus, in accordance with an embodiment of the invention, biological fuel cell 100 is usually assembled without the case, the seal, and the compartment-separating membrane required by conventional batteries. As a result, biological fuel cell 100 can be manufactured with a footprint smaller than about 3 mm², preferably smaller than about 1 mm², and most preferably smaller than about 0.3 mm². The biological fuel cell, with dimensions on the millimeter to sub-millimeter level, can power devices such as an implanted sensor, a sensor/transmitter, an actuator, or a receiver/actuator system, as further described herein. Further, this small biological fuel cell can be constructed so that none of its components, including its catalytic components, will be dissolved or leached while residing in the body.

The Electrodes

[0060] Five exemplary structures, including anode 102 and cathode 104, are illustrated in FIGS. 3A-3E. Merely by way of simplification, these structures are illustrated with similar anode and cathode geometries. It should be noted, however, that these are merely simplified examples of these structures, as the dimensions of the two electrodes may differ because the current densities of the two electrodes are usually not the same, and may be adjusted to ensure that the current densities of the two electrodes are the approximately the same. The optimal ratio of anode area to cathode area depends on the ratio of the respective current densities of the two electrodes in the tissue in which biological fuel cell 100 is used. When the dimensions of the electrodes are larger than about 0.1 mm, their current densities are generally determined by local flow and mass transport. When the dimensions of the electrodes are smaller, their current densities, which may not be limited by mass transport, are generally determined by the kinetics of the electrocatalysts.

[0061] In FIG. 3A, the biological fuel cell 600 appears as a bipolar sandwich, similar to conventional fuel cell stacks and button-type batteries. An electronically insulating separator 602 between anode 102 and cathode 104 is penetrated by the blood or by the interstitial fluid, minimizing the ohmic resistance of the cell. Single-cell sandwiches
5 can be stacked to generate a current that is an aggregate or a multiple of the current of the single-cell components. Such a configuration provides a high surface area in a small volume, at the likely expense of increased mass transport resistance. This configuration is preferred when kinetics, rather than mass transport, limits the current.

[0062] In the coplanar biological fuel cell 604 of FIG. 3B, a separator for penetration
10 by blood or interstitial fluid (such as the separator 602 in cell 600 of FIG. 3A) is not required. Advantageously, coplanar cell 604 facilitates mass transport to anode 102 and cathode 104 and is of relatively simple construction. In this construction, the electrodes 102 and 104 of the cell 604 can be reduced in width to minimize the ohmic loss. Preferably, these electrodes are long and narrow, in the form of parallel strips.

[0063] The biological fuel cells 606, 608 and 610, respectively, of FIGS. 3C, 3D and
15 3E, have stent-like, cylindrical geometries that are well suited for implantation in blood vessels. The single-walled tubular structures of FIGS. 3C and 3D, namely cells 606 and 608, are comparable to the coplanar structure of FIG. 3B. As shown in FIG. 3C, cell 606 comprises a half-annular anode 102 joined in parallel with a half-annular
20 cathode 104, via an insulating spacer 607, to form a complete annular structure. As shown in FIG. 3D, the cell 608 comprises an annular anode 102, and an annular cathode 104, joined in series, via a ring-like insulating spacer 609, to form a relatively elongated annular structure. In this embodiment, the products of the upstream electrode reaction are swept past the downstream electrode.

[0064] Cell 610 of FIG. 3E comprises an annular cathode 104 within an annular anode
25 102. The cathode and anode may be concentrically arranged as shown. Cell 610 offers less ohmic resistance than the cells of FIGS. 3B to 3D, but has a high mass-transport resistance. Even though HbO_2 is in rapid equilibrium with dissolved O_2 , the lesser diffusivity of HbO_2 is likely to lead to a preference for an arrangement of cell
30 610 in which the cathode 104 is the inner electrode.

[0065] Cell 604 of FIG. 3B and cell 608 of FIG. 3D are particularly advantageous in

that they are easily optimized in terms of the ratio of the areas of their respective anodes 102 and cathodes 104. In both cell 604 and cell 608, this ratio varies simply with the lengths of the electrode segments. In cell 606 of FIG. 3C, the ratio can be optimized by varying the radius of the radial segments.

- 5 [0066] According to an embodiment of the invention, anode 102 and cathode 104 are made of a non-corroding metal, such as gold, palatinum, palladium, iridium, osmium, rhenium, ruthenium, ruthenium dioxide, and preferably, carbon. By way of example, carbon particles, carbon fibers, carbon cloth, or the like may be used to make carbon-based anodes and cathodes. Carbon particles have effective diameters that range from
10 about 10 nm to about 100 μm , and preferably range from about 2 μm to about 50 μm . Carbon fibers have diameters that normally range from about 2 μm to about 20 μm . Carbon cloth is made of fibers, having diameters similar to those of carbon fibers, and has a void fraction greater than about 10 to about 30 percent by volume, and preferably, greater than about 50 percent by volume.
- 15 [0067] Each of anode 102 and cathode 104 is coated by crosslinking an electron-conducting redox polymer and an enzyme, each of which is further discussed below, on its surface. Crosslinking a water-soluble redox polymer and an enzyme on a treated carbon electrode produces a hydrogel with an immobilized and wired enzyme. The anode and cathode hydrogels are permeable to water-soluble biochemicals and
20 ions.

Redox Polymers

- [0068] The redox polymer of the anode electrocatalyst layer 106 electrically connects, or wires, the reaction centers of the anodic enzyme to the anode 102 and the redox polymer of the cathode electrocatalyst layer 108 wires the reaction centers of the
25 cathodic enzyme to the cathode 104. This wiring is accomplished without using a diffusing mediator. The redox polymer preferably forms some type of bond with the enzyme. Preferably, the redox polymer is a polycation that forms an electrostatic adduct with the enzyme. For example, the redox polymer and the enzyme may be, and preferably are, oppositely charged polyelectrolytes. In one particular example,
30 polycationic redox polymers are most effective in the wiring of GOx, because GOx is polyanionic at neutral pH. A current density of about 2 mA/cm^2 can be reached with

carbon-cloth-based electrodes even in air where the redox potential of the wire of GOx is about +0.05 V vs. Ag/AgCl and the electrode is poised at 0.2 V (Ag/AgCl). At this potential, most of the GOx electrons are collected by the wire, with only one-sixth of the current being lost to O₂.

5 [0069] A suitable redox polymer is one having a redox species that is a transition metal compound or complex. A preferred transition metal compound or complex is one in which the transition metal is osmium, ruthenium, iron, or cobalt, preferably, the former. According to an embodiment of the invention, the redox polymer has several desirable characteristics, including but not limited to, the following: (1) a flexible,
10 hydrophilic backbone, which provides segmental mobility when the redox polymer is hydrated; (2) redox functions pendant on flexible and hydrophilic spacers, which tend to maximize electron exchange between the colliding redox centers; and (3) small complexes of Os^{2+/3+}, having high rates of self-exchange, which small complexes allow the close approach of the reaction centers of the enzymes. For example, an
15 exemplary redox polymer, PVP-[Os(N,N'-dialkylated-2,2'-bi-imidazole)₃Cl]^{2+/3+}, has long and flexible tethers that bind the redox centers to the polymer backbone and allow for efficient collection of electrons from elements such as GOx. This redox polymer is illustrated in FIG. 4 and further described in Mao *et al.*, *Long Tethers Binding Redox Centers to Polymer Backbones Enhance Electron Transport in Enzyme*
20 *"Wiring" Hydrogels*, J. Am. Chem. Soc. 2003, 125, 4951-4957.

[0070] The redox polymer is important to the effective functioning of cell 100. For example, when a cell lacks the redox-polymer-based electrical connections, or wires, discussed above, the internal resistance of the cell is so high that no current will flow. Further by way of example, when BOD enzyme is used in a cell that lacks a redox
25 polymer, only a very small fraction of the molecules of the BOD enzyme are properly oriented to allow electron transfer with cathode 104 and to thereby contribute to the current in the cell. By contrast, when a redox polymer hydrogel is present in cell 100, the enzyme molecules need not be oriented toward the surface of the electrode because virtually all of the reaction centers of the enzyme are wired to the electrode via the
30 redox centers of the redox polymer hydrogel. The hydrogel has mobile segments that can effectively approach these reaction centers of the enzyme to effect this wiring. Additionally, the three-dimensional volume of the hydrogel can contain not just one

layer, but multiple layers, of the enzyme that is wired to the electrode.

[0071] In summary, in cells lacking the wiring provided by redox polymers, electron transfer between an enzyme and an electrode may be poor or may not take place at all. For example, in such a cell, as effective electron transfer between an electrode and an enzyme requires that the active site of the enzyme face toward the surface of the electrode, only a small fraction of a monolayer of the randomly oriented enzyme will be electroreduced or electrooxidized. Therefore, the current densities associated with cells that lack redox-polymer wiring cannot approach the current densities associated with the redox-polymer-wired cells 100 described herein. Advantageously, extraordinarily high current densities, such as from about 0.1 to about 10 mA/cm², can be obtained from cells 100 containing electrodes that have been modified with redox polymer hydrogels that wire enzymes such as GOx and BOD.

[0072] The redox potentials of the redox polymers that wire the anode enzyme and the cathode enzyme can be tailored to increase the power output of biological fuel cell 100. The difference in these redox potentials affects the optimal operating potential of biological fuel cell 100. The redox potential of the anode redox polymer is reducing relative to the redox potential of the cathode redox polymer. The preferred redox potential of the anode redox polymer depends on the anode enzyme, and that of the cathode polymer on the cathode enzyme. Usually the redox potential of the anode polymer is tailored to function under physiological conditions, and if the anode enzyme is GOx, the redox polymer is also tailored to function in the range from about -300 mV to about +200 mV, and preferably from about -150 mV to about +70 mV, versus the potential of the Ag/AgCl (3 M KCl) electrode. The redox potential of the cathode redox polymer is tailored to be in the range of from about +250 mV to about +600 mV, and preferably from about +300 mV to about +500 mV, versus the potential of the Ag/AgCl (3 M KCl) electrode.

Composite Electrodes

[0073] Anode electrocatalyst layer 106 and cathode electrocatalyst layer 108 are composed of redox polymers that form hydrogels upon swelling in water, as previously described. In these layers, electron transport occurs by way of collisions between redox centers that are tethered to crosslinked polymers. When the redox

polymers are crosslinked and swelled in water, chain segments of the polymers are mobile, electron diffusivity via the polymers is high ($>10^{-8}$ cm²/s), but the hydrogels are soft. When the redox polymers are highly crosslinked, the polymers are mechanically tough even after forming hydrogels, but the segmental mobility and the electron diffusivity associated with the polymer are reduced. Composite electrodes (e.g., a composite anode and a composite cathode) are composed of redox polymers that are highly crosslinked, yet still form hydrogels having mobile chain segments.

[0074] In an embodiment of the invention, a composite anode is formed by combining electrocatalyst layer 106 with a carbon anode 102, and a composite cathode is formed by combining electrocatalyst layer 108 with a carbon cathode 104. The carbon anode 102 and/or carbon cathode 104 is preferably composed of carbon in the form of carbon particles, carbon fibers, or most preferably, carbon cloth. The electrocatalyst layer and the electrode can be combined by binding the hydrogel to hydrophilic carbon particles, carbon fibers, or carbon cloth, to produce a relatively strong composite electrode. The specific area (area per unit weight) of the carbon cloth is high, and carbon fibers, coated with a thin film of well-crosslinked hydrogel, have a high water-wetted surface area. The composite electrode is a well-crosslinked, leather-like, hydrophilic composite electrode that can maintain mechanical integrity and high current density under the shear stress exerted by rapidly flowing solutions at flow velocities similar to those of blood in major arteries.

[0075] In one embodiment of the invention, 10- μ m-diameter carbon fibers, on which the electrostatic redox-polymer-enzyme adduct is crosslinked, can be used. FIG. 8 shows a scanning electron microscope image (at 500 times magnification) of a composite electrode, in which the crosslinking of the redox-polymer-enzyme adduct on carbon fibers, of about 10 μ m in diameter, can be seen. The carbon fibers may be treated to render their surfaces hydrophilic. The surfaces can be plasma-oxidized for this purpose, although other known methods can be used. The composite electrodes of this embodiment can withstand a shear stress of 0.08 N/m² that is predicted for blood flowing at a linear velocity of 10 cm/s.

[0076] In another embodiment of the invention, disc-shaped carbon cloth electrodes can be used to form composite electrodes. The currents associated with these composite electrodes are limited by mass transport. When these composite electrodes

are rotated, the currents increase with the square root of their angular velocity, in accordance with the Levich Equation, until the kinetic limit defined by the electrocatalyst is reached. For carbon cloth discs with a diameter of 4 mm, this limit is about 2 to about 5 mA/cm² of geometrical surface area (as opposed to true surface area) for the anode, and about 5 to about 9 mA/cm² of geometrical surface area for the cathode. This carbon-cloth embodiment differs from a previously mentioned, carbon-fiber embodiment in which single carbon fibers of about 7 μm in diameter are used to build the electrodes. For these carbon-fiber electrodes, the associated currents are, for the most part, kinetically limited, having a limit of about 1 mA/cm² of true area, which is about equal to the geometric area.

Anodes

[0077] Anode 102 of biological fuel cell 100 effectuates the electrooxidation of the fuel of the cell, such as the electrooxidation of glucose to gluconolactone schematically illustrated in FIG. 2. As described previously, anode enzymes, examples of which are oxidases and dehydrogenases, catalyze this electrooxidation of the cell's fuel. These anode enzymes are wired to the anodes via an anode redox polymer. An example of a redox polymer of an anode electrocatalyst layer 106 is the polymer X5, sometimes referred to herein as polymer I, the representative structure of which is shown in FIG. 4. Polymer X5 is derived from the copolymer of poly(acrylamide) and poly(4-vinyl pyridine) and comprises an Os complex. Another example of a redox polymer of an anode electrocatalyst layer 106 is shown in FIG. 5. This redox polymer is derived from poly(N-vinyl imidazole) and comprises an Os complex. In these examples, the Os(II) and Os(III) centers of the anode redox polymers and the anode enzymes are immobilized in electron-conducting films on the surfaces of the anodes.

Cathodes

[0078] Cathode 104 of biological fuel cell 100 effectuates the four-electron electroreduction of O₂ to water under physiological conditions. This electroreduction reaction is catalyzed by the cathode enzymes, which are wired to the cathodes via a cathode redox polymer. A representative structure of an exemplary redox polymer, PAA-PVI-[Os(4,4'-dichloro-2,2'-bi-pyridine)₂Cl]⁺²⁺, of a cathode electrocatalyst

layer 108 is shown in FIG. 6, and a representative structure of another exemplary redox polymer, sometimes referred to herein as polymer II, is shown in FIG. 7.

[0079] As described previously, cathode enzymes catalyze the four-electron reduction of O₂ to water. The cathode enzymes are copper-containing oxidases, examples of which include laccases, ascorbate oxidases, ceruloplasmines, and bilirubin oxidases (BODs). The preferred enzymes are exemplified by BODs, which unlike laccases, retain more than 80%, and usually retain more than 90%, of their maximal activity under physiological pH and salinity.

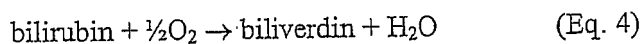
[0080] The catalytic reduction of O₂ to water depends on the coordination of the copper ions of the enzymes, or more particularly, the four Cu⁺²⁺ ions of the enzymes. The Cu⁺²⁺ ions are classified by the ligands that coordinate them into three "types", types I, II, and III. The centers of type I Cu⁺²⁺ ions show an intense Cys to Cu(II) charge transfer band at around 600 nm. The type I copper center accepts electrons from an organic substrate, such as a phenol, ascorbate, or bilirubin, and relays the electrons to the O₂-reduction site. The O₂-reduction site is a tri-nuclear cluster, consisting of one type II Cu⁺²⁺ center and a pair of type III Cu⁺²⁺ centers with a characteristic 330-nm shoulder.

[0081] In non-physiological conditions, laccase monolayers on vitreous carbon catalyze the four-electron electroreduction of O₂ to water. (See, for example, Barton *et al.*, *The "Wired" Laccase Cathode: High Current Density Electroreduction of O₂ to Water at +0.7 V (NHE) at pH 5*, J. Am. Chem. Soc. 2001, 123, 5802-5803; Chen *et al.*, *A Miniature Biofuel Cell*, J. Am. Chem. Soc. 2001, 123, 8630-8631; Barton *et al.*, *Electroreduction of O₂ to Water on the "Wired" Laccase Cathode*, J. Phys. Chem. B 2001, 105, 11917-11921; and Barton *et al.*, *Electroreduction of O₂ to water at 0.6 V (SHE) at pH 7 on the 'wired' *Plueuotus ostreatus* laccase cathode*, Biosensors and Bioelectronics 17 (2002), 1071-1074.) For example, it has been shown that a composite electrode formed using laccase from *Coriolus hirsutus* crosslinked with a redox polymer on a hydrophilic cloth of 10 μm-diameter carbon fibers can electroreduce oxygen to water in the absence of chloride, in a pH 5 citrate buffer, at a current density of 5 mA/cm² at -0.13 V versus the reversible potential of the O₂/H₂O electrode at 37.5 °C. In this example, the redox polymer was PVI-Os(tpy)(dme-bpy)^{2+/3+} [poly-N-vinylimidazole, with one-fifth of the imidazoles complexed with

$[\text{Os}(\text{tpy})(\text{dme-bpy})]^{2+/3+}$, where tpy = terpyridine, and dme-bpy = 4,4'-dimethyl-2,2'-bipyridine]. This redox polymer electrically connected, or wired, the *C. hirsutus* laccase reaction centers to the carbon fibers.

- [0082] Under physiological conditions, however, the current density of the wired *C. hirsutus* laccase-carbon cloth composite cathode was very small. At a pH of about 7.4, the *C. hirsutus* laccase was practically inactive, and the *C. hirsutus* laccase was inhibited by Cl^- at a chloride concentration of about 0.14 M. Therefore, under physiological conditions, the laccase-based electrode is not a viable option for the electroreduction of O_2 to water.
- 10 [0083] According to an embodiment of the invention, the BOD enzyme can be used in biological fuel cell 100 to electroreduce O_2 to water under physiological conditions. There are different forms of BOD available, such as BOD from *Myrothecium verrucaria* (*Mv*-BOD) and BOD from *Trachyderma tsunodae* (*Tt*-BOD). BODs are usually monomeric proteins and have molecular weights ranging from about 52 kDa to
- 15 about 65 kDa. By way of example, *Tt*-BOD is a monomeric protein that has a molecular weight of about 64 kDa, and *Mv*-BOD has a molecular weight of about 52 kDa. Both *Mv*-BOD and *Tt*-BOD are multi-copper oxidases, each containing one type I, one type II, and two type III copper ions. These three types are defined by their optical and magnetic properties. Type I (blue) copper ions have a characteristic Cys to
- 20 Cu(II) charge-transfer band near 600 nm. The type I copper center accepts electrons from the electron-donating substrate of the enzyme and relays these to the O_2 -reduction site. The O_2 -reduction site is a tri-nuclear cluster, consisting of a type II copper ion and a type III pair of cupric ions with a characteristic 330-nm shoulder.

- [0084] In an electroreduction reaction, BOD catalyzes the oxidation of bilirubin to biliverdin, as represented by Eq. 4 below.
- 25



- [0085] In one embodiment of the invention, *Mv*-BOD can be used in cathode electrocatalyst layer 108. In a cathode 104 constructed using *Mv*-BOD, the electrostatic adduct of the polyanionic *Mv*-BOD and its wire, the polycationic redox
- 30 copolymer of polyacrylamide and poly(N-vinylimidazole) complexed with $[\text{Os}(4,4'$

dichloro-2,2'-bipyridine) $_2\text{Cl}]^{+/2+}$, are immobilized on cathode 104. The current density of a cathode 104 built according to this embodiment, when rotated, is O_2 -transport-limited up to about 8.8 mA/cm^2 and has a kinetic limit of about 9.1 mA/cm^2 . When this *Mv*-BOD cathode 104 is rotated at around 300 rpm and is poised at around -
5 256 mV versus the potential of the reversible $\text{O}_2/\text{H}_2\text{O}$ electrode, cathode 104 will have an initial current density of about 2.4 mA/cm^2 that may decline to around 1.3 mA/cm^2 after approximately six days of continuous operation at 37.5°C .

[0086] In another embodiment of the invention, *Tt*-BOD can be used in cathode electrocatalyst layer 108. In *Tt*-BOD, all of the ligands of the type II and type III
10 $\text{Cu}^{+/2+}$ centers are histidines (His), similar to ligands of ascorbate oxidase. It is believed that the full His coordination of the type II $\text{Cu}^{+/2+}$ center is the underlying cause of the relative insensitivity of BODs to inhibition by the chloride and hydroxide anions at their physiological concentration. Accordingly, other enzymes having the three types of copper centers, would also be useful as components of cathode
15 electrocatalysts in cathodes operating under physiological conditions.

[0087] While the type I $\text{Cu}^{+/2+}$ center of *Mv*-BOD has an axial, weakly coordinating methionine, that of *Tt*-BOD has a non-coordinating phenylalanine. In a comparison of two laccases, one with methionine and the other with phenylalanine in the axial position of the type I $\text{Cu}^{+/2+}$ center, it was found that the redox potential of the type I
20 $\text{Cu}^{+/2+}$ center was approximately 100 mV more oxidizing when the ligand was phenylalanine. It has been shown that the use of *Tt*-BOD shifts the operating potential of cathode 104 upward and improves its operational stability over that of *Mv*-BOD. It is believed that any observed differences between the wired *Mv*-BOD and the wired *Tt*-BOD cathodes, such as differences in the redox potentials, current densities, pH
25 ranges and the operational stabilities, are derived from the more oxidizing redox potential of the type I $\text{Cu}^{+/2+}$ center of *Tt*-BOD, and from differences in the electrostatic adducts that the two polyanionic enzymes form with their respective wiring redox polymers.

Tailoring of the Biological Fuel Cell

30 [0088] In a preferred embodiment, electrons cascade energetically downhill in small potential steps via the anode 102 and the cathode 104 of the biological fuel cell 100.

Using this embodiment, one can tailor the cell to obtain a desired cell voltage, a usable or an optimal cell current, and efficient operation. The electron cascade associated with anode 102 involves small potential steps between the anode enzyme, such as GOx, and the anode redox polymer, and between the anode redox polymer and the anode, as the electrons are transferred from the fuel of the cell, such as glucose, to the anode. The electron cascade associated with the electron transfer between the anode 102 and the cathode 104 involves a further potential step, the thermodynamic limit of which is the cell voltage. The electron cascade associated with cathode 104 involves small potential steps between the cathode and the cathode redox polymer, and between the cathode redox polymer and the cathode enzyme, such as BOD, as the electrons are transferred from the cathode to molecular oxygen.

[0089] In the above-described embodiment, the size of the small potential steps, which should be measurable voltages, can be selected to obtain desirable voltage, current, and efficiency characteristics of the cell. For example, the potential steps, each, some, or all of which may vary in size, can be selected to be from about 10 mV to about 200 mV, such as from about 20 mV to about 100 mV, as is preferred when the cell operates to electrooxidize glucose at anode 102 and electroreduce oxygen at the cathode 104, as previously described. Preferably, the operating voltage of the cell, or the difference between the electrode potential at the cathode and the anode at certain current densities, is greater than or equal to 0.6 V. The current densities are selected according to the application, where the selection may be based on factors such as the enzyme turnover rate, electron-transport resistance and mass-transport resistance. The power density per unit area of the cell is the product of the operating voltage and the current density of the cell.

Exemplary Applications

Operation of a Miniature Biological Fuel Cell in a Biological System

[0090] As previously described, the biological fuel cell of the present invention can be tailored such that its operating voltage is greater than or equal to 0.6 V, a relatively high voltage for a miniature biological fuel cell. Such an operating voltage is of particular interest, as it is sufficient to drive electronic circuits, such as silicon-based integrated circuits or organic circuits, composed of printed, electrodeposited, or

otherwise formed circuit patterns. For example, for silicon-based circuits, preferably, a cell voltage of greater than about half the value of the silicon electron-conducting gap (at about 1.106 V), should be used, as this may simplify the design of the circuits. These circuits can be mounted on or packaged in a biocompatible material, such as a biocompatible plastic, polymer, or ceramic material, for applications calling for implanted biofuel cells, for example.

- [0091] A miniature, membrane-free, biofuel cell operating at 0.78 V has been reported in Mano *et al.*, *A Miniature Biofuel Cell Operating at 0.78 V*, Chem. Commun., 2003, 518-519. Operation at this relatively high voltage was attributed to the use of PVI-
10 $[\text{Os}(\text{N},\text{N}'\text{-biallylated-2,2'-biimidazole})_3\text{Cl}]^{2+/3+}$, the representational structure of which is shown in FIG. 4, as opposed to another anode redox polymer. The cell produced 1.2 μW , with a power density of 2.68 $\mu\text{W}/\text{mm}^2$. As the cathode enzyme of the biofuel cell was a laccase, the cell was operated at 37°C, in a pH 5 buffer, and in the absence of chloride.
- 15 [0092] In an embodiment of the invention, the cathode enzyme of the biofuel cell is a BOD, rather than a laccase, such that the cell can operate at relatively high voltage, but under physiological conditions. In Experimental Example 3, set forth and further described below, such a biofuel cell, consisting of two, electrocatalyst-coated, carbon fibers (7- μm in diameter, 2 cm in length), was tested for operation in a biological
20 system. When the miniature biofuel cell was implanted in a grasshopper, no power was produced. This was attributed to the fact that the sugar in the biological fluid of the grasshopper is disaccharide trehalose, rather than glucose. When the cell was implanted in a grape, a fruit having a high glucose concentration (> 30 mM) in its sap, power was produced.
- 25 [0093] The power output of the grape-implanted cell was O_2 -transport-controlled and depended on the position of the cathode fiber. When the cathode fiber was near the center of the grape, where the fruit was oxygen-deficient, the power density was only 0.47 $\mu\text{W}/\text{mm}^2$ at 0.52 V. When the cathode fiber was shallowly implanted near the skin of the grape, where the sap was better oxygenated, the power density was 2.4
30 $\mu\text{W}/\text{mm}^2$ at 0.52 V. The grape-implanted cell retained 85% of its initial power output of 1.1 μW after a day of operation.

[0094] When the above-described miniature biofuel cell was tested in an aerated, glucose-containing physiological buffer (pH 7.2, 0.14 M NaCl, 20 mM phosphate) at 37 °C, it operated continuously for a week. The output of the cell in the physiological buffer solution was 1.9 μ W, which is sufficient for powering low-power CMOS circuits, and the operating voltage of 0.52 V is adequate for operation of low-voltage CMOS/SIMOX integrated circuits. The cell is thus suitable for powering implanted, autonomous sensor-transmitter systems, such as those of relevance to physiological research and medicine. Examples of such systems and their applications are provided in United States Patent Application No. 09/753,746, of Heller, Funderburk, Drucker and Jin, entitled "Analyte Monitoring Device and Methods of Use" which was filed on January 2, 2001. Various such devices and applications are further described below.

Applications for an Implantable Miniature Biofuel Cell

[0095] An implantable biofuel cell suitable for medical applications is preferably inexpensive (~sub-dollar), small (~sub-mm² footprint; ~sub-mm³ volume), disposable or short-lived (~1-week), low-power (~ μ W for continuous operation, ~milliW for intermittent operation), and low-voltage (~0.52-0.78 V, and preferably, >0.6 V, operating voltage). Here, the term "low-power" or "low-voltage" refers to a power or voltage low enough to be suitable or safe for implantation in a biological system, such as a human body, although such power or voltage may be a relatively high power or voltage, as described above, in the context of an achievable operating power or voltage for a miniaturized biofuel cell. For these applications, the implantable biofuel cell is preferably miniaturized, for example, small relative to the size of the electronic package of the device it powers, and designed to have an operational life, operating voltage, current density, power density per unit area, and the like, suitable for the application.

[0096] The implantable biofuel cell is useful in a variety of medical applications. For example, it may be used in various medical devices that operate intermittently, continuously, or autonomously. In a particular example, the biofuel cell may be used to power miniature, *in vivo*, trans- or sub-cutaneous, lactate and/or pyruvate sensor-transmitter devices for signaling the extent of ischemia resulting from internal or external bleeding or other stress. Further, the biofuel cell may be used to power various miniature, intermittent, continuous or autonomous, *in vivo*, medical devices,

such as preferably continuous, trans- or sub-cutaneous glucose monitors that can autonomously activate the administration of insulin to diabetic patients; preferably continuous monitors of the condition of surgical sites, such as post-surgical sites, that can autonomously activate the administration of agents to reduce bleeding, to reduce pain, and/or to promote healing; preferably continuous monitors of harmful or poisonous agents, or biological- or chemical-warfare agents, such as monitors that can autonomously activate the administration of an antidote; and similar intermittent, continuous or autonomous monitoring and/or treatment devices.

[0097] An example of an autonomous, trans- or sub-cutaneous, analyte-monitoring device is now described in relation to FIG. 9. The device 700 preferably has two, physically separate sections, namely, a sensor section 800 and a receiver-transmitter section 900, as depicted in the schematic diagram of FIG. 9. This physical separation simplifies manufacture of the device. The two sections of the device may be in the form of patches that can be worn on the skin of a patient or user of the device, via adhesive or other attachment mechanism, for example.

[0100] The sensor section 800 comprises a physiological, analyte sensor 802 that is configured for trans- or sub-cutaneous implantation via the skin of the patient. Such a sensor may be used for the direct testing of analyte levels in the biological fluid associated with the tissue at or adjacent to the implantation site. This level may be correlated and/or converted to analyte levels in blood or other fluids. The site and depth of insertion may affect the particular shape, components, and configuration of the sensor 802. Examples of suitable sensors for use in the analyte-monitoring systems of the invention are described in United States Patent Application Serial No. 09/034,372.

[0101] The sensor section 800 further comprises a miniature biofuel cell 100, as described herein, that is electrically coupled to the sensor 802 and electrically coupled to a transmitter 804, such as an antenna, for transmitting a signal from the sensor to the receiver-transmitter section 900. Preferably, the miniature biofuel cell 100 is integrated with various electrical components, including the transmitter 804, on an integrated circuit chip 820, such as an organic or a silicon-based integrated circuit, constructed for biological compatibility, such as being mounted on or housed in a biologically compatible material, as previously described. The transmitter, or antenna,

is typically the largest, or longest, component of the sensor section 800 to ensure adequate signal transmission. That is, its length may be on the order of about one-fourth or more of the wavelength of the signal it transmits, such as on the order of that used in cellular telephones. Preferably, the transmitter comprises a carbon fiber that is of the same length as a carbon fiber electrode of the biofuel cell 100, so that the size of the sensor section 802 can be reduced or minimized. The transmitter 804 may take the form of an antenna protruding from the sensor section 800, in a manner similar to that of an antenna that protrudes from a cellular telephone, or it may take form of a typical integrated circuit component, such as a component printed, electrodeposited, or otherwise patterned on an integrated circuit substrate, as previously described.

[0102] Other electrical components may include a potentiostat, a capacitor, a resistor, an amplifier, a converter, such as current-to-voltage or a current-to-frequency converter, control or logic sub-circuitry (such as subcircuitry for the control of the sensor 802 or the cell 100, the control of signal receipt or transmission, or the evaluation of signals from the sensor), and/or the like. The biofuel cell 100 may be used to provide a voltage across the electrodes of the sensor 802, such as via a potentiostat, to charge a capacitor for the storage of signals from the sensor 802, to provide power for relaying a signal from the sensor 802 to the transmitter 804 and transmitting a signal from the transmitter 804 to the receiver-transmitter section 900, and/or the like.

[0103] The biofuel cell 100 is designed to accommodate the various power and energy requirements of the sensor section 800, particularly those of the transmitter 804, which typically consumes the most energy. According to an embodiment of the invention, the biofuel cell can provide about $2\mu\text{W}$ or more of power for an autonomous, three-day, physiological, glucose biosensor-transmitter system having a sub- mm^2 footprint and a sub- mm^3 volume. As the power requirement of the transmitter 804 increases with a square of the distance, d , between it and the receiver-transmitter section 900, preferably this distance is kept to a minimum, so that the biofuel cell 100 and the sensor section 800 are as small as possible or desired. For example, when the duty cycle is about 1:100, this distance may be on the order of up to and including about 20 cm (although longer distances may be possible), and more preferably, up to and including about 5 cm. Preferably, the transmitter 804 of the sensor section 800 is

located as close as possible to the receiver-transmitter section 900, and more particularly, a receiver 902 of the receiver-transmitter section.

[0104] In operation of the analyte-monitoring device 700, the transmitter 804 of the sensor section 800 transmits a signal, representative of the concentration or level of analyte in the subcutaneous tissue, to the receiver-transmitter section 900. The receiver-transmitter section 900 has a receiver 902, communicatively coupled to the transmitter 804, for receiving the signal from the transmitter 804 of the sensor section 800 of the device. The receiver 902 is formed using known receiver and antenna circuitry. The receiver-transmitter section 900 also has a transmitter 904, electrically coupled to the receiver 902, for receiving the signal from the receiver 902 and transmitting or displaying or otherwise processing information from the signal, such as transmitting or displaying the information (such as analyte-concentration information) to the patient, transmitting the information to a remote device 1000, such as a communication device (such as an alarm or a remote display) or a drug delivery device (such as a device adapted to deliver a drug or a medicine to the patient, based on the information, as further described below), or processing the information to evaluate a condition of the patient, for example. While the transmitter 904 is schematically shown in FIG. 9 as an antenna for the transmission of information, merely by way of example, it may take the form of a display, such as a digital read-out display. The receiver-transmitter section 900 may comprise other various electrical components and sub-circuitry to facilitate its functioning, such as the various electrical components described in the above-referenced United States Patent Application No. 09/753,746.

[0105] As mentioned above, the receiver-transmitter section 900 of the device 700 may be used to transmit information to a remote drug delivery device, as represented by remote device 1000 in FIG. 9, via any sufficient communicative coupling between the transmitter 904 and the remote device 1000. Alternatively, as schematically depicted in FIG. 10, the receiver-transmitter section 900 of the device 700 could be replaced by a receiver-delivery section 1100 comprising a receiver 1200, communicatively coupled to the transmitter 804, and a drug reservoir 1300, operatively or electrically coupled to the receiver 1200, in which the receiver 1200, upon receiving a certain signal from the sensor section 800, triggers the delivery of a

drug or a medicine from the drug reservoir to the patient. By way of example, the delivery may be accomplished by way of a drug delivery pump 1250 and delivery conduit 1320, such as biocompatible surgical tubing, each of which is operatively coupled to the drug reservoir 1300, as shown, where the delivery conduit 1320, which
5 may be controlled by a check valve 1310, is connected to a trans- or sub-cutaneous insertion device 1330. In this embodiment, an interim receiver-transmitter section, such as receiver-transmitter section 900 previously described, may be omitted from the device 700, and the device may serve as an analyte-monitoring and treatment device.

10 [0106] For the drug delivery embodiments described above, a suitable drug delivery pump system is a disposable system, as described in a United States Provisional Application Serial No. 60/417,464, of Benjamin M. Rush, entitled "Disposable Pump for Drug Delivery System," which was filed on October 9, 2002, or more preferably, a
15 States Provisional Application Serial No. 60/424,613, of Christopher V. Reggiardo, entitled "Disposable Pump and Actuation Circuit for Drug Delivery," which was filed on November 6, 2002. As the drug delivery pump generally requires a great deal of power, an energy source other than a biofuel cell described herein is needed.

[0107] The autonomous, subcutaneous, analyte-monitoring and/or treatment devices
20 just described can be used for the monitoring and/or treatment of diabetics, where the analyte is glucose and the drug is insulin; for the monitoring and/or treatment of poison victims, such as snake-bite victims, where the drug is a poison antidote, such as a venom antidote; for the monitoring and/or treatment of ischemia, where the analyte is lactate or pyruvate, indicative of bleeding or other stress, and the drug is an
25 appropriate medicament; and for like applications. Alternatively, the autonomous, analyte-measuring device and/or may be cutaneous, or located on the skin, where the sensor is in contact with the skin, and used for applications such as the monitoring and/or treatment of a skin contaminant, such as a nerve gas or other biological- or chemical-warfare agent, where the drug is atropine or some other appropriate antidote
30 or medicine. For a number of such applications, the device could be a wearable monitoring or monitoring and treatment device by virtue of its small size.

[0108] An embodiment of an autonomous, analyte-monitoring and treatment device, which includes a drug delivery system, is now described in relation to a schematic, block-diagram illustration of FIG. 11. In this illustration, a sensor-based drug delivery system 1400 is shown as having a sensor control section 1412, a portion of which is trans- or sub-cutaneously inserted into the patient, namely, an insertion portion of the sensors 1410 that is schematically shown in dashed lines. The system may provide a drug to counteract the high or low level of the analyte in response to the signals from one or more sensors 1410. Alternatively, the system monitors the drug concentration to ensure that the drug remains within a desired therapeutic range. The drug delivery system includes one or more (and preferably two or more) subcutaneously implanted sensors 1410, an on-the-skin sensor section 1412, a receiver/display unit 1414, a data storage and controller module 1416, and a drug administration system 1418. In some cases, the receiver/display unit 1414, data storage and controller module 1416, and drug administration system 1418 may be integrated in a single unit. The sensor-based drug delivery system 1400 uses data from the one or more sensors 1410 to provide necessary input for a control algorithm/mechanism in the data storage and controller module 1416 to adjust the administration of drugs. As an example, a glucose sensor could be used to control and adjust the administration of insulin.

[0109] In this embodiment, sensor 1410 produces signals correlated to the level of the drug or analyte in the patient. The level of the analyte will depend on the amount of drug delivered by the drug administration system. A processor 1420 in the on-the-skin sensor section 1412, as illustrated in FIG. 11, or in the receiver/display unit 1414 determines the level of the analyte, and possibly other information, such as the rate or acceleration of the rate in the increase or decrease in analyte level. This information is then transmitted to the data storage and controller module 1416 using a transmitter 1422 in the on-the-skin sensor section 1412, as illustrated in FIG. 11, or a non-integrated receiver/display unit 1414.

[0110] If the drug delivery system 1400 has two or more sensors 1410, the data storage and controller module 1416 may verify that the data from the two or more sensors 1410 agrees within predetermined parameters before accepting the data as valid. This data may then be processed via the data storage and controller module 1416, optionally with previously obtained data, to determine a drug administration

protocol. The drug administration protocol is then executed using the drug administration system 1418, which may be an internal or external infusion pump, syringe injector, transdermal delivery system (e.g., a patch containing the drug placed on the skin), or inhalation system. Alternatively, the drug storage and controller module 1416 may provide a drug administration protocol so that the patient or another person may provide the drug to the patient according to the profile.

[0111] In one embodiment of the invention, the data storage and controller module 1416 is trainable. For example, the data storage and controller module 1416 may store glucose readings over a predetermined period of time, e.g., several weeks. When an episode of hypoglycemia or hyperglycemia is encountered, the relevant history leading to such event may be analyzed to determine any patterns that might improve the system's ability to predict future episodes. Subsequent data might be compared to the known patterns to predict hypoglycemia or hyperglycemia and deliver the drug accordingly. In another embodiment, the analysis of trends is performed by an external system or by a processing circuit (not shown) in the on-the-skin sensor section 1412 or an analyzer (not shown) in the receiver/display unit 1414 and the trends are incorporated in the data storage and controller 1416. Examples of suitable processing circuits and suitable analyzers are described in the above-referenced United States Patent Application No. 09/753,746.

[0112] According to one embodiment, the data storage and controller module 1416, a processing circuit, and/or an analyzer utilize patient-specific data from multiple episodes to predict a patient's response to future episodes. The multiple episodes used in the prediction are typically responses to a same or similar external or internal stimulus. Examples of stimuli include periods of hypoglycemia or hyperglycemia (or corresponding conditions for analytes other than glucose), treatment of a condition, drug delivery (e.g., insulin for glucose), food intake, exercise, fasting, change in body temperature, elevated or lowered body temperature (e.g., fever), and diseases, viruses, infections, and the like. By analyzing multiple episodes, the data storage and controller module 1416, processing circuit, and/or analyzer can predict the course of a future episode and provide, for example, a drug administration protocol or administer a drug based on this analysis. An input device (not shown) may be used by the patient or another person to indicate when a particular episode is occurring so that, for

example, the data storage and controller module 1416, processing circuit, and/or analyzer can tag the data as resulting from a particular episode, for use in further analyses.

5 [0113] In addition, the drug delivery system 1400 may be capable of providing on-going drug sensitivity feedback. For example, the data from the sensor 1410 obtained during the administration of the drug by the drug administration system 1418 may provide data about the individual patient's response to the drug which can then be used to modify the current drug administration protocol accordingly, both immediately and in the future. An example of desirable data that can be extracted for each patient
10 includes the patient's characteristic time constant for response to drug administration (e.g., how rapidly the glucose concentration falls when a known bolus of insulin is administered). Another example is the patient's response to administration of various amounts of a drug (e.g., a patient's drug sensitivity curve). The same information may be stored by the drug storage and controller module and then used to determine
15 trends in the patient's drug response, which may be used in developing subsequent drug administration protocols, thereby personalizing the drug administration process for the needs of the patient.

Use of the Oxygen Electroreducing Cathode to Assay HbA1c

20 [0114] In an embodiment of the invention, one or more components of biological fuel cell 100 can be used to build a cell that can be operated to assay HbA1c. The HbA1c molecule is a hemoglobin molecule that has been combined with a glucose molecule. Unlike a glucose measurement, which reflects the current blood sugar level of a person, such as a medical patient, an HbA1c measurement can reflect how well a
25 person has been controlling his or her glucose levels over a period of several months. In accordance with an embodiment of the invention, a "desktop" HbA1c assay can be developed.

[0115] The basis for the HbA1c assay of the invention comes from the ability to wire reaction centers of an enzyme, e.g., BOD, to cathode 104. As explained herein, BOD
30 catalyzes the four-electron reduction of oxygen to water. Cathode 104, when

constructed with BOD as the redox enzyme, can operate under physiological conditions and can therefore be used with a biological fluid of a person or other animal to provide an HbA1c measurement.

[0116] Hemoglobin, being the oxygen carrier of blood, reversibly binds oxygen, forming HbO₂. The equilibrium of the reaction, $\text{Hb} + \text{O}_2 \leftrightarrow \text{HbO}_2$, is rapid. Because O₂ is rapidly released by HbO₂ when O₂ is depleted from the solution in an electrochemical cell, the concentration of HbO₂ can be measured coulometrically based on the reaction, $4\text{H}^+ + 4\text{e}^- + \text{HbO}_2 \rightarrow 2 \text{H}_2\text{O} + \text{Hb}$. The concentration of available oxygen in arterial blood is about 8 mM. In a coulometric assay, the red blood cells (optionally captured on Nylon or similar cloth) would be lysed in pH 5 citrate buffer under air, and the HbO₂ would be coulometrically assayed. Because the concentration of O₂ in water in equilibrium with air at 25°C is known to be 0.24 mM, the amount of non-Hb-bound O₂ would be subtracted in calculating the amount of HbO₂. The HbA1c/Hb ratio would be measured by one of the methods (1) – (3) set forth below.

[0117] (1) Magnetic beads that are < 1 μm (available from Bangs Laboratories), on which antibodies against HbA1c would be immobilized, can be mixed with a citrate-solution diluted blood sample. Two measurements would be performed, one on the entire sample, and a second on the re-oxygenated HbA1c bound to the magnetic beads, after their removal to a chamber of an electrochemical cell. Alternatively, the second measurement could be performed on the residual Hb, after the magnetic separation of the bead-bound HbA1c.

[0118] (2) Two samples of the lysed red blood cells in citrate buffer can be coulometrically assayed in two chambers. The total HbO₂ would be measured coulometrically in the first chamber. Immobilized HbA1c-specific antibody would be in the second chamber. Either of the two (HbO or the immobilized antibody) would capture HbA1c without capturing Hb. After rinsing or passage of citrate buffer through the second chamber (e.g., by repeatedly filling through capillary action and touching the edge of the chamber to filter paper), the second chamber would contain only HbA1cO₂. The HbA1cO₂ would be assayed coulometrically based on its electroreduction reaction, $4\text{H}^+ + 4\text{e}^- + \text{HbA1cO}_2 \rightarrow 2 \text{H}_2\text{O} + \text{HbA1c}$. The HbA1c/Hb ratio could then be calculated from the two coulometric measurements.

[0119] (3) This method is like that of method (2) above, except that the two coulometric measurements would be performed in a single chamber. The chamber, which would contain the immobilized HbA1c capture agent, would be filled with a citrate solution of the lysed red blood cells. First, the total HbO₂ would be coulometrically measured. Next, the unbound Hb, but not the bound HbA1c, would be rinsed out, the HbA1c would be re-equilibrated with air, and its amount would be coulometrically measured.

[0120] Thus, in one form of the invention, the assay can comprise a method of determining the ratio of HbA1c to total Hb in blood, the method comprising the steps of obtaining a blood sample; electrochemically determining the total amount of hemoglobin in the sample; electrochemically determining the amount of HbA1c in the sample; and calculating the ratio of HbA1c to total hemoglobin. In a preferred form, the method of electrochemically determining the total amount of hemoglobin in the sample is accomplished by placing the sample in an electrochemical cell in which, at the cathode, a cathode enzyme is bound. Binding may be accomplished using a redox polymer. In this method, it is preferred that the enzyme be a laccase or a BOD which will electrooxidize oxygen bound to the hemoglobin to water. The hemoglobin content is determined from the oxygen content.

[0121] In another form of the invention, the electrochemical determination of HbA1c fraction can be accomplished by one of two methods. In a first method, the A1c-containing fraction of the hemoglobin is separated by physical means, such as by use of an HbA1c-specific antibody. Under appropriate conditions, the HbA1c, then present in the form of HbA1cO₂, can be electrochemically determined by electroreduction of the oxygen (again with an enzyme selected to accomplish the four-electron reduction of oxygen). In a second method, the glycated protein (in the form of a fructosyl amine) can be directly oxidized on crosslinked, poly(N-vinyl imidazole)-based redox polymer films (without an enzyme) of sufficiently positive oxidizing potential. Alternatively, enzymatic electrooxidation of the fructosyl amines can be used for this part of the determination.

[0122] Thus, the invention comprises an electrochemical method for the determination of HbA1c (or a ratio of HbA1c/Hb) comprising the steps of determining from a starting sample, in an electrochemical cell, the total amount of hemoglobin (e.g., by

measuring bound oxygen), separating the HbA1c component from the sample using an HbA1c-capturing agent, and measuring hemoglobin content in the captured or non-captured portion of the sample.

Experimental Examples

5 [0123] The following examples are provided to demonstrate biological fuel cells 100, and particular cathodes 104, that were experimentally produced in accordance with embodiments of the invention. Experimental Example 1 is reported in Mano et al., *An Oxygen Cathode Operating in a Physiological Solution*, J. Am. Chem. Soc. 2002, 124, 6480-6486, and Experimental Example 2 is reported in Mano et al., *On the*
10 *Relationship between the Characteristics of Bilirubin Oxidases and O Cathodes Based on Their "Wiring"*, J. Phys. Chem. B 2002, 106, 8842-8848. The following examples include the chemicals and materials used in the experiment, the techniques used to assemble the electrodes, the results of the experiments, as well as discussions of the results. It should be noted that these experiments are provided herein mainly for
15 illustrative purposes, and should not be construed as placing limitations on the invention.

Experimental Example 1: *M.v.-BOD* On The Cathode

[0124] Chemicals and Materials: Bilirubin oxidase (EC 1.3.3.5) from *M. Verrucaria*, catalase from bovine liver (EC 1.11.1.6), uric acid (sodium salt), spermine
20 (hydrochloride salt), neomycin, gentamycin, 1,4,8,11-tetraazacyclotetradecane (cyclam), L-sodium ascorbate, 4-acetaminophen, NaIO₄, NaCl, NaOH, KCNS, KBr, MgCl₂, CaCl₂, and NaF were purchased from Sigma (St. Louis, MO). Poly(ethylene glycol) (400) diglycidyl ether (PEGDGE) was purchased from Polysciences Inc. (Warrington, PA). A fresh solution of BOD in pH 7.4 20 mM phosphate buffer (PB)
25 was prepared daily. The uric acid was dissolved in dilute NaOH and then neutralized with dilute H₃PO₄ to yield a 10 mM aqueous solution. The electrochemical measurements were performed in phosphate buffered saline (PBS) (pH 7.4 20 mM phosphate-buffered 0.15 M NaCl) except in the experiments where the pH and anion dependence of the steady-state electroreduction of O₂ were studied. In these, borate,
30 citrate, acetate, phosphate, and Tris buffers were employed. All solutions were made with deionized water that was passed through a purification train (Sybron Chemicals

Inc., Pittsburgh, PA). Carbon cloth (Toray TGPB-030) was received, as a sample, from E-TEK (Somerset, NJ). Ultrapure O₂ and argon were purchased from Matheson (Austin, TX).

[0125] Synthesis of the Redox Polymer PAA-PVI-[Os(4,4'-dichloro-2,2'-bipyridine)₂Cl]⁺²⁺: 4,4'-Dinitro-2,2'-bipyridine *N,N'*-dioxide was prepared as described in Anderson, S.; Constable, E. C.; Seddon, K. R.; Turp, E. T.; Baggott, J. E.; Pilling, J. *J. Chem. Soc., Dalton Trans.* 1985, 2247-2250, and Kenausis, G.; Taylor, C.; Rajagopalan, R.; Heller, A. *J. Chem. Soc., Faraday Trans.* 1996, 92, 4131-4135. 4,4'-dichloro-2,2'-bipyridine (dcl-bpy) was synthesized from 4,4'-dinitro-2,2'-bipyridine *N,N'*-dioxide by modifying the procedure of Maerker et al. (see Anderson, S., *supra* and Maerker, G.; Case, F. H. *J. Am. Chem. Soc.* 1958, 80, 2475-2477). Os(dcl-bpy)₂Cl₂ was prepared as follows: (NH₄)₂OsCl₆ and "dcl-bpy were dissolved in ethylene glycol in a 1:2 molar ratio and refluxed under argon for 1 hour (yield 85%). The Os(dcl-bpy)₂Cl₂ was then complexed with the 1:7 polyacrylamide-poly(*N*-vinylimidazole) (PAA-PVI) copolymer and purified as described in Zakeeruddin, S. M.; D. M. Fraser, D. M.; Nazeeruddin, M.-K.; Gratzel, M. *J. Electroanal. Chem.* 1992, 337, 253-256. PAA-PVI-[Os(4,4'-dichloro-2,2'-bipyridine)₂Cl]⁺²⁺ redox polymer was thus synthesized.

[0126] Electrodes: The carbon cloth electrodes were made by the three-step procedure reported in Barton, S. C.; Kim, H.-H.; Binyamin, G.; Zhang, Y.; Heller, A. *J. Phys. Chem.* 2001, 105, 11917-11921. Their substrates were 3 mm-diameter vitreous carbon electrodes mounted in Teflon sleeves. In the first step, the substrates were polished with 0.05 μm Al₂O₃ powder (Buehler, Lake Bluff, IL) rinsed and sonicated for 10 minutes in ultrapure water. The polishing step was repeated until no voltammetric features beyond water oxidation were observed in a 50 mV/s scan in PBS through the 0.2 and 1.0 V range. The electrodes were then dried in an air stream. In the second step, the 350 μm-thick carbon cloth (nominal 78% void fraction, composed of 10 μm diameter fibers) was cut into 4 mm-diameter disks. These were cemented, using conductive carbon paint (SPI, West Chester, PA), to the surface of the substrate electrodes. The substrate bound cloth was made hydrophilic by exposure to a 1 Torr O₂ plasma for 5 minutes. The rotating ring-disk electrodes (RRDE), with 3 mm-diameter vitreous carbon disks and platinum rings were similarly made. In these,

the platinum electrodes were cycled in 0.5 M H₂SO₄ until the voltammograms showed the characteristics of a clean platinum electrode. In the third step, the electrocatalyst was deposited on the carbon cloth. The deposition solution consisted of 10 µL of 10 mg/mL aqueous redox polymer solution, 2 µL of PB, 2 µL of 46 mg/mL BOD in PB, and 2 µL of 7 mg/mL PEGDGE in water. A 5 µL aliquot of the mixed solution was pipetted onto the mounted hydrophilic carbon cloth, which was promptly wetted and penetrated by the solution. The electrodes were cured for at least 18 hours at room temperature before they were used.

[0127] Instrumentation and Cell: The measurements were performed using a bi-potentiostat (CH-Instruments, electrochemical detector model CHI832) and a dedicated computer. The temperature was controlled with an isothermal circulator (Fisher Scientific, Pittsburgh, PA). The dissolved O₂ concentration was monitored with an O₂ electrode purchased from BAS (West Lafayette, IN). The electrodes were rotated using a Pine Instruments rotator (Austin, TX). The measurements were carried out in a water-jacketed electrochemical cell at 37.5°C containing 50 mL of PBS. At the start of the experiments, argon was bubbled through the solution for at least 15 minutes, followed by oxygen. To maintain a fixed volume of solution in the cell, the bubbled gases were pre-saturated with water by passage through a bubbler, which also contained PBS. The potentials were measured versus a commercial Ag/AgCl (3 M KCl) reference electrode. The counter electrode was a platinum wire (BAS). In the coulometric measurements, the scan rate was 1 mV/s.

[0128] BOD Assay: The absorption spectra of the BOD solutions were measured at 25°C with an Agilent 8453 UV-visible spectrophotometer following the procedure of Hirose (see Hirose, J.; Inoue, T.; Sakuragi, H.; Kikkawa, M.; Minakami, M.; Morikawa, T.; Iwamoto, H.; Hiromi, K. *Inorg. Chim. Acta* 1998, 273, 204-212). The concentration of BOD was calculated using its reported molar absorption coefficient of 3870 M⁻¹cm⁻¹ at 610 nm.

[0129] Results: The open-circuit potential of a vitreous carbon electrode on which BOD (without redox polymer) was adsorbed was +360 mV versus Ag/AgCl in pH 7.4 PBS under 1 atm O₂ at 37.5°C or -196 mV versus the potential of the reversible O₂/H₂O under the same conditions. The open-circuit potential of a similar electrode,

but with a thin, adsorbed film of the electrostatic adduct of the redox polymer and BOD, was remarkably higher, +530 mV versus Ag/AgCl, only -26 mV versus the potential of the reversible O_2/H_2O electrode. No spectroscopic evidence was found for complex formation between the copper ions of BOD and the polymer. When the
5 water-soluble copolymer of acrylamide and *N*-vinylimidazole was added to the BOD solution in PB, the spectrum of the enzyme did not change.

[0130] A cyclic voltammogram of the composite wired BOD-coated carbon cloth electrode, with a coating consisting of 44.6 wt % BOD, 48.5 wt % polymer, and 6.9 wt % PEGDGE, under argon at 50 mV/s in PBS at 37.5°C, was produced. The
10 voltammogram is characteristic of a polymer-bound osmium complex with an apparent redox potential of +350 mV versus Ag/AgCl. At 1 mV/s scan rate, the voltammogram exhibited a symmetrical wave, with only slight separation of the oxidation and reduction peaks ($\Delta E_p = 5$ mV). At 50 mV/s the separation was substantially increased ($\Delta E_p = 53$ mV). The width of the peaks at half-height, E_{whm} ,
15 was 90 mV, close to the theoretical width of 90.6 mV for an ideal Nernstian one-electron-transfer reaction. In contrast with wired laccases, where ΔE_p and E_{whm} increased with the PEGDGE weight fraction in the catalyst, ΔE_p and E_{whm} did not vary with the PEGDGE weight fraction in the wired BOD electrodes. As will be shown below, the kinetic limit of current density of the wired BOD electrodes depended,
20 however, on the weight fraction of the PEGDGE crosslinker. Upon 4-hour cycling of the potential at 50 mV/s between 0.0 and +0.5 V versus Ag/AgCl, the heights of the voltammetric peaks of the electrodes rotating at 1000 rpm decreased only by less than 5%, at 37.5°C.

[0131] The reproducibility of the O_2 electroreduction currents of the electrodes
25 rotating at 1000 rpm was $\pm 10\%$ or better both for different batches ($n = 4$) and within batches ($n = 12$). When the electrodes were rotated at 4000 rpm, the reproducibility was only $\pm 28\%$ between the batches and $\pm 20\%$ within the batches.

[0132] Because two-electron BOD-catalyzed electroreduction of O_2 to H_2O_2 might compete with the desired four-electron reduction, production H_2O_2 was tested for
30 using RRDEs having wired BOD carbon cloth disks and platinum rings. If H_2O_2 were produced on the disk, it would have been detected at the ring poised at +0.750 mV

versus Ag/AgCl, the H_2O_2 being electrooxidized to O_2 on the platinum ring at this potential (a similar experiment was performed to investigate the formation of H_2O_2 during the electroreduction of O_2 on disks of RRDE electrodes modified with cytochrome *c*).

5 [0133] When O_2 was electroreduced on the disk at increasing current densities of between 0 and 5 mA/cm^2 , the ring current remained unchanged and was negligibly small, showing that H_2O_2 was not produced on the disk. Furthermore, catalase, which would have decomposed any H_2O_2 that might have been produced into O_2 , had no effect on the ring current, confirming that H_2O_2 was not a byproduct of the
10 electroreduction of O_2 to water. After 10 hours of O_2 electroreduction at approximately 1 mA current, the 50 mL solution of the cell tested negative for H_2O_2 in a colorimetric ABTS-horseradish peroxidase test that would have detected 1 μM H_2O_2 .

[0134] The dependence of the current density I on the square root of the angular
15 velocity of the rotating electrode, $\omega^{1/2}$, was determined. Up to 3500 rpm, where the current density reached 8.8 mA/cm^2 , the current increased linearly with $\omega^{1/2}$ in accordance with the Levich equation, showing that it was O_2 -transport-limited under 1 atm O_2 when the electrode was poised at +300 mV versus Ag/AgCl. Above 3500 rpm, the current density continued to increase with $\omega^{1/2}$, but no longer linearly, until it
20 reached the kinetic limit of 9.1 mA/cm^2 .

[0135] The optimal composition of the electrocatalyst was determined for electrodes rotating at 1000 rpm and poised at +300 mV versus Ag/AgCl. In the first group of experiments, the crosslinker (PEGDGE) was fixed at 6.9 wt %, and the total loading of all film components was fixed at 0.6 mg/cm^2 . The dependence of the current
25 density of BOD through the 20 to 70 wt % range was determined. From 20 to 45 wt %, the current density increased with the weight percentage of BOD, reaching 4.6 mA/cm^2 at 45.2 wt %. Above 50 wt % BOD, the current density declined rapidly. At 60 wt % BOD, precipitation was observed. The precipitation is attributed to the formation of a charge-neutral electrostatic adduct between the cationic polymer and
30 the anionic enzyme ($\text{pI} = 4.1$). In experiments where the weight percentage of the cross-linker was varied, while the BOD to redox polymer weight ratio was fixed at

1:1, the optimal PEGDGE weight percentage was found to be 6.9. The resulting optimal catalyst was composed of 44.6 wt % BOD, 48.5 wt % polymer, and 6.9 wt % PEGDGE at 0.6 mg/cm² total loading. The effect of the total loading on the kinetic limit of the catalytic current was not optimized, because the optimum would have varied with the ratios of the components.

[0136] Unlike in the cases of wired glucose oxidase and of wired laccases, crosslinking by periodate oxidation of the BOD oligosaccharides did not lead to useful wired BOD electrodes, even though BOD contains 6.3 wt % carbohydrate.

[0137] The pH dependence of the steady-state current density of O₂ electroreduction was measured with the electrode poised at +300 mV versus Ag/AgCl in 0.15 M NaCl while the electrode rotated at 1000 rpm. Phosphate, borate, citrate, or Tris was added at 20 mM concentration to maintain the desired pH. The dependence of the current on the pH was determined. The current density increased with pH until it reached a plateau at pH 7.5 and then declined above pH 10.5. In the pH 6-10.5 range, the current density was nearly independent of pH, varying by less than ±10%. Up to pH 9, there was no irreversible change in the current characteristics; above pH 10.5, the drop in the current density was irreversible.

[0138] Because copper-binding anions, particularly halide anions, inhibit the laccases and because blood contains 0.14 M chloride, the effect of added anions was investigated. In these experiments, the electrode rotated at 1000 rpm and was poised at +300 mV versus Ag/AgCl in a pH 7.4, 20 mM phosphate buffer solution. The current density was nearly independent of the concentration of chloride, added as NaCl, through the 0-1 M range. Above 1.5 M NaCl concentrations, a decline in the current density was, nevertheless, observed. When bromide was added, the current density declined monotonically as the KBr concentration was raised from 0 and 1 M. At 1 M KBr, the current density was about 25% lower than in the absence of bromide. A steeper decline was again observed at >1.5 M KBr concentration. Adding of fluoride (as NaF) inhibited the electroreduction of O₂, about 30% of the current density being lost when the concentration of fluoride was raised from 0 to 0.5 M and about 90% being lost when the concentration was further raised to 1 M. Thiocyanate, added as KCNS, strongly inhibited the electroreduction, the current density dropping

to 0 already at 0.25 M KCNS. The maximum current density was about the same when the solutions were buffered at pH 7 with Tris, acetate, or phosphate.

[0139] The temperature dependence of the current density of the electrode poised at +300 mV versus Ag/AgCl, rotating at 1000 rpm in PBS under 1 atm O₂ was determined. The current density increased with temperature up to 60°C and then declined rapidly. The increase was reversible only up to 50°C, the enzyme being denatured at higher temperatures. The Arrhenius plot (not shown) of the temperature dependence yielded an activation energy of $E_{\text{act}} = 28.2$ kJ/mol. The observed activation energy for the denaturing of the enzyme was 77 kJ/mol.

10 [0140] When rotating at 4000 rpm, where the shear stress on the rim on the fiber cloth was 0.7 N/m², the electrodes were mechanically unstable. For this reason, their stability was tested at 300 rpm, where the current was O₂ transport limited. At 300 rpm, the shear stress acting on the rim of the 4 mm diameter electrode was 1.4×10^{-2} N/m². The time dependence of the current density of an electrode poised at +300 mV
15 versus Ag/AgCl rotating at 300 rpm in PBS under 1 atm O₂ at 37.5°C was determined. In the first six days of operation, the current dropped by less than 10 % per day. The initial 2.4 mA/cm² current density dropped to 1.3 mA/cm² after six days of continuous operation. After storage of the dry electrodes for 1 month at 4°C under air, 95 ± 3 % of the initial current density was retained. The presence of electrooxidizable blood
20 constituents did not harm the electrodes. A transient 5 % increase in the current density was observed when either 0.1 mM ascorbate or 0.1 mM ascorbate and 0.17 mM acetaminophen was added, and a transient 25 % increase in current density was observed with 0.48 mM urate in the solution.

[0141] Potentials: Xu et al. measured spectrophotometrically the redox potential of an
25 aerated pH 5.3 solution of recombinant *M. Verrucaria* BOD at 20 °C, reporting +260 mV versus Ag/AgCl or -440 mV relative to the potential of the reversible O₂/H₂O electrode at the same pH. In pH 7.8 50 mM Tris buffer, others have reported a potential of +373 mV versus Ag/AgCl at ambient temperature, -174 mV versus the reversible O₂/H₂O electrode potential at this pH. The open-circuit potential of the O₂
30 electrode made by adsorbing BOD on vitreous carbon was +360 mV versus Ag/AgCl under 1 atm O₂ at 37.5°C and at pH 7.4, consistent with the latter value. This potential was -196 mV versus that of the reversible O₂/H₂O electrode under these conditions.

The open circuit potential of the wired BOD electrode, made by cross-linking the electrostatic adduct of BOD, a polyanion above pH 4.1, and a redox polycation, on carbon cloth, was 530 mV versus Ag/AgCl, only 26 mV below that of the reversible O_2/H_2O electrode, at pH 7.4 under 1 atm O_2 and at 37.5°C. Two redox polycations
5 that can be used here are shown in FIGS. 6A and 6B. The wiring of the BOD caused a remarkable increase in potential. The redox potential of the PAA-PVI-[Os(4,4'-dichloro-2,2'-bipyridine) $_2$ Cl] $^{+/2+}$ wire (shown in FIG. 6) was +350 mV versus Ag/AgCl or -180 mV versus the pH 7.4 open-circuit potential of the wired BOD electrode under 1 atm O_2 .

10 [0142] Voltammetric Characteristics: The slight separation of the voltammetric peak heights at 1 mV/s scan rate is indicative of a reversible surface-bound couple. From the linear dependence of the peak heights on the scan rate, the redox couples of the polymer were determined to be surface-confined. The voltammetric peaks were narrower and less separated than those in the earlier PVI-Os(tpy)(dme-bpy) $^{2+/3}$ -based
15 laccase electrode, where ΔE_p was 120 mV. The difference is attributed to faster charge transport through the wire of this study. Repetitive cycling over a 4-hour period at 37.5°C did not change the shape of the voltammograms of the electrodes rotating at 1000 rpm, and their peak currents decreased only by less than 5 %.

[0143] Reproducibility: When the electrodes rotated at 1000 rpm, the apparent batch-to-batch reproducibility, as well as the within-the-batch reproducibility, of the O_2
20 electroreduction currents was better than $\pm 10\%$. This reproducibility does not necessarily imply that the composite catalysts were identical within $\pm 10\%$, because at 1000 rpm the current was limited by O_2 transport, not by the kinetics of the electrocatalyst. When the electrodes were rotated at 4000 rpm, where the currents
25 were already limited by the kinetics of the catalytic films, but the electrodes were already mechanically unstable, the reproducibility was only $\pm 28\%$ between the batches and $\pm 20\%$ within the batches.

[0144] Composition: The optimal enzyme-to-polymer weight ratio was near 1:1. At a lower weight fraction of enzyme, the current was limited by the BOD-catalyzed rate of
30 O_2 reduction. When the weight fraction of enzyme was higher, the current was limited by the electronic resistance of the film, the redox polymer being an electron conductor and the enzyme an insulator. Above 60 wt % BOD, where the electrostatic adduct

precipitated, the increased resistance resulted in increased separation of the voltammetric peaks. The observed optimal weight ratio is that of the composition where the upper limits of three currents are equal, a first current based on the flow of electrons from the electrode to the redox polymer, a second current based on the flow of electrons from the redox polymer to the BOD, and a third current based on the flow of electrons from the BOD to O_2 . The optimal ratio decreases when the maximum turnover rate of the enzyme is higher and decreases when electrons diffuse more rapidly through the redox polymer. The ratio also depends on the nature of the bond between the wire and the enzyme, which determines the maximum electron current from the redox polymer to BOD. In the absence of bonding, the BOD and the redox polymer would phase-separate, the entropy of mixing of two macromolecules being too low prevent their separation. As discussed above, intimate contact between the electrostatically bound BOD and its wire lowers the kinetic resistance for electron transfer from the wire to BOD.

[0145] Crosslinking reduces the segmental mobility on which the electron conduction in the redox polymer films depends. Because electrons diffuse as they are transferred when reduced and oxidized redox centers collide, the highest electron diffusivities are being reached when the film is not crosslinked. However, in absence of crosslinking, the films dissolve, and when inadequately crosslinked, they are sheared off the rotating electrodes. With 6.9 wt % PEGDGE cross-linker, the films were mechanically stable at 300 rpm where the maximum shear stress at the rims of the electrodes was $1.4 \times 10^{-2} \text{ N/m}^2$. At this angular velocity, the current density was 2.4 mA/cm^2 .

[0146] Polarization: Electroreduction of O_2 started at the open-circuit potential of the wired BOD electrode, +530 mV versus Ag/AgCl. When the electrode rotated at 4000 rpm where, as will be shown below, the current was no longer O_2 -transport-limited, the current density was 6.8 mA/cm^2 at +380 mV versus Ag/AgCl (-176 mV versus the potential of the reversible O_2/H_2O electrode at the same pH) and the current density reached 9.1 mA/cm^2 at 300 mV versus Ag/AgCl, -276 mV versus the reversible potential. The value of 6.8 mA/cm^2 at -176 mV versus the potential of the reversible O_2/H_2O electrode represents a more than 13-fold increase over current density reported by Tsujimura et al., (see Tsujimura, S.; Tatsumi, H.; Ogawa, J.; Shimizu, S.;

Kano, K.; Ikeda, T. *J. Electroanal. Chem.* 2001, 496, 69-75), whose solution was not a physiological buffer, and whose cathodes operated only for a few hours.

[0147] Mass Transport and Kinetics: The Levich-Koutecky plot for electrode rotating at an angular velocity ω demonstrates that the Levich equation $I = 0.62 nFAcD^{2/3}\nu^{-1/6}\omega^{1/2}$ is rigorously obeyed up to 3500 rpm, where the current density is 8.8 mA/cm². The correspondence between the measured and the predicted currents is exact for the O₂ diffusivity $D = 2.4 \times 10^{-5}$ cm²/s¹, the O₂ solubility $c = 1.07 \times 10^{-6}$ mol/cm³, and the kinematic viscosity $\nu = 0.091$ cm²/s¹ of the 0.15 M NaCl solution at 37.5°C when n , the number of electrons electroreducing the O₂, equals 4 and the area A is 0.126 cm². Above 3500 rpm, the current is controlled by the kinetics of the electrocatalytic reaction. When the electrode rotates at 4000 rpm and the current is kinetically controlled, the measured Tafel slope is -122 mV/decade, and the theoretical for O₂ electroreduction at 37.5°C.

[0148] Absence of Inhibition in Physiological Solution: The pH dependence of the current density of the wired BOD electrode differed from the pH dependence of the maximal turnover rate V_{\max} of the dissolved enzyme. When the enzyme is dissolved, V_{\max} was high only through the pH 6-8 range. V_{\max} declined rapidly at both higher and lower pH, only one-third of V_{\max} being retained at pH 9.26. In contrast, the wired BOD electrode retained its high current density through the pH 6-10 range. Importantly, the variation of the current was negligibly small within the pH 7.35-7.45 range of normal human arterial blood. Above pH 10.5, the electrode was irreversibly damaged because of enzyme denaturation. The observed damage above pH 10.5 is consistent with results of Samejima et al., who found, by tracking the circular dichroism as a function of pH, that the enzyme is denatured upon ionization of its tyrosine residues. The voltammetric characteristics of the redox polymer did not change up to pH 11.

[0149] Laccases are strongly inhibited by halide anions, including the chloride anion, because these bind with their catalytic type II Cu centers and prevent electron transfer from their type I Cu to their type III Cu clusters. The current density of the wired laccase electrodes declined at pH 5 by 60% when the chloride concentration was raised from 0 to 0.1 M. In contrast, the current density of the wired BOD electrode

declined only by 6%. The loss remained small even in 1 M NaCl at pH 7.4 (FIG. 10). Other copper-binding anions inhibited the electroreduction of O₂, with inhibition declining in the order CNS⁻ >> F⁻ >> Br⁻ > Cl⁻. This order is only in partial agreement with the order CNS⁻ > F⁻ >> Cl⁻ > Br⁻ of solution-phase inhibition of the free enzyme reported by Hirose et al. (see Hirose, J.; Inoue, T.; Sakuragi, H.; Kikkawa, M.; Minakami, M.; Morikawa, T.; Iwamoto, H.; Hiromi, K. *Inorg. Chim. Acta* 1998, 273, 204-212) for BOD and by Xu et al. (see Xu, F.; Shin, W.; Brown, S. H.; Walhleithner, J. A.; Sundaram, U. M.; Solomon, E. I. *Biochim. Biophys. Acta* 1996, 1292, 303-311 and Xu, F. *Biochemistry* 1996, 35, 7608-7614) for laccases. Significantly, the inhibition of the wired BOD cathode by chloride at its 0.096-0.106 M concentration in normal human blood was so small that physiological variation in chloride concentration will not affect the O₂ electroreduction current. The electrode differed in this respect from the dissolved BOD-based cathode of Tsujimura et al., the current of which depended strongly on the concentration of KCl in the 0-0.1 M range. The observed partial loss of O₂ electroreduction current at very high chloride concentration (>1.5 M NaCl) is not attributed to specific binding of chloride to copper centers of BOD. Its likely cause is the screening of the charges of the electrostatically bound polycationic and polyanionic segments of the cross-linked redox polymer-BOD adduct at high ionic strength, causing their dissociation and making the wiring of the enzyme ineffective.

[0150] Temperature Dependence: The O₂ electroreduction current increased with the temperature up to 60°C when the rate of increase was about 10°C/h¹ and declined rapidly when the temperature exceeded 60°C. The decline is attributed to the denaturation of the enzyme. The apparent stability of the wired enzyme electrode was better than that of the dissolved enzyme, for which an optimal temperature of 40°C was reported. The apparent activation energy for O₂ electroreduction was $E_{\text{act}} = 28.2$ kJ/mol¹ for the pH 7.4 solution with the electrode rotating at 1000 rpm under 1 atm O₂, where the current was O₂ transport controlled. Because the current was O₂-transport-limited at 1000 rpm, the 28.2 kJ/mol¹ value represents the activation energy for diffusion of oxygen in the solution. The 77 kJ/mol¹ activation energy for current loss is similar to that for the thermal denaturation of other enzymes.

[0151] Stability: At high angular velocity (>1000 rpm), the electrode was mechanically unstable, its catalytic film being sheared off. When the electrode, poised at +300 mV versus Ag/AgCl, was rotated at 300 rpm under 1 atm O₂ at 37.5 °C, it lost less than 10 % of its current per day of continuous operation for 6 days. The wired
5 BOD electrode was far more stable than suggested by Tanaka's study of the stability of the dissolved enzyme, showing loss of half the activity after 1 hour in phosphate buffer at 37°C (see Tanaka, N.; Murao, S. *Agric. Biol. Chem.* 1982, 46, 2499-2503). It was also more stable than that of an immobilized BOD electrode used in the clinical
10 monitoring of the concentration of bilirubin. The half-life of the clinical bilirubin-monitoring electrode was much shorter than that of the cathode of this study, only 17 hours at 37°C and 8 hours at 40°C.

[0152] The most readily cathode-electrooxidized constituents of blood, urate, ascorbate and acetaminophen, at their physiological concentrations, did not damage the cathode poised at +300 mV/Ag/AgCl in PBS buffer at 37.5°C. When 0.1 mM ascorbate was
15 added, or 0.1 mM ascorbate and 0.17 mM acetaminophen were added, the current transiently decreased by 5 %, and when 0.48 mM urate was added, the decrease was 25 %. While Binyamin et al. showed that the electrooxidative polymerization of urate in a redox polymer film with a higher density of cationic sites and thus a higher urate concentration in the film caused degradation of its electrocatalytic properties, no such
20 damage was observed in the present films (see Binyamin, G.; Chen, T.; Heller, A. *J. Electroanal. Chem.* 2001, 500, 604-611).

[0153] Conclusion: In Experimental Example 1, the first electrode on which O₂ is electroreduced to water under physiological conditions at a current density of 9.1 mA/cm² and at a potential -0.26 V relative to the reversible potential of the O₂/H₂O
25 electrode, is described. The electrode has no leachable components, making it suitable for use in flow systems, and with a yet-to-be-added, thin bioinert film, for use in animals. The electrode could well serve as the cathode of a miniature biofuel cell that might power implanted sensors and actuators for about 1 week.

Experimental Example 2: *T.t.*-BOD On The Cathode

30 [0154] Chemicals and Materials: BOD (EC 1.3.3.5, 1.3 U/mg¹) from *Trachyderma tsunodae* was a gift from Amano, Lombard, IL. NaCl, NaOH, KCNS, KBr, MgCl₂,

CaCl₂, and NaF were purchased from Sigma, St. Louis, MO. Poly(ethylene glycol) (400) diglycidyl ether (PEGDGE) was purchased from Polysciences Inc. (Warrington, PA). A fresh solution of BOD in pH 7.4 20 mM phosphate buffer (PB) was prepared daily. The uric acid was dissolved in dilute NaOH then neutralized with dilute H₃PO₄ to yield a 10 mM aqueous solution. The electrochemical measurements were performed in pH 7.4 phosphate buffered saline (PBS, 20 mM phosphate, 0.15 M NaCl) except in the experiments where the pH and anion dependences of the steady-state, O₂ electroreduction currents were determined. In these, borate, citrate, acetate, phosphate and Tris buffers were employed. All solutions were made with de-ionized water, passed through a purification train (Sybron Chemicals Inc, Pittsburgh, PA). Carbon cloth (Toray TGPB-030) was received, as a sample, from E-TEK (Somerset, NJ). Ultra-pure O₂ and argon, were purchased from Matheson (Austin, TX). The synthesis of the BOD-wiring redox polymer PAA-PVI-[Os(4,4'-dichloro-2,2'-bipyridine)₂Cl]⁺²⁺ was previously reported (see Mano, N.; Kim, H.-H.; Zhang, Y.; Heller, A. *J. Am. Chem. Soc.* 2002).

[0155] Carbon Cloth Electrodes: The carbon cloth electrodes were made by the three-step procedure reported in Barton, S. C.; Kim, H.-H.; Binyamin, G.; Zhang, Y.; Heller, A. *J Phys. Chem.* 2001, 105, 11917, and Mano, N.; Kim, H.-H.; Zhang, Y.; Heller, A. *J. Am. Chem. Soc.* 2002. A deposition solution was prepared by mixing 10.3 µL of a 10 mg/mL¹ aqueous redox polymer solution, 2 µl of PBS, and 1.7 µL of 55 mg/mL¹ BOD in PBS and 2 µl of 7 mg/mL¹ PEGDGE in water. A 5 µl aliquot of the mixed solution was pipetted onto the mounted hydrophilic carbon cloth, which was promptly wetted and penetrated by the solution. The electrodes were cured for at least 18 hours at room temperature before they were used.

25 [0156] Carbon Fiber Electrodes: Prior to coating, the 7 µm-diameter fibers (0.0044 cm²) were made hydrophilic by exposure to 1 Torr O₂ plasma for 3 minutes. The cathodic catalyst consisted of the crosslinked adduct of 44.4 wt % Tt-BOD, 49 wt % redox polymer, and 6.6 wt % PEGDGE.

[0157] Instrumentation and Cell: The measurements were performed using a bipotentiostat (CH-Instruments, Austin, TX, Model #CHI832) and a dedicated computer. The temperature was controlled with an isothermal circulator (Fisher Scientific, Pittsburgh, PA). The dissolved O₂ concentration was monitored with an

oxygen O₂-electrode purchased from BAS (West Lafayette, IN). The electrodes were rotated using a Pine Instruments Rotator (Austin, TX). The measurements were carried out in a water-jacketed electrochemical cell at 37.5°C containing 50 mL PBS. At the start of the experiments argon was bubbled through the solution for a least 15 min, followed by oxygen. To maintain a fixed volume of solution in the cell the bubbled gasses were pre-saturated with water by passage through a bubbler, which also contained PBS. The potentials were measured versus a commercial Ag/AgCl (3 M KCl) reference electrode. The counter electrode was a platinum wire (BAS, West Lafayette, IN). In the coulometric measurements the scan rate was 1 mV/s¹.

10 [0158] BOD Assay: The absorption spectra of the BOD solutions were measured at 25°C with an Agilent 8453 UV-Visible spectrophotometer following the procedure of Amano (Lombard, IL).

[0159] Results: The open-circuit potential of the vitreous carbon electrode on which *Tt*-BOD (without redox polymer) was adsorbed was +440 mV versus Ag/AgCl in pH 7.4 PBS under argon at 37.5°C (-116 mV versus the potential of the reversible O₂/H₂O electrode). The open-circuit potential of a similar electrode, but with a thin adsorbed film of the electrostatic adduct of the redox polymer and *Tt*-BOD, was remarkably higher, +530 mV versus Ag/AgCl (-26 mV versus the potential of the reversible O₂/H₂O electrode). No spectroscopic evidence was found for complex formation between the Cu⁺²⁺ ions of BOD and the redox polymer. When the water-soluble copolymer of acrylamide and *N*-vinylimidazole was added to a solution of *Tt*-BOD in PBS, the spectrum of the enzyme did not change.

[0160] A cyclic voltammogram of the composite wired *Tt*-BOD coated carbon cloth electrode, with a coating consisting of 44.4 wt % BOD, 49 wt % polymer and 6.6 wt % PEGDGE, under argon at 50 mV/s¹ in PBS buffer at 37.5°C, was produced. The voltammogram was characteristic of the Os complex bound to the redox polymer, with an apparent redox potential of + 350 mV versus Ag/AgCl. At 1 mV/s¹ scan rate the voltammogram exhibited a symmetrical wave, with a 25 mV separation (ΔE_p) of the oxidation and reduction peaks. At 50 mV/s¹ the separation increased to 110 mV. The width of the peaks at half height, E_{whm} , was 113 mV, whereas in the wired *Mv*-BOD it was 90 mV, close to the theoretical width of 90.6 mV for an ideal Nernstian, one-electron-transfer reaction. As observed earlier in wired laccases, but not in wired *Mv*-

BOD, ΔE_p and E_{whm} increased with the PEGDGE weight fraction in the catalyst. Upon 4-hour cycling of the potential at 50 mV/s¹ between 0.0 V and +0.5 V versus Ag/AgCl, the heights of the voltammetric peaks of the electrodes rotating at 1000 rpm decreased only by less than 6 % at 37.5°C.

5 [0161] The reproducibility of the O₂ electroreduction currents of electrodes rotating at 1000 rpm under air, or under 1 atm O₂, was ± 10 % or better, both for different batches (n=4) and within batches (n=12). When the electrodes were rotated at 4000 rpm the reproducibility of their currents was ± 15 % between batches and ± 11 % within batches.

10 [0162] Because two-electron BOD-catalyzed electroreduction of O₂ to H₂O₂ might compete with the desired four-electron reduction, the solutions were tested for accumulation of H₂O₂. No trace of H₂O₂ was detected when they were assayed by established procedures.

[0163] The dependence of the current I on the square root of the angular velocity of the rotating electrode, $\omega^{1/2}$, was determined. Up to 3000 rpm, where the current density reached 2.74 mA/cm², it increased linearly with $\omega^{1/2}$, precisely as predicted by the Levich equation, showing that the current was O₂-transport-limited in air when the electrode was poised at + 300 mV versus Ag/AgCl. Above 3000 rpm the current continued to increase with $\omega^{1/2}$, but no longer linearly, until it reached 2.9 mA/cm².
15 Under 1 atm O₂, at 1000 rpm, the current density reached 3.5 mA/cm², 30 % less than reported for the *Mv*-BOD cathode, under the same conditions. Under 1 atm O₂ and at 4000 rpm, where the current density was no longer mass transport limited, the current density was 4.6 mA/cm² at +380 mV versus Ag/AgCl and reached its kinetic limit of 6.25 mA/cm² at 300 mV versus Ag/AgCl. The kinetic limit of the *Tt*-cathode was
20 approximately 30 % lower than that of the *Mv*-cathode (9.1 mA/cm²).
25

[0164] The optimal composition of the electrocatalyst was determined for electrodes rotating at 1000 rpm and poised at + 300 mV versus Ag/AgCl. In the first group of experiments, the crosslinker (PEGDGE) weight percentage was fixed at 6.6 wt %, and the total loading of all film components was fixed at 0.6 mg/cm². The dependence of the current density on the wt % of *Tt*-BOD through the 20 to 60 wt % range was
30 determined. Between 10 wt % and 45 wt %, the current density increased with the wt

- 5 % of *Tt*-BOD, reaching 3.5 mA/cm² at 44.9 wt %. Above 47 wt % *Tt*-BOD, the current density declined rapidly. At 50 wt % *Tt*-BOD, the adduct of the enzyme (isoelectric point pH 4.1) and the redox polymer, a polycation, precipitated. The precipitation was similar to that observed in the case of GOx and other polyanionic enzymes, and is attributed to the formation of an electrostatic adduct between the polycationic polymer and the polyanionic enzyme. Above 55 wt % BOD, where the electrostatic adduct precipitated, the separation of the voltammetric peaks increased. These results differed sharply from those for *Mv*-BOD, where precipitation was observed only above 60 wt % and where the decline in current density above 60 wt % was not as sharp. In experiments where the weight percentage of the crosslinker was varied with the *Tt*-BOD to redox polymer weight ratio fixed at 1:1.1, the optimal PEGDGE wt % was 6.6. Thus, at 0.6 mg/cm² total loading, the optimized catalyst was composed of 44.4 wt % *Tt*-BOD, 49 wt % redox polymer, and 6.6 wt % PEGDGE. Because it depended on the composition, the total loading was not optimized.
- 15 [0165] The pH-dependence of the steady state current density of O₂ electroreduction was measured with the electrode poised at +300 mV versus Ag/AgCl in 0.15 M NaCl while the electrode rotated at 1000 rpm. Phosphate, borate, citrate or Tris were added at 20 mM concentration to maintain the desired pH. The current density increased with pH until it reached a plateau at pH 7.5, then declined slightly above pH 10.5. In the pH 6 to 10.5 range, the current density was nearly independent of pH, varying by less than ±10 %. Up to pH 10.5, there was no irreversible change in the current characteristics, and above pH 11, the drop in the current was irreversible. The window of operation of the *Tt*-BOD cathode was up-shifted relative to that of *Mv*-BOD, from 5-10 to 6-10.5.
- 25 [0166] Because copper-binding anions, particularly halide anions, inhibit the laccases and because serum and other physiological fluids contain 0.14 M chloride, the effect of added anions was investigated. In these experiments, the electrode was rotated at 1000 rpm while it was poised at + 300 mV versus Ag/AgCl in the pH 7.4 20 mM phosphate buffer solution. The current density was nearly independent of the concentration of NaCl through the 0-1 M range. As found also in the case of *Mv*-BOD, the current density declined above 1.5 M NaCl. When the concentration of KBr was raised from 0 and 1 M, the current density declined monotonously; at 1 M KBr it
- 30

was approximately 20 % lower than at 0 M KBr. A steeper decline was again observed at >1.5 M KBr concentration. Adding of fluoride (as NaF) inhibited the electroreduction of O₂, approximately 30 % of the current density being lost when the concentration of fluoride was raised from 0 to 0.25 M, and 100 % being lost when the concentration was further raised to 0.5 M. Thiocyanate, added as KCNS, strongly inhibited the electroreduction, the current density dropping to nil already at 0.135 M KCNS. The maximum current density was about the same when the solutions were buffered at pH 7 with Tris, acetate or phosphate.

[0167] The temperature dependence of the current density of the electrode poised at +300 mV versus Ag/AgCl, rotating at 1000 rpm in PBS under 1 atm O₂, was determined. The current density increased with temperature up to 40°C, then declined rapidly above 55°C. With *Mv*-BOD, the current density increased up to 60°C, then declined rapidly. For both *Mv*- and *Tt*-BOD enzymes, the increase was reversible only up to 50°C, the enzymes being denatured at higher temperatures. For *Tt*-BOD, the Arrhenius plot of the temperature dependence of the current yielded an activation energy of $E_{\text{act}} = 34.3 \text{ kJ/mol}^1$. The observed activation energy for the thermal denaturing of the enzyme was 88.2 kJ/mol¹.

[0168] Repetitive cycling over a 4-hour period at 37.5°C in air or under 1 atm O₂ did not change the shape of the voltammograms of electrodes rotating at 1000 rpm, their peak currents decreasing only by less than 5 %.

[0169] Consistently with earlier results, the carbon cloth electrodes rotating at 4000 rpm (shear stress on the rim 0.7 N/m²) were mechanically unstable. For this reason, the extended stability tests were performed at 300 rpm, where the current was O₂-transport-limited. At this angular velocity, the shear stress acting on the rim of the 4 mm-diameter electrode was 1.4×10⁻² N/m². The time dependence of the current density of an electrode poised at + 300 mV versus Ag/AgCl, rotating at 300 rpm in PBS under 1 atm O₂ at 37.5°C, was determined. The current dropped by about 5 % per day, the current density declining from 1.9 mA/cm² to 1.4 mA/cm² after six days of continuous operation. After storage of the dry electrodes for three weeks at 4°C under air, 95 ± 3 % of the initial current density was retained.

[0170] The presence of electrooxidizable serum constituents did not harm the electrodes. A transient 5 % increase in the current density was observed when either 0.1 mM ascorbate or 0.1 mM ascorbate and 0.17 mM acetaminophen was added, and a transient 18 % increase in current density was observed with 0.48 mM urate in the solution.

[0171] The polarization curves of miniature carbon fiber cathodes (7 μm in diameter, 2 cm in length) modified with wired *Mv*-BOD or with wired *Tt*-BOD in a quiescent air solution at 37.5°C in PBS were compared. On the *Mv*-BOD fiber, O_2 was electroreduced at + 0.25 V versus Ag/AgCl at a current density of 0.73 mA/cm^2 . On the *Tt*-BOD fiber, O_2 was electroreduced at + 0.3 V versus Ag/AgCl at 0.88 mA/cm^2 .

[0172] Open-circuit potentials of the non-wired BOD electrodes under argon: The open-circuit potential of the electrode made by adsorbing non-wired *Tt*-BOD on vitreous carbon, is, under argon, +440 mV versus Ag/AgCl, or -116 mV versus the potential of the reversible $\text{O}_2/\text{H}_2\text{O}$ electrode, while that of *Mv*-BOD is +360 mV versus Ag/AgCl, or -196 mV versus the potential of the reversible $\text{O}_2/\text{H}_2\text{O}$ electrode. In the absence of redox polymer, the only redox center of BOD exchanging electrons with the carbon electrode is the type I $\text{Cu}^{+/2+}$ center. This center, unlike the cluster of type II and type III $\text{Cu}^{+/2+}$ centers, is close to the periphery of the globular proteins of the two BODs. The type I $\text{Cu}^{+/2+}$ center of *Mv*-BOD differs from that of *Tt*-BOD in the axial amino acid residue of its $\text{Cu}^{+/2+}$ center. In *Mv*-BOD, the amino acid is methionine; while in *Tt*-BOD, it is phenylalanine. In the F463 M laccase, mutant replacement of the non-complexing, axial phenylalanine by the weakly complexing methionine decreases the redox potential of the type I $\text{Cu}^{+/2+}$ center by 100 mV. In laccases, the redox potential of the type I $\text{Cu}^{+/2+}$ center decreases by approximately 100 mV when it is four-coordinated rather than three-coordinated. It is believed that the higher redox potential of *Tt*-BOD relative to that of *Mv*-BOD can be attributed to the replacement of the methionine by phenylalanine in the type I $\text{Cu}^{+/2+}$ center.

[0173] Dependence of the potential of the type I BOD $\text{Cu}^{+/2+}$ centers on pH in the absence of O_2 : For a typical Nernstian electrode reaction in which a proton is consumed upon oxidation, the potential is up-shifted at 25°C by 59 mV when the pH is decreased by one unit. The redox potential of the type I $\text{Cu}^{+/2+}$ of *Tt*-BOD, the centers of which are titrated with $\text{Li}_2[\text{Co}(2)(2,6\text{-pyridine-dicarboxylate})_2]$, at 25°C has

been measured under anaerobic conditions. In pH 6.8, 50 mM phosphate buffer, the potential was +400 mV versus Ag/AgCl, and in pH 5.0, 0.2 M acetate buffer, it was +442 mV versus Ag/AgCl. The redox potentials of the copper proteins azurin and rusticyanin also increase as the pH is decreased. In contrast, the redox potentials of *Mv*-BOD decrease as the pH is lowered, possibly because of a structural change leading to a change in the coordination of the $\text{Cu}^{+/2+}$.

[0174] Open-circuit potentials of the wired BOD electrodes under 1 atm O_2 : Because in both *Mv*-BOD and *Ti*-BOD the electroreduced O_2 is reversibly bound to the cluster of type II and type III $\text{Cu}^{+/2+}$ centers, this cluster is poised at or near the potential of the reversible $\text{O}_2/\text{H}_2\text{O}$ electrode. At open-circuit potential, where no current flows, it is not required that each of the four electrocatalytic reaction steps be fast. Specifically, it is not necessary that the redox potentials (which are the potentials when the concentrations of the oxidized and the reduced species are equal) increase in each of the following steps: (a) electron transfer from the electrode to $\text{Os}^{2+/3+}$ centers of the redox polymer; (b) electron transfer from the $\text{Os}^{2+/3+}$ centers to the type I $\text{Cu}^{+/2+}$ centers; (c) electron transfer from the type I $\text{Cu}^{+/2+}$ centers to the type II and the type III $\text{Cu}^{+/2+}$ center-comprising clusters; and (d) electron transfer from the clusters to their bound O_2 molecules. When no current flows, each of the centers can increase or decrease its potential, until the potentials are the same, by adjusting the concentration ratio of its oxidized and reduced species, $[\text{Os}^{2+}]:[\text{Os}^{3+}]$ or $[\text{Cu}^{+}]:[\text{Cu}^{2+}]$. For this reason the open-circuit potentials of both the wired *Mv* and the *Ti* cathodes are, under 1 atm O_2 , close to (within less than 30 mV of) the potential of the reversible $\text{O}_2/\text{H}_2\text{O}$ electrode at pH 7.4.

[0175] Polarization: After the redox centers poise themselves near the open-circuit potential by adjusting their $[\text{Os}^{2+}]:[\text{Os}^{3+}]$ or $[\text{Cu}^{+}]:[\text{Cu}^{2+}]$ ratio, the concentration of one or more of the electron donors or acceptors can be so far reduced that the reaction rate, which is the current, becomes very small. In the four-step cascade, this will be avoided, and the overall rate will remain high, when the $[\text{Os}^{2+}]:[\text{Os}^{3+}]$ and the $[\text{Cu}^{+}]:[\text{Cu}^{2+}]$ ratios of each of the centers is not much larger or much smaller than 1. When the ratio is not too far from 1, the potential of the redox center is, by definition, near its Nernstian redox potential. Thus, the current will be high when the redox potentials of the centers are in the order $\text{O}_2/\text{H}_2\text{O} > (\text{type II and type III}) \text{Cu}^{+/2+}$ cluster

- > type I $\text{Cu}^{+/2+}$ center > wire $\text{Os}^{2+/3+}$ > electrode. The maximum current, which is the short circuit current, is reached when the rates of the four electron-transfer steps are equal. The equalization of the rates necessitates, however, $[\text{Os}^{2+}]:[\text{Os}^{3+}]$ and $[\text{Cu}^+]:[\text{Cu}^{2+}]$ ratios somewhat different than 1, because the centers differ in their self-exchange rates and because the concentration of $\text{Os}^{2+/3+}$ differs from that of the $\text{Cu}^{+/2+}$ centers. Upon adjusting the ratios, the rates of the four steps are equalized and the short circuit current reaches its maximum. Note that for ratios in the 0.1-10 range, the potentials of the centers at short circuit will differ from their redox potentials by -59 to +59 mV.
- 10 [0176] In a polarization study, O_2 was electroreduced on the *Mv*-BOD fiber at +0.25 V versus Ag/AgCl at a current density of 0.73 mA/cm², while on the *Tt*-BOD fiber it was electroreduced at + 0.3 V versus Ag/AgCl at 0.88 mA/cm². The simultaneous gain in potential and current is attributed to the approximately 100 mV higher redox potential of the type I $\text{Cu}^{+/2+}$ center of *Tt*-BOD relative to that of the *Mv*-BOD. The
- 15 O_2 -binding, type II and type III $\text{Cu}^{+/2+}$ center-cluster is buried in the globular BOD protein and may not be directly reduced by electron transfer from an Os^{2+} -complex of the redox polymer. It is the type I $\text{Cu}^{+/2+}$ center that accepts electrons from Os^{2+} , as it is nearer to the protein's surface. When the rates of electron transfer between the type I center and the cluster, and between the cluster and its bound O_2 are fast, then the
- 20 current-controlling step is the transfer of electrons from Os^{2+} of the polymer to the type I $\text{Cu}^{+/2+}$ center. Increasing the redox potential of the type I $\text{Cu}^{+/2+}$ center increases the rate constant of electron transfer by increasing the transfer-driving potential difference. As a result, the rate of $\text{Os}^{2+} \rightarrow (\text{type I } \text{Cu}^{2+})$ transfer can increase to match the $(\text{type I } \text{Cu}^+) \rightarrow (\text{type II } \text{Cu}^{2+})$ rate at a lower $[\text{Os}^{2+}]:[\text{Os}^{3+}]$ ratio, and therefore,
- 25 when the redox polymer and the electrode are poised at a more oxidizing potential than in the *Mv*-cathode where the redox potential of the type I center is approximately 100 mV more reducing.

- [0177] Composition: The key difference between the optimal *Tt* and *Mv* compositions is that the *Tt*-films contain less enzyme. If the turnover rates of *Tt* and *Mv* were
- 30 similar, the wt % of the 64 kDa *Tt* would be higher than the approximately 50 wt % of the 52 kDa *Mv*-cathode, which is its optimal composition. The higher wt % cannot be reached because of precipitation of the electrostatic adduct of the enzyme and the

redox polymer above 55 wt % BOD. In the absence of precipitation up to 60 wt % BOD, the *Mv*-electrodes can have the optimal BOD wt %, which is the wt % where the rates of consumption of electrons by the enzyme and the rate of electron permeation from the electrode to the enzyme are equal. Because there is no difference
5 between the isoelectric points (pH 4.1) of *Mv*-BOD and *Tt*-BOD, the abrupt precipitation of *Tt* at 55 wt % is attributed to electrostatic bonding of clusters of anions on the *Tt*-globule and the redox polymer, leading to crosslinking. When the redox polymer is highly crosslinked, its segmental mobility, which underlies the transport of electrons (via collisions between reduced and oxidized, redox-couple-carrying
10 segments) is reduced. For this reason, the wired *Tt*-BOD is a poorer electron conductor, even though the weight fraction of redox polymer in its adduct is higher. The poorer conductivity is evidenced by increased separation of the voltammetric peaks above 55 wt % *Tt*-BOD.

[0178] Crosslinking by PEGDGE further reduces the segmental mobility on which the
15 electron conduction in the redox polymer film depends. Though high electron diffusivities are reached in films that are less crosslinked, the poorly crosslinked films dissolve, or swell excessively, and are sheared off the rotating electrodes. With 6.6 wt % PEGDGE crosslinker, the films were mechanically stable at 300 rpm, where the maximum shear stress at the rims of the electrodes was 1.4×10^{-2} N/m². At this
20 angular velocity, the current density was 1.9 mA/cm².

[0179] The polarization and the current density of the wired *Tt*-BOD fiber cathode are considerably improved over those of the wired *Mv*-BOD fiber cathode. In carbon cloth electrodes, the 4.6 mA/cm² current density at -176 mV versus the potential of the reversible O₂/H₂O electrode represents a nine-fold increase over that of the less stable
25 and chloride-inhibited dissolved *Mv*-BOD-based O₂ cathode.

[0180] Voltammetric characteristics: When the weight fraction of *Tt*-BOD exceeded 55 wt %, the current was limited by the high electronic resistance of the film caused by the electrostatic crosslinking of the redox polymer and the polyanionic enzyme, leading to lesser mobility of the redox centers. The $\Delta E_p = 25$ mV separation of the
30 voltammetric peaks at 1 mV/s scan rate of the wired *Tt*-BOD cathode exceeded the 5 mV separation of the *Mv*-BOD cathodes. The slower charge transport in the *Tt*-

electrode was a consequence of the reduced segmental mobility of in the *Tt*-films. The 113 mV width of the peaks at half height also exceeded the 90 mV width of the *Mv*-electrode, also reflecting the loss of segmental mobility.

[0181] Reproducibility: When the electrodes were rotated at 1000 rpm, the apparent batch-to-batch reproducibility, as well as the within-batch reproducibility, of the O₂ electroreduction currents were better than ± 10 %, as they also were for *Mv*-BOD. This reproducibility does not necessarily imply that the composite catalysts are identical within ± 10 %, because at 1000 rpm the current is limited by O₂ transport, not by the kinetics of the electrocatalyst. When the electrodes were rotated under O₂ at 4000 rpm, where the currents are limited by the kinetics of the electrocatalyst, the batch-to-batch reproducibility was ± 15 % and the within-batch reproducibility was ± 11 %. The spread was only half that between and within batches of *Mv*-electrodes, where loss of the catalytic films by shearing worsened the reproducibility at high angular velocity (>1000 rpm). The better reproducibility and stability are attributed to the enhanced electrostatic crosslinking of the enzyme and the redox polymer, which reduces the swelling and improves the mechanical stability of the sheared films.

[0182] Absence of inhibition at physiological pH and physiological chloride concentration: The dissolved *Tt*-BOD electrode retained its current through pH 7 to 10 range and the wired *Mv*-BOD electrode retained its current through the pH 5 to pH 10 range, while the wired *Tt*-BOD electrode retained its current through the pH 6 to 10.5 range. The decrease in current above pH 11 is irreversible. This decrease is caused by the denaturation of the enzyme, and is attributed, in the case of *Mv*-BOD, to the ionization of tyrosine residues. The variation of the current is negligibly small across the pH range of human serum or blood.

[0183] At pH 5, the current density of the wired *Coriolus hirsutus* laccase cathode declined by 60 % when the chloride concentration was raised from nil to 0.1 M. Laccases are inhibited by halide anions, including chloride anions, because these anions bind with the type II Cu⁺²⁺ centers and slow the transfer of electrons from the type I Cu⁺²⁺ center to the type III Cu⁺²⁺ pair. The dissolved *Tt*-BOD cathode is inhibited by chloride at 0.1 M concentration as well. Unlike these cathodes, the wired *Tt*-BOD cathode is the least inhibited by chloride, its current density declining only by

3 % when the chloride concentration is raised from 0 to 0.1 M, while that of the wired *Mv*-BOD cathode declines by 6 %. The loss remains small even at 1 M NaCl. Significantly, the inhibition of the wired *Tt*-BOD cathode by chloride at its 0.096-0.106 M concentration in normal human blood is so small that physiological variation
5 in chloride concentration will not affect the O₂ electroreduction current. Other copper-binding anions inhibit the electroreduction of O₂, the inhibition declining in the order CNS⁻ > F⁻ >> Br⁻ > Cl⁻. This order is only in partial agreement with the order CNS⁻ >> F⁻ >> Br⁻ > Cl⁻ found for the wired *Mv*-BOD and with the order CNS⁻ > F⁻ >> Cl⁻ > Br⁻ for the inhibition of dissolved *Tt*-BOD and for laccases. The order has been
10 attributed, in the case of the dissolved enzymes, to differences in the blockage of the access to their type II and type III Cu⁺²⁺ clusters.

[0184] The observed partial loss of O₂ electroreduction current at very high chloride concentration (> 1.5 M NaCl) is not attributed to specific binding of chloride to copper centers of the wired BOD, but to the screening of the charges of the electrostatically
15 bound polycationic and polyanionic segments of the redox-polymer-BOD adduct at high ionic strength, causing their dissociation and making the wiring of BOD less effective.

[0185] Temperature dependence and stability of the current: The O₂ electroreduction current increased with the temperature up to 60°C when the rate of increase was about
20 10°C/h, and declined rapidly when the temperature exceeded 60°C. The decline is attributed to the denaturation of the enzyme. The wired *Tt*-BOD cathode was more stable than the cathode made of with the dissolved enzyme, for which an optimal temperature of 45°C was reported. The apparent activation energy for O₂ electroreduction was $E_{act} = 34.3$ kJ/mol ($E_{act} = 28.2$ kJ/mol for *Mv*-BOD) at pH 7.4
25 when the electrode rotated at 1000 rpm under 1 atm O₂, and the current was O₂-transport controlled. Because the current is O₂-transport-limited at 1000 rpm, the 34.3 kJ/mol activation energy is that for the diffusion of oxygen in the solution. Its value is consistent with the temperature dependence of the diffusivity of O₂. The thermal-denaturation-caused 88.2 kJ/mol activation energy for current loss of the *Tt*-cathode
30 shows that the cathode is more stable than the *Mv*-cathode (77.2 kJ/mol), explaining why the *Tt*-cathode loses only 5 % of its current per day of operation at 37.5°C, while the *Mv*-cathode loses 10 %. The wired *Tt*-BOD cathode is much more stable than the

cathode of Tanaka made with the dissolved enzyme, which had a half-life of one hour in phosphate buffer at 37°C. It was also more stable than that of an immobilized-BOD electrode used in the clinical monitoring of the concentration of bilirubin having a half life of 17 hours at 37°C and 8 hours at 40°C.

- 5 [0186] At their physiological concentrations the most readily electrooxidized constituents of blood urate, ascorbate and acetaminophen do not damage the *Tt*-cathode when poised at +300 mV/Ag/AgCl in PBS at 37.5°C. When 0.1 mM ascorbate was added, or 0.1 mM ascorbate and 0.17 mM acetaminophen were added, the current transiently decreased by 5 %, and when 0.48 mM urate was added, the
10 current decreased by 22 %. While the electrooxidative polymerization of urate in a redox polymer film with a higher density of cationic sites and thus a higher urate concentration in the film causes severe fouling, the present films were not fouled by urate electro-polymerization.

- [0187] Conclusion: Wired BOD films catalyze the electroreduction of O₂ to water
15 under physiological conditions. When the oxygen electroreducing cathodes are poised at potentials that are as little as -136 mV reducing relative to the potential of the reversible O₂/H₂O, the current density of the wired *Tt*-BOD cathode exceeds 2 mA/cm² at 37°C. The cathode operates for six days, with 5 % of the current being lost per day. The improvement in operating current density and potential is attributed to
20 the higher redox potential of the type I Cu⁺²⁺ redox center of *Tt*-BOD, and the improved stability is attributed to the enhanced electrostatic bonding of *Tt*-BOD and its polymeric wire.

Experimental Example 3: Characteristics of a Miniature Glucose Oxygen Biofuel Cell and Its Operation in a Living Plant

- 25 [0188] In this experimental example, the temperature, pH, glucose concentration, NaCl concentration, and operating atmosphere dependence of the power output of a compartment-less, miniature glucose-O₂ biofuel cell, comprised only of two bioelectrocatalyst-coated carbon fibers, each of 7-μm diameter and 2-cm length (Mano, N.; Mao, F.; Heller, A. J. Am. Chem. Sec. 2002, 124, 12962), was
30 investigated. The bioelectrocatalyst of the anode consists of glucose oxidase from *Aspergillus niger* electrically wired by polymer I, having a redox potential of -0.19 V

vs Ag/AgCl. That of the cathode consists of bilirubin oxidase from *Trachyderma tsunodae* wired by polymer II, having a redox potential of +0.36 V vs Ag/AgCl (Mano, N.; Kim, H.-H.; Zhang, Y.; Heller, A. *J. Am. Chem. Soc.* 2002, 124, 6480. Mano, N.; Kim, H.-H.; Heller, A. *J. Phys. Chem. B* 2002, 106, 8842). Implantation of
5 the fibers in a grape leads to an operating biofuel cell. The cell, made of 7- μ m diameter, 2-cm long fibers, produces in the grape 2.4 μ W at 0.52 V.

[0189] The anode and cathode compartments of most fuel cells are separated by an ion-conducting membrane. In the most widely used H₂-O₂ cell, hydrogen is oxidized to water at the anode at a reducing potential and oxygen is reduced to water at the
10 cathode at an oxidizing potential. In the phosphoric acid electrolyte H₂-O₂ cell, a NafionTM membrane excludes oxygen from the anode compartment and hydrogen from the cathode compartment. (Hillman, A. R. In *Electrochemical Science and Technology of Polymers*; Linford, R.G., Ed.; Elsevier: London, 1987; p 103; *Fuel Cells and Their Applications*; Kordesch, K., Simader, G., Eds.; VCH Publisher: New
15 York, 1996; p 384; Ormerod, R. M. *Chem.Soc.Rev.* 2003, 32, 17-28.) Because the anode is poised at a reducing potential with respect to the cathode, and because both the anode and the cathode comprise platinum group metal catalysts, hydrogen would be more readily oxidized at the cathode, and oxygen would be more readily reduced at the anode. As a result, the power output would be nil or negligibly small. In all but a
20 few of the earlier reported biofuel cells, the anode and cathode compartments were also separated by an ion-exchange membrane. (Appleby, A. J.; Ng, D. Y. C.; Weinstein, H.J. *Appl. Electrochem.* 1971, 1, 79-90; Rao, J. R.; Richter, G.; Von Sturm, F.; Weidlich, E. *Ber. Bunsen-Ges Phys Chem.* 1973 77, 787-790; Wan, B. Y. C.; Tseung, A. C. C. *Med. Biol. Eng.* 1974, 12, 14-28; Affrossman, S.; Courtney, J.
25 M.; Gilchrist, T.; Martin, I. *Med. Biol. Eng.* 1975, 13, 539-543; Turner, A. P. F.; Ramsay, G.; Higgins, I. J. *Biochem Soc. Trans.* 1983, 11, 445-448; Palmore, G.T.; Kim, H.-H. *J. Electroanal. Chem.* 1999, 464, 110-117; Palmore, G. T.; Bertschy, H.; Bergens, S.H.; Whitesides, G. M. *J. Electroanal. Chem.* 1998, 443, 155-161; Sasaki, S.; Karube, L. *Trends Biotechnol* 1999, 17, 50-52.) In cells having platinum group
30 metal-based O₂ cathodes, separation was necessary because the anodic reactant's electrooxidation products poisoned the metallic platinum group electrocatalyst of the cathode. (Appleby, A. J.; Ng, D. Y. C.; Weinstein, H.J. *Appl. Electrochem.* 1971, 1, 79-90; Rao, J. R.; Richter, G.; Von Sturm, F.; Weidlich, E. *Ber. Bunsen-Ges Phys*

Chem. 1973 77, 787-790; Wan, B. Y. C.; Tseung, A. C. C., Med. Biol. Eng. 1974, 12, 14-28; Affrossman, S.; Courtney, J. M.; Gilchrist, T.; Martin, I. Med. Biol. Eng. 1975, 13, 539-543.) In cells containing a dissolved redox mediator in the anode compartment, to transport electrons from its substrate-reduced oxidase or dehydrogenase to the anode, the membrane was essential to prevent electrooxidation of the mediator at the cathode. In cells containing a dissolved redox mediator in the cathode compartment, to transport electrons from the cathode to its O₂-oxidized laccase or other enzyme, the membrane was essential to prevent reduction of the mediator at the anode. (Turner, A. P. F.; Ramsay, G.; Higgins, I. J, Biochem Soc. Trans. 1983, 11, 445-448; Palmore, G.T.; Kim, H.-H. J Electroanal Chem 1999, 464, 110-117; Palmore, G. T.; Bertschy, H.; Bergens, S.H.; Whitesides, G. M. J. Electroanal. Chem. 1998, 443, 155-161; Sasaki, S.; Karube, L. Trends Biotechnol 1999, 17, 50-52; Kang, C.; Xie, Y.; Anson, F. C. J Electroanal. Chem. 1996, 413, 165-174; Pizzariello, A.; Stred'ansky, M.; Miertus, S. Bioelectrochemistry 2002, 56 99-105.)

[0190] The electrocatalysts of this study are wired enzymes. (Heller, A. Acc. Chem. Res. 1990, 23, 128-134; Heller, A. J Phys. Chem. B 1992, 96, 3579-3587.) They are electrostatic adducts of redox enzymes, which are polyanions at neutral pH, and electron-conducting redox polymers, which are polycations. The adduct prevents phase separation of the redox polymer and the enzyme. The redox potential of polymer I wiring the anodic enzyme (see FIG. 4), glucose oxidase (GOx), is tailored to be just slightly oxidizing with respect to the redox potential of GOx, and polymer II (see FIG. 7) wiring the cathodic enzyme, bilirubin oxidase (BOD), is just slightly reducing with respect to the potential of BOD. This provides for an electron cascade in the direction glucose → glucose oxidase → polymer I → anode → external resistance → cathode → polymer II → O₂, with the external resistance, rather than the kinetic resistance of any of the six electron-transfer steps, dominating the potential difference between glucose and O₂ (see FIG. 2). By basing the anode and cathode electrocatalysts on wired enzymes, it is possible to make both electrodes so selective for their respective reactants that the current-depleting oxidation of glucose at the cathode, and reduction of O₂ at the anode, are slower than the desired electrooxidation and electroreduction of reactants at their intended electrode. Beyond the key condition of selectivity, two additional conditions should be met in order to allow the

elimination of the compartment-separating membrane: the readily poisoned, platinum-group, metal catalysts should be avoided, and neither compartment should contain a dissolved redox mediator. Thus, preferably, dissolved redox mediators are not present in the cell, the enzymes and redox polymers are countercharged polyelectrolytes that form bound adducts, such as electrostatic adducts, and the electrodes are selective.

[0191] In the compartment-less biofuel cell (as schematically shown in FIG. 2), the electrons of glucose reduce GOx, β -D-glucose being electrooxidized to δ -gluconolactone (see Eq. 1, above). The electrons are collected and transported to the anode via the redox polymer I shown in FIG. 4. Electrons are transported from the cathode via redox polymer II, shown in FIG. 7, to O_2 -oxidized bilirubin oxidase, catalyzing its electroreduction of O_2 to water (see Eq. 2, above). The overall cell reaction is represented by (see Eq. 3, above).

[0192] The current densities of the anode and the cathode of a biofuel cell based on the wiring of enzymes are limited by the amount and the turnaround rate of the enzyme that is wired. While in the H_2 - O_2 and in the methanol-air fuel cells, which can be miniaturized and chip-mounted, (Kelley, S. C.; Deluga, G. A.; Smyrl, W.H. *AIChE J* 2002, 48, 1071-1082) the current densities are of hundreds of milliamperes per square centimeter, the current densities of smooth wired enzyme electrodes are only ~ 1 mA/cm² and reach only 2-10 mA/cm² when the electrodes are porous. Furthermore, the operational lives of the H_2 - O_2 and methanol-air fuel cells are of years, while the operational lives of biofuel cells based on wiring of enzymes are ~ 1 week. Nevertheless, because the enzyme wiring-based cells are structurally simpler, are uniquely easy to miniaturize, and their electrodes are potentially mass-manufacturable at the same cost as glucose anodes used in glucose monitors for diabetes management ($<10\%$), the cells are likely to find applications. As the size of microelectronic circuits and sensors shrinks, the size of the low-power sensor-transmitter package (of potential value in physiological research and in medicine) becomes increasingly dependent on the size of its power source. The miniature biofuel cells are likely to meet the need for a small power source in low-power sensor-transmitter systems.

[0193] Earlier, progress toward a compartment-less biofuel cell anode was made by Persson and Gorton, who electrooxidized glucose on a carbon anode on which a redox mediator was chemisorbed and glucose dehydrogenase was immobilized. (Persson, B.; Gorton, L. *Enzyme Microb. Technol.* 1985, 7, 549-552; Persson, B.; Gorton, L.; Johansson, G. *Bioelectrochem. Bioenerg.* 1986, 16, 479-483.) Katz et al. reported a compartment-less enzyme-based fuel cell with an operating voltage of 60 mV and a power density of 50 nW/mm². (Katz, E.; Willner, I.; Kotlyar, A. B. *J. Electroanal. Chem.* 1999, 479, 64-68.) Katz et al. also proposed a "self-powered enzyme-based biosensor," in which the current passing between a glucose-transport-limited anode and a cathode, not limited by O₂ transport, would be indicative of the glucose concentration. However, they did not address the essential issue of the source of the power for amplifying, measuring, and transmitting the signal from such a biosensor. (Katz, E.; Buckmann, A. F.; Willner, I. *J. Am. Chem. Soc.* 2001, 123, 10752-10753.) Tsujimura et al. reported a membrane-less glucose-O₂ biofuel cell operating in O₂-saturated 30 mM MOPS buffer in the presence of 50 mM glucose, producing 580 nW/mm² at an operating potential of 0.19 V. (Tsujimura, S.; Kano, K.; Ikeda, T. *Electrochemistry* 2002, 70, 940-942.) Chen et al. describe a compartment-less biofuel cell based on the wiring of glucose oxidase and of laccase to 7-μm-diameter, 2-cm-long carbon fiber electrodes. (Chen, T.; Barton, S. C.; Binyamin, G.; Gao, Z.; Zhang, Y.; Kim, H.-H.; Heller, A. *J. Am. Chem. Soc.* 2001, 123, 8630-8631.) The output of their cell at 37°C is 0.6 μW, or 1.4 μW/mm² at 0.38 V. Because their cathode is laccase-based, and because laccase loses much of its activity in 0.14 M NaCl and at pH 7.2, (Baron, S. C.; Kim, H.-H.; Binyamin, G.; Zhang, Y.; Heller, A. *J. Phys. Chem. B* 2001, 105, 11917 - 11921; Barton, S. C.; Kim, H.-H.; Binyamin, G.; Zhang, Y.; Heller, A. *J. Am. Chem. Soc.* 2001, 123, 5802-5803; Baron, S. C.; Pickard, M.; Vasquez-Duhalf, R.; Heller, A. *Biosens Bioelectron.* 2002, 17, 1071-1074; Xu, F. *Appl. Biochem. Biotechnol* 2001, 95, 125-133) the cell is operated at pH 5 and in the absence of chloride. Mano et al. report a laccase-comprising, compartment-less cell with an improved redox polymer connecting the reaction centers of glucose oxidase to the carbon fiber. It produces 1.2 μW, or 2.7 μW/mm², at an operating potential of 0.78 V, the highest reported for a miniature membrane-less biofuel cell. (Mano, N.; Mao, F.; Shin, W.; Chen, T.; Heller, A. *Chem. Commun.* 2003, 518-519.) Replacement of the laccase by bilirubin oxidase, an oxygen-electroreduction-catalyzing enzyme that

maintains its activity at neutral pH and in the presence of 0.14 M NaCl, (Tsujimura, S.; Kano, K.; Ikeda, T. *Electrochemistry* 2002, *70*, 940-942; Mano, N.; Kim, H.-H.; Zhang, Y.; Heller, A. J. *Am. Chem. Soc.* 2002, *124*, 6480-6486; Mano, N.; Kim, H.-H.; Heller, A. *J Phys. Chem B* 2002, *106*, 8842-8848; Tsujimura, S.; Tatsumi, H.; Ogawa, J.; Shimizu, S.; Kano, K.; Ikeda, T. J., *Electroanal. Chem.* 2001, *496*, 69-75.)

allows operation of the wired enzyme-based, compartment-less, biofuel cell under physiological conditions. The cell produces 1.9 μW at 37°C under physiological conditions, or 4.3 $\mu\text{W}/\text{mm}^2$ at 0.52 V at 37°C. In week-long operation, it generates 0.9 J of electrical energy while passing a charge of 1.7 C. (Mano, N.; Mao, F.; Heller, A. J. *Am Chem. Soc.* 2002, *124*, 12962-12963.) If a zinc fiber of similar dimensions were utilized in a battery, and if the current efficiency of zinc utilization were 100%, only 0.005 C would be passed. Thus, the dimensions of a biofuel cell operating for a week can be much smaller than those of a battery. The characteristics of this membrane-less biofuel cell, which produces electrical power when implanted in a living organism (a grape), are now described.

[0194] Chemicals and Materials: Bilirubin oxidase (BOD) (EC 1.3.3.5, 1.3 U/mg¹) from *Trachyderma Tsunodae* was purchased from Amano (Lombard, IL), and glucose oxidase (GOx) (EC 1.1.3.4, 191 U/mg¹) from *Aspergillus niger* was purchased from Fluka (Milwaukee, WI). Poly(ethylene glycol) (400) diglycidyl ether (PEGDGE) from Polysciences, Inc. (Warrington, PA), and NaIO₄ and NaCl from Sigma (St. Louis, MO), were used as received. A fresh solution of BOD in pH 7.4, 20 mM phosphate buffer (PB) was prepared daily. All solutions were made with deionized water passed through a purification train (Sybron Chemicals Inc., Pittsburgh, PA). The syntheses of the BOD-wiring redox polymer II (PAA-PVI [Os(4,4'-dichloro-2,2'-bipyridine)₂Cl]⁺²⁺) (shown in FIG. 7) and the GOx-wiring redox polymer I (PVP-[Os(N,N'-alkylated-2,2'-bi-imidazole)₃]^{2+/3+}) (shown in FIG. 4) were as previously reported. (Mano, N.; Kim, H.-H.; Zhang, Y.; Heller, A. J. *Am. Chem. Soc.* 2002, *124*, 6480-6486; Mano, N.; Kim, H.-H.; Heller, A. *J Phys. Chem B* 2002, *106*, 8842-8848; Mano, N.; Mao, F.; Heller, A. J. *Am Chem. Soc.* 2002, *124*, 12962-12963; Kim, H.-H.; Mano, N.; Zhang, Y.; Heller, A. J. *Electrochem.Soc.* 2003, *150*, A209-A213.)

[0195] Instrumentation and Electrodes: The measurements were performed using a bipotentiostat (CH Instruments, Austin, TX, model CH1832) and a dedicated computer.

- [0196] The 2-cm-long, 7- μ m-diameter, carbon-fiber electrodes (Goodfellow, Cambridge, UK) were contacted and coated by reported procedures. (Chen, T.; Barton, S. C.; Binyamin, G.; Gao, Z.; Zhang, Y.; Kim, H.-H.; Heller, A. J. Am. Chem. Soc. 2001, *123*, 8630-8631; Mano, N.; Kim, H.-H.; Zhang, Y.; Heller, A. J. Am. Chem. Soc. 2002, *124*, 6480-6486; Mano, N.; Kim, H.-H.; Heller, A. J. Phys. Chem B 2002, *106*, 8842-8848; Mano, N.; Mao, F.; Heller, A. J. Am. Chem. Soc. 2002, *124*, 12962-12963; Kim, H.-H.; Mano, N.; Zhang, Y.; Heller, A. J. Electrochem. Soc. 2003, *150*, A209-A213.) Each end of the fibers was cemented to a copper wire using conductive carbon paint (SPI, West Chester, PA). The carbon paint was allowed to dry and then insulated with the epoxy. The active area of each fiber was 0.44 mm². Prior to their coating, fibers were made hydrophilic by exposure to a 1-Torr O₂ plasma for 3 min. (Sayka, A.; Eberhart, J.G. Solid State Technol. 1989, *32*, 69-70.) The cathodic catalyst was made, as described, of 44.6 wt % bilirubin oxidase, 48.5 wt % polymer II, and 6.9 wt % of the cross-linker PEGDGE. (Mano, N.; Kim, H.-H.; Zhang, Y.; Heller, A. J. Am. Chem. Soc. 2002, *124*, 6480-6486; Mano, N.; Kim, H.-H.; Heller, A. J. Phys. Chem B 2002, *106*, 8842-8848; Mano, N.; Mao, F.; Heller, A. J. Am. Chem. Soc. 2002, *124*, 12962-12963.) The anodic catalyst solution was made as follows: 100 μ L of 40 mg/mL of GOx in 0.1 M NaHCO₃ was oxidized by 50 μ L of 7mg/mL of NaIO₄ in the dark for 1 h, and then 2 μ L of the periodate-oxidized GOx was mixed with 8 μ L of 10 mg/mL of polymer I and a 0.5- μ L droplet of 2.5 mg/mL of PEGDGE. A 5- μ L, aliquot of this solution was applied to the carbon fiber. The resulting anodic catalyst consisted of the cross-linked adduct of 39.6 wt % GOx, 59.5 wt % polymer I, and 0.9 wt % PEGDGE. The glucose concentration was determined by using a FreeStyleTM blood glucose monitor (TheraSense Inc., Alameda, CA). The bulk cell used for the characterization of the electrodes in vitro had an Ag/AgCl (3 M KCl) reference electrode and a platinum wire counter electrode (BAS, West Lafayette, IN).
- [0197] Implantation in the Grape: The fibers were implanted by making a pair of 2-cm-long cuts with a razor blade, so as to create a triangular groove and allow

temporary removal of the cut part. After the fiber was implanted, the cut part was replaced in its groove.

- [0198] Results: FIG. 12A shows the polarization curves of the 7- μ m carbon fiber anode [modified with wired GOx (bold line)] and of the fiber cathode [modified with wired BOD (fine line)], in a quiescent 15 mM glucose solution in air at 37 °C in pH 7.2, 0.1 M NaCl and 20 mM phosphate buffer solution. Catalytic electrooxidation of glucose was observed at -0.2 V vs Ag/AgCl, and it reached its plateau of 10 μ A/mm² near -0.1 V vs Ag/AgCl. Catalytic electroreduction of O₂ was observed at +0.48 V vs Ag/AgCl and reached its 9.5 μ A/mm² plateau near +0.35 V vs Ag/AgCl.
- 10 [0199] FIG. 12B shows the power density of the biofuel cell at 25°C (fine line) and at 37°C (bold line). The dependence of the power output on the cell voltage in air (bold line) and under O₂ (fine line) is shown in FIG. 13A. In the quiescent PBS buffer, the power density at 1 atm O₂ was 30% lower than that in air. FIG. 13B shows the dependence of the power density on the glucose concentration in air (●) and under
- 15 O₂(○). The current density increased with the glucose concentration up to 20 mM, where a plateau of 4.4 μ W/mm² was reached in air and a plateau of 3.4 μ W/mm² was reached under O₂. At 2 mM glucose concentration, the power density was 80% lower under O₂ than it was in air; at 35 mM glucose concentration, it was 35% lower under O₂ than it was in air. FIG. 14 shows the temperature dependence of the power density
- 20 for the cell operating at +0.52 V in a quiescent solution in air at 37°C in a pH 7.2, 0.14 M NaCl, 20 mM phosphate, and 15 mM glucose solution. The power density increased with temperature, reaching a plateau at 40°C, and then declined above 50 °C.
- [0200] The pH dependence of the power density for the cell operating at +0.52 V is seen in FIG. 15A. The power density increased with pH, reaching a plateau at pH 6.2, and then declined slowly above pH 8.4. The NaCl concentration dependence of the power density for the cell operating at +0.52 V is shown in FIG. 15B. The power was nearly independent of the NaCl concentration through the 0-0.1 M range and then declined, dropping at 1 M NaCl to one-fifth of its value at 0.1 M NaCl.
- 25 [0201] No power was produced when the fibers were implanted in a grasshopper. Implantation of the fibers in a grape (>30 mM glucose, pH 5.4), however, did yield an
- 30

- operating biofuel cell. FIG. 16A shows a photograph of the sliced grape and the contacts of the implanted fibers. Because the fibers of 7- μm diameter were barely visible in the photograph, lines representing their positions were drawn. The dependence of the power density on the operating voltage is shown in FIG. 16B. The power output of the cell depended on the position of the cathode fiber. When the cathode fiber was located near the center of the grape, the power density was 0.47 $\mu\text{W}/\text{mm}^2$; when the cathode fiber was near the skin of the grape, the power density was 2.4 $\mu\text{W}/\text{mm}^2$. After 24 h of continuous operation, 85% of the initial power output was retained.
- 10 [0202] The reversible redox potential of GOx from *A. niger* at pH 7.4 is -0.35 vs Ag/AgCl, (Hirose, J.; Inoue, T.; Sakuragi, H.; Kikkawa, M.; Minakami, M.; Morikawa, T.; Iwamoto, H.; Hiromi, K. Inorg. Chim. Acta 1998, 273, 204-212.) and that of BOD from *T. Tsunodae* is about +0.36 vs Ag/AgCl (Hirose, J.; Inoue, T.; Sakuragi, H.; Kikkawa, M.; Minakami, M.; Morikawa, T.; Iwamoto, H.; Hiromi, K. Inorg. Chim. Acta 1998, 273, 204-212.) (as schematically shown in FIG. 17). Thus, the redox potentials of GOx and BOD differ by 0.71 V. This value, representing the limit of the operating voltage of the cell, is close to the difference between the observed threshold potentials for electrooxidation of glucose (-0.20 V vs Ag/AgCl) and electroreduction of oxygen +0.48 V vs Ag/AgCl). Concentration polarization and overpotentials for the six electron-transfer steps of the anode and the cathode (as schematically shown in FIG. 1) decrease the operating voltage at the point of maximum power to 0.52 V.

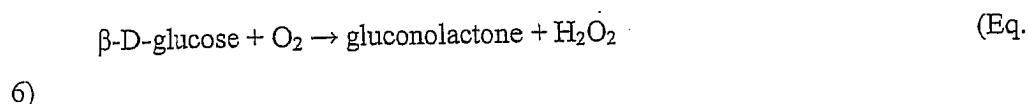
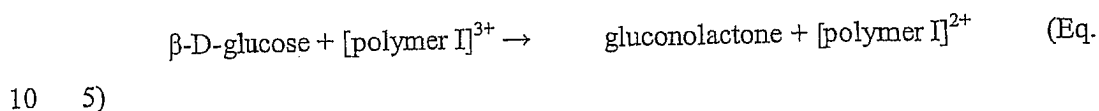
- [0203] Redox polymer I (FIG. 4), connecting the GOx reaction centers to the anode fiber, enables the electrooxidation of glucose at -100 mV vs Ag/AgCl at a current density of 1.1 mA/cm^2 (FIG. 12A, bold line), (Mano, N.; Mao, F.; Heller, A. J. Am. Chem. Soc. 2002, 124, 12962-12963; Mao, F.; Mano, N.; Heller, A. J. Am. Chem. Soc. 2003, 125, 4951-4957.) a potential only 260 mV oxidizing versus the estimated GOx redox potential at pH 7.3. (Stankovich, M.T.; Schopfer, L.M.; Massey, V.J. Biol. Chem. 1978, 253, 4971-4979.) It differs from the earlier redox polymer (Kim, H.-H.; Mano, N.; Zhang, Y.; Heller, A. J. Electrochem. Soc. 2003, 150, A209-A213) in its redox center and in the tethering of it, redox centers to the polymer backbone through a 13-atom-long flexible spacer arm. The redox potential of its [Os(N,N' -alkylated-
- 25
30

2,2'-bi-imidazole)^{2+/3+}] redox center is -190 mV vs $\overline{\text{Ag}}/\text{AgCl}$, about 0.8 V reducing relative to that of the familiar $\text{Os}(\text{bpy})_3^{2+/3+}$ Complex. (Mano, N.; Mao, F.; Heller, A. J. Am Chem. Soc. 2002, *124*, 12962-12963; Mao, F.; Mano, N.; Heller, A. J Am. Chem Soc. 2003, *125*, 4951-4957.) Although the potential difference between the GOx redox centers and the redox polymer is only 170 mV, the polymer effectively wires the enzyme redox centers. The long tether binding the redox centers to the backbone reduces the overvoltage for driving the electrons from the GOx-FADH₂ centers to the redox polymer and through the polymer to the electrode. It provides for close approach of the redox centers of the polymer and of the enzyme and facilitates collisional electron transfer between neighboring polymer redox centers, as the tethered centers "wipe" the electrons from large overlapping proximal volumes of the hydrated cross-linked redox polymer. (Mano, N.; Mao, F.; Heller, A. J. Am Chem. Soc. 2002, *124*, 12962-12963.)

[0204] Redox polymer II (FIG. 7) is an electron-conducting redox copolymer of polyacrylamide and poly (N-vinylimidazole) complexed with $[\text{Os}(4,4'\text{-dichloro-2,2'\text{-bipyridine}})_2\text{Cl}]^{+/2+}$ (Mano, N.; Kim, H.-H.; Zhang, Y.; Heller, A. J. Am. Chem. Soc. 2002, *124*, 6480-6486; Mano, N.; Kim, H.-H.; Heller, A. J Phys. Chem B 2002, *106*, 8842-8848; Mano, N.; Mao, F.; Heller, A. J. Am Chem. Soc. 2002, *124*, 12962-12963.) It electrically wires the BOD $\text{Cu}^{+/2+}$ centers to the cathode fiber. As illustrated in FIG. 12A (fine line), the overpotential for oxygen reduction to water is remarkably low. Even though the oxygen concentration in air-saturated pH7 phosphate buffer is only about 0.1 mM, the current density of the oxygen cathode reaches 1.1 mA/cm² at -140 mV vs the potential of the reversible O₂/H₂O couple. (Mano, N.; Kim, H.-H.; Zhang, Y.; Heller, A. J. Am. Chem. Soc. 2002, *124*, 6480-6486; Mano, N.; Kim, H.-H.; Heller, A. J Phys. Chem B 2002, *106*, 8842-8848.) Glucose is not electrooxidized on the cathode poised at +0.4 V vs Ag/AgCl.

[0205] When the anode and cathode fibers are of equal length, the currents of the two are equal when the anode is poised at -0.19 V vs Ag/AgCl and the cathode at +0.34 mV vs Ag/AgCl, the cell operating at +0.52 V (FIG. 12B). In a quiescent physiological buffer solution, the power output is 2.8 $\mu\text{W}/\text{mm}^2$ at 25°C (FIG. 12B, fine line) and 4.4 $\mu\text{W}/\text{mm}^2$ at 37°C (FIG. 12B, bold line).

[0206] Oxygen Pressure Dependence: At low partial pressures of O₂, where electroreduction of O₂ to water is O₂ mass-transport-limited in the quiescent solution, the power increases with the partial pressure of O₂ until the kinetic limit of the cathodic electrocatalyst is reached. As the O₂ partial pressure is increased, the anodic glucose electrooxidation current decreases, because O₂ competes with the wire for GOx FADH₂ electrons (see Eqs. 5 and 6 below). As can be seen in FIG. 13A, at 37 °C and 15 mM glucose concentration, switching the bubbled gas from air to oxygen results in the loss of one-third of the power when the cell operates at 0.52 V.



[0207] As illustrated in FIG. 13B, the loss depends on the glucose concentration. Although above 15 mM glucose concentration about one-third of the power is lost when the atmosphere is switched from air to oxygen, the loss is much greater, four-fifths of the output, at 2 mM glucose concentration. The difference is attributed to the slower electrooxidation of the solution side of the film than its electrode side. At high glucose concentration, the glucose-reduced front moves toward the electrode, and the effective kinetic resistance is reduced. Excessive loss of current by electroreduction of O₂ at the glucose-oxidizing anode is avoided because of the rapid diffusion of electrons in GOx wiring redox polymer I (FIG. 4); the apparent electron diffusion coefficient is as high as 5.8 x 10⁻⁶ cm²/s. (Mano, N.; Mao, F.; Heller, A. J. Am Chem. Soc. 2002, 124, 12962-12963; Mao, F.; Mano, N.; Heller, A. J. Am. Chem Soc. 2003, 125, 4951-4957.) The redox centers of the film are rapidly electrooxidized even at 0.1 V vs Ag/AgCl, and in an aerated solution, most of the electrons of GOx are captured by polymer I rather than by dissolved O₂.

[0208] While the H₂O₂ produced in the competing side reaction of O₂ with reduced glucose oxidase could damage the glucose electrooxidizing anode if the H₂O₂ were allowed to accumulate, the damage it causes to the anode when diluted or decomposed by catalase, an abundant enzyme in many organisms, is not significant. (Binyamin, G.; Heller, A. J. Electrochem. Soc. 1999, 146, 2965-2967.)

[0209] Temperature Dependence: The temperature dependence of the cell operating at 0.52 V at 15 mM glucose concentration in a quiescent PBS buffer solution in air and at 37 °C is seen in FIG. 14. The power density increases up to 50°C and then declines rapidly as one or both of the enzymes are denatured. The activation energies are 28.3 kJ/mol for the anode reaction (Mano, N.; Mao, F.; Heller, A. J. Am. Chem. Soc. 2002, 124, 12962-12963.) and 34.3 kJ/mol¹ for the cathode reaction. (Mano, N.; Kim, H.-H.; Zhang, Y.; Heller, A. J. Am. Chem. Soc. 2002, 124, 6480-6486.) At ambient temperature, the power density is limited by the kinetics of the cathodic bioelectrocatalyst. The observed activation energy for the thermal denaturing of bilirubin oxidase is 88.2 kJ/mol¹, and for glucose oxidase it is 96 kJ/mol. (Mano, N.; Kim, H.-H.; Zhang, Y.; Heller, A. J. Am. Chem. Soc. 2002, 124, 6480-6486; Mano, N.; Mao, F.; Heller, A. Unpublished results, 2003.) Even though the activation energy for denaturing glucose oxidase is higher, it is the denaturing of bilirubin oxidase (Mano, N.; Kim, H.-H.; Zhang, Y.; Heller, A. J. Am. Chem. Soc. 2002, 124, 6480-6486.) that causes the observed decline from 4.5 to 3.45 $\mu\text{W}/\text{mm}^2$ upon increasing the temperature from 45 to 55°C at a rate of 10°C/h, because in this temperature domain the power output is controlled by the cathode in the 15 mM aerated glucose solution. Because both enzymes are denatured and the activation energy for the denaturing of GOx exceeds that of BOD, (Mano, N.; Kim, H.-H.; Zhang, Y.; Heller, A. J. Am. Chem. Soc. 2002, 124, 6480-6486; Mano, N.; Mao, F.; Heller, A. Unpublished results, 2003.) at temperatures above 55°C the cell becomes anode-limited, and heating at a rate of 10°C/h from 55 to 60°C causes the power to drop rapidly, from 3.45 to 2.0 $\mu\text{W}/\text{mm}^2$.

[0210] pH Dependence: FIG. 15A shows the pH dependence of the power density when the cell operates at +0.52 V in air. The current density of the anode is near its maximum between pH 6 and 8.2. (Mano, N.; Mao, F.; Heller, A. Unpublished results, 2003.) The current density of the cathode is nearly independent of pH in the pH 6-10.5 range. (Mano, N.; Kim, H.-H.; Zhang, Y.; Heller, A. J. Am. Chem. Soc. 2002, 124, 6480-6486; Mano, N.; Kim, H.-H.; Heller, A. J Phys. Chem B 2002, 106, 8842-8848.) At pH<6, (Mano, N.; Kim, H.-H.; Zhang, Y.; Heller, A. J. Am. Chem. Soc. 2002, 124, 6480-6486; Mano, N.; Kim, H.-H.; Heller, A. J Phys. Chem B 2002, 106, 8842-8848; Mano, N.; Mao, F.; Heller, A. Unpublished results, 2003.) the power is limited by the kinetics of the anode; at pH 5, where the current density of the anode is

2.0 $\mu\text{A}/\text{mm}^2$ and that of the cathode is 4.5 $\mu\text{A}/\text{mm}^2$, the power density drops to 1.0 $\mu\text{W}/\text{mm}^2$. As the pH is raised to pH 6, the kinetics of the anode improves and, as shown in FIG. 15A, the power density increases. (Mano, N.; Mao, F.; Heller, A. Unpublished results, 2003.) Above pH 6, the current of the cathode is lower than that of the anode. At pH 7, (Mano, N.; Mao, F.; Heller, A. J. Am Chem. Soc. 2002, 124, 12962-12963.) where the anode current density is 12 $\mu\text{A}/\text{mm}^2$ and the cathode current density is 10 $\mu\text{A}/\text{mm}^2$, the cathode controls the power. Thus, the optimal operating pH for the cell consisting of two carbon fibers of equal length is 6. Above pH 8.4, the power decreases because of denaturation of bilirubin oxidase. (Mano, N.; Kim, H.-H.; Zhang, Y.; Heller, A. J. Am. Chem. Soc. 2002, 124, 6480-6486; Mano, N.; Kim, H.-H.; Heller, A. J Phys. Chem B 2002, 106, 8842-8848. In the pH range of human serum or blood (pH 7.1-7.4), the variation in power is negligibly small.

[0211] Effect of NaCl: Serum, blood, and other physiological fluids contain 0.14 M chloride. Copper-binding anions, particularly halide anions, inhibit multi-copper oxidases. In addition, the electrostatic bond between the polyanionic enzyme and the polycationic redox polymer, which prevents their phase separation, is weakened at high ionic strength, where the enzyme and polymer charges are screened by their respective counterions. (Heller, A. J Phys. Chem. B 1992, 96, 3579-3587; Degani, Y.; Heller, A.J. Am. Chem. Soc. 1989, 111, 2357-2358; Katakis, I.; Ye, L.; Heller, A.J. Am. Chem. Soc. 1994, 116, 3617-3618.) At greater cross-linking, the phase separation is reduced. The dependence of the power output on the NaCl concentration is seen in FIG. 15B. Above 0.15 M, the anodic current monotonically declines upon increasing the NaCl concentration. Because increasing the salt concentration from 0.1 to 1 M decreases the current density of the wired BOD cathode only by 2%, (Mano, N.; Kim, H.-H.; Zhang, Y.; Heller, A. J. Am. Chem. Soc. 2002, 124, 6480-6486; Mano, N.; Kim, H.-H.; Heller, A. J Phys. Chem B 2002, 106, 8842-8848) the decrease in the power output is attributed to the partial unwiring of the GOx. (Mano, N.; Mao, F.; Heller, A. Unpublished results, 2003.)

[0212] Operation in the Grape: For the experiment demonstrating that the cell consisting merely of two coated carbon fibers actually operates in a living organism, the cell was implanted in a grasshopper and in a grape. In the grasshopper, no power was produced. As we learned later, the sugar in the fluid of the grasshopper is not

glucose but the disaccharide trehalose. (Harrison, R. R.; Koch, C. *Analog Integr. Circuits Signal Process* 2000, 24, 213-216.) Power was produced, however, in the grape, a fruit having a high (>30 mM) glucose concentration in its sap. The power output of the cell functioning in the grape was O₂-transport-controlled and depended on the position of the cathode fiber. When the cathode fiber was near the center of the grape, where the fruit was oxygen-deficient, the power density was only $\mu\text{W}/\text{mm}^2$ at 0.52 V. When the fiber was shallowly implanted near the skin of the grape, where the sap was better oxygenated, the power density was $2.4 \mu\text{W}/\text{mm}^2$ at 0.52 V.

[0213] Conclusion: The area of the electrodes of the compartment-less, glucose-O₂ biofuel cell, consisting of two electrocatalyst-coated 7- μm diameter, 2-cm long carbon fibers, is 180 times smaller, its operating voltage is 8 times higher (0.52 vs 0.06 V), and its power density 12 times higher (4.3 vs $0.35 \mu\text{W}/\text{mm}^2$) than those of an earlier reported compartment-less, glucose-O₂ cell which also operated under physiological conditions. (Katz, E.; Willner, I.; Kotlyar, A. B. *J. Electroanal. Chem.* 1999, 479, 64-68.) At neutral pH, where the power output of the cell is cathode-limited, the activation energy for power increase is 34.3 kJ/mol. Above 50°C, the decline is caused by the thermal denaturing of bilirubin oxidase, having an activation energy of 88.2 kJ/mol¹. When the lengths of the anode and cathode fibers are the same, the power output is limited in the aerated solution below pH 6 by the anode and above pH 6 by the cathode. In the pH range of human serum or blood, the variation of power output is negligibly small. The power output does not vary substantially with NaCl concentration in the 0.05-0.15 M range; in the 0.15-1 M range, it declines as the NaCl concentration is raised. The cell operates continuously at 37°C in an aerated, glucose-containing physiological (pH 7.2, 0.14 NaCl, 20 mM phosphate) buffer for a week, and, as shown here, it retains 85% of its initial power output of $1.1 \mu\text{W}$ after operating for a day in a living organism, a grape. The power output of the cell at 37 °C in a physiological buffer solution is $1.9 \mu\text{W}$, sufficient for powering low-power CMOS circuits, (Harada, M.; Tsukahara, T.; Kodate, J.; Yamagishi, A.; Yamada, L. *IEEE J. Solid State Circuits* 2000, 15, 2000-2004.) and its operating voltage of 0.52 V is adequate for operation of low-voltage CMOS/SIMOX integrated circuits. It is hoped, that after considerable further development, the simple and disposable cell will power implanted autonomous sensor-transmitter systems of relevance to physiological

research and medicine. These miniature systems would operate for about a week to monitor, for example, the temperature at a site following surgery, indicative of inflammation.

5 [0214] As described herein, the present invention provides power sources, or fuel cells, capable of operating without a membrane, such that their size can be reduced to a sub-mm² footprint and a sub-mm³ volume, for example. This reduced size is of great advantage for a variety of applications, such as applications calling for the implantation of fuel cells in biological systems.

10 [0215] In fuel cells of the present invention, the rate of electrooxidation of fuel at the wired cathode of the cell is much slower than the rate of oxygen electroreduction, and the rate of oxygen electroreduction at the wired anode of the cell is much slower than the rate of fuel electrooxidation, such that no membrane is required. Thus, the fuel cell of the present invention can operate with the anode and the cathode in the same compartment, in the presence of both oxygen and the fuel of the cell, such as glucose.

15 [0216] Not only can the fuel cell operate without cumbersome components, such as membranes, seals and cases, it can do so effectively. For example, according to one aspect of the invention, the fuel cell of the present invention can produce a current density of from about 0.1 to about 10 mA/cm². In addition, the effective fuel cell of the present invention can be manufactured relatively inexpensively, such as on the
20 order of about 10¢ per cell. The very low cost of the inventive fuel cells is a particular advantage with respect to applications that call for fuel cells having a short life span, such as disposable fuel cells used in biological systems for medical purposes, which may be in use for only a week, or even less.

25 [0217] The fuel cell of the present invention is further advantageous in that it can operate under physiological conditions. As such, the biofuel cell of the present invention may be used within a biological system, such as a human body. For example, according to an embodiment of the invention, the biofuel cell electrooxidizes oxidizable components of a body fluid within a human, such as glucose in a diabetic, and electroreduces oxygen within that fluid. Power is generated in the biofuel cell via
30 the electrooxidation and electroreduction occurring in the same fluid.

Advantageously, this biofuel cell is small, effective, powerful, and easy and inexpensive to manufacture.

[0218] Various references, publications, and provisional and non-provisional United States patent applications, have been identified herein, each of which is incorporated
5 herein in its entirety by this reference. Various aspects and features of the present invention have been explained or described in relation to beliefs or theories, although it will be understood that the invention is not bound to any particular belief or theory. Various modifications, processes, as well as numerous structures to which the present invention may be applicable will be readily apparent to those of skill in the art to
10 which the present invention is directed, upon review of the specification. Although the various aspects and features of the present invention have been described with respect to various embodiments and specific examples herein, it will be understood that the invention is entitled to protection within the full scope of the appended claims.

CLAIMS

1. A fuel cell comprising:
an anode and an anode enzyme in electrical communication; and
a cathode and a copper-containing cathode enzyme in electrical
5 communication.
2. The fuel cell of claim 1, further comprising an anode redox polymer
disposed on the anode.
- 10 3. The fuel cell of claim 1, further comprising a cathode redox polymer
disposed on the cathode.
4. The fuel cell of claim 1, the cathode sufficient for electroreduction of
oxygen.
- 15 5. The fuel cell of claim 1, the cathode enzyme comprising four copper
ions per functional unit thereof.
6. The fuel cell of claim 1, the cathode enzyme comprising a laccase,
20 ascorbate oxidase, a ceruloplasmine, or a bilirubin oxidase.
7. The fuel cell of claim 1, the anode sufficient for electrooxidation of at
least one of a sugar, an alcohol, or a carboxylic acid in a biological system.
- 25 8. The fuel cell of claim 1, the anode sufficient for electrooxidation of
glucose, lactate, or pyruvate.
9. The fuel cell of claim 1, the anode enzyme comprising an oxidase or a
dehydrogenase.
- 30 10. The fuel cell of claim 1, the anode enzyme comprising an oxidase or a
dehydrogenase of glucose, lactate, or pyruvate.

11. The fuel cell of claim 1, further comprising an additional enzyme for breaking down a carbohydrate into at least one of a sugar, an alcohol, or a carboxylic acid.
- 5 12. The fuel cell of claim 1, the cathode enzyme immobilized relative to the cathode.
13. The fuel cell of claim 12, the cathode enzyme immobilized via a redox polymer.
- 10 14. The fuel cell of claim 12, the cathode and the cathode enzyme being oppositely charged polyelectrolytes.
- 15 15. The fuel cell of claim 1, the anode enzyme immobilized relative to the anode.
16. The fuel cell of claim 15, the anode enzyme immobilized via a redox polymer.
- 20 17. The fuel cell of claim 15, the anode and the anode enzyme being oppositely charged polyelectrolytes.
18. The fuel cell of claim 13 or 16, the redox polymer comprising a Osmium-complex.
- 25 19. The fuel cell of claim 1, the anode and the cathode being in a single compartment.
20. The fuel cell of claim 1, the fuel cell operable under physiological conditions.
- 30 21. The fuel cell of claim 1, the fuel cell having an operating cell voltage of greater than or equal to about 0.52 V.

22. The fuel cell of claim 1, the fuel cell producing a current density of from about 0.1 to about 10 mA/cm².

5 23. The fuel cell of claim 1, the fuel cell having a footprint of less than or equal to about 3 mm².

24. The fuel cell of claim 1, the fuel cell having a volume of less than or equal to about 1 mm³.

10 25. The fuel cell of claim 1, the fuel cell electrically coupled to an electrical device.

26. A fuel cell comprising:
15 an anode, an anode redox polymer, and an anode enzyme, in electrical communication; and
a cathode, a cathode redox polymer, and a copper-containing cathode enzyme, in electrical communication.

20 27. The fuel cell of claim 26, the cathode enzyme comprising four copper ions per functional unit thereof.

28. The fuel cell of claim 26, the cathode enzyme comprising a laccase, an ascorbate oxidase, a ceruloplasmine, or a bilirubin oxidase.

25 29. The fuel cell of claim 26, wherein each of the potential differences between the anode and the anode redox polymer, the anode redox polymer and the anode enzyme, the cathode and the cathode redox polymer, the cathode redox polymer and the cathode enzyme, is from about 10 mV to about 200 mV.

30 30. The fuel cell of claim 26, the fuel cell having an operating cell voltage of greater than or equal to about 0.52 V.

31. The fuel cell of claim 26, the anode and the cathode being in a single compartment.

32. The fuel cell of claim 26, the fuel cell operable under physiological
5 conditions.

33. A method of generating electrical power, comprising:
electrooxidizing an anode reductant via an anode in the presence of an anode
enzyme; and
10 electroreducing a cathode oxidant via a cathode in the presence of a copper-
containing cathode enzyme.

34. The method of claim 33, the cathode enzyme comprising four copper
ions per functional unit thereof.
15

35. The method of claim 33, the cathode enzyme comprising a laccase, an
ascorbate oxidase, a ceruloplasmine, or a bilirubin oxidase.

36. The method of claim 33, the electrooxidizing and the electroreducing
20 occurring in a single compartment.

37. The method of claim 33, the electrooxidizing and the electroreducing
occurring under physiological conditions.

25 38. A method of generating electrical power, comprising:
providing a fuel cell, having an anode and a cathode, in operable
communication with a biological system;
electrooxidizing a biological component of the biological system via the anode
in the presence of an anode enzyme; and
30 electroreducing oxygen via the cathode in the presence of a copper-containing
cathode enzyme.

39. The method of claim 38, the cathode enzyme comprising four copper ions per functional unit thereof.

40. The method of claim 38, the cathode enzyme comprising a laccase, an ascorbate oxidase, a ceruloplasmine, or a bilirubin oxidase.

41. The method of claim 38, the anode and the cathode being in a single compartment.

42. The method of claim 38, the electrooxidizing and the electroreducing occurring under physiological conditions.

43. The method of claim 38, wherein the biological system comprises an animal, a plant, or any component thereof.

44. The method of claim 43, wherein the animal is a human.

45. The method of claim 38, wherein a fluid of the biological system is pumped through the fuel cell, the fluid comprising the biological component.

46. The method of claim 45, wherein the biological fluid is blood.

47. The method of claim 38, wherein the fuel cell is provided within the biological system.

48. An electrically-operated device comprising:
at least one electrically-operated component; and
a fuel cell for operation in a biological system, the fuel cell comprising:
an anode and an anode enzyme in electrical communication, the anode coupled to the electrically-operated component; and
a cathode and a copper-containing cathode enzyme in electrical communication, the cathode coupled to the electrically-operated component.

49. The device of claim 48, the cathode enzyme comprising four copper ions per functional unit thereof.

50. The device of claim 48, the cathode enzyme comprising a laccase, an ascorbate oxidase, a ceruloplasmine, or a bilirubin oxidase.

51. The device of claim 48, the anode and the cathode being in a single compartment.

52. The device of claim 48, the fuel cell operable under physiological conditions.

53. The device of claim 48, the fuel cell sufficient for implantation in an animal.

54. The device of claim 48, the device sufficient for implantation in an animal.

55. The device of claim 53 or 54, wherein the animal is a human.

56. A fuel cell comprising:
an anode and an anode electrolysis layer on at least a portion of the anode, the anode electrolysis layer comprising an anode enzyme; and
a cathode and a cathode electrolysis layer on at least a portion of the cathode, the cathode electrolysis layer comprising a copper-containing cathode enzyme.

57. The fuel cell of claim 56, the anode enzyme comprising an oxidase or a dehydrogenase.

58. The fuel cell of claim 56, the anode electrolysis layer further comprising an anode redox polymer that comprises a redox species.

59. The fuel cell of claim 56, the cathode enzyme comprising four copper ions per functional unit thereof.

60. The fuel cell of claim 56, the cathode enzyme comprising a laccase, an ascorbate oxidase, a ceruloplasmine, or a bilirubin oxidase.

5 61. The fuel cell of claim 56, the cathode electrolysis layer further comprising a cathode redox polymer that comprises a redox species.

62. The fuel cell of claim 58, the anode redox polymer comprising a redox hydrogel.

10 63. The fuel cell of claim 61, the cathode redox polymer comprising a redox hydrogel.

64. The fuel cell of claim 58, the redox species comprising a transition
15 metal compound or complex.

65. The fuel cell of claim 61, the redox species comprising a transition metal compound or complex.

20 66. The fuel cell of claim 64 or 65, wherein the transition metal is osmium.

67. The fuel cell of claim 56, the anode and the cathode being in a single compartment.

25 68. The fuel cell of claim 56, the fuel cell operable under physiological conditions.

69. A fuel cell comprising:
an anode and an anode electrolysis layer on at least a portion of the anode, the
30 anode electrolysis layer comprising an anode enzyme and an anode redox polymer that comprises a redox species; and

a cathode and a cathode electrolysis layer on at least a portion of the cathode, the cathode electrolysis layer comprising a copper-containing cathode enzyme and a cathode redox polymer that comprises a redox species.

5 70. The fuel cell of claim 69, wherein the anode enzyme comprises an oxidase or a dehydrogenase and wherein the cathode enzyme comprises a laccase, an ascorbate oxidase, a ceruloplasmine, or a bilirubin oxidase.

10 71. The fuel cell of claim 69, the anode and the cathode being in a single compartment.

 72. The fuel cell of claim 69, the fuel cell operable under physiological conditions.

15 73. A method of powering an electrical device, comprising:
 providing a fuel cell in electrical communication with the device and in contact with a biological fluid comprising glucose and oxygen, the fuel cell comprising an anode and an anode enzyme in electrical communication, and a cathode and a copper-containing cathode enzyme in electrical communication; and
20 electrooxidizing glucose via the anode and electroreducing oxygen via the cathode.

 74. The method of claim 73, the cathode enzyme comprising four copper ions per functional unit thereof.

25 75. The method of claim 73, the cathode enzyme comprising a laccase, an ascorbate oxidase, a ceruloplasmine, or a bilirubin oxidase.

 76. The method of claim 73, where the anode and the cathode are in a
30 single compartment.

 77. The method of claim 73, wherein the electrooxidizing and the electroreducing occur under physiological conditions.

78. The method of claim 73, wherein a source of the biological fluid is an animal.
- 5 79. The method of claim 73, wherein a source of the biological fluid is a human.
80. The method of claim 73, wherein the fuel cell is within a human.
- 10 81. The method of claim 73, wherein the device is within a human.
82. An analyte-monitoring device comprising:
a sensor for producing a sensor signal representative of a level of an analyte in a biological fluid within an animal, the sensor adapted for trans- or sub-cutaneous
15 contact with the biological fluid;
a biofuel cell of claim 1, 26, or 69, electrically coupled with the sensor; and
a transmitter electrically coupled to the biofuel cell for transmitting a transmission signal representative of the level of analyte in the biological fluid.
- 20 83. The device of claim 82, further comprising a receiver for receiving the transmission signal from the transmitter.
84. The device of claim 83, wherein the receiver is located up to and including about 20 cm away from the transmitter.
- 25 85. The device of claim 83, further comprising a second transmitter for transmitting information from the receiver.
86. The device of claim 83, further comprising a source of a treatment
30 agent operably coupled to the receiver.
87. The device of claim 83, where the source is operably coupled to a system for delivery of the treatment agent from the source to the animal.

88. The device of claim 87, wherein the system comprises a pump for pumping the treatment agent from the source.

5 89. The device of claim 87, wherein the system is adapted for trans- or sub-cutaneous delivery of the treatment agent from the source to the animal.

90. The device of claim 82, wherein the animal is a human.

10 91. A method of sensing a level of analyte in a biological fluid within an animal, comprising:

providing a sensor of the level of the analyte in the biological fluid, a biofuel cell of claim 1, 26, or 69, electrically coupled with the sensor, and a transmitter electrically coupled to the biofuel cell;

15 providing trans- or sub-cutaneous contact between the sensor and the biological fluid; and

transmitting a signal representative of the level of the analyte in the biological fluid.

20 92. A method of treating an animal, comprising:

providing a sensor of the level of the analyte in the biological fluid, a biofuel cell of claim 1, 26, or 69, electrically coupled with the sensor, and a transmitter electrically coupled to the biofuel cell;

25 providing trans- or sub-cutaneous contact between the sensor and the biological fluid;

transmitting a signal representative of the level of the analyte in the biological fluid;

providing a system for trans- or sub-cutaneous delivery of a treatment agent from a source thereof in response to the signal; and

30 delivering the treatment agent.

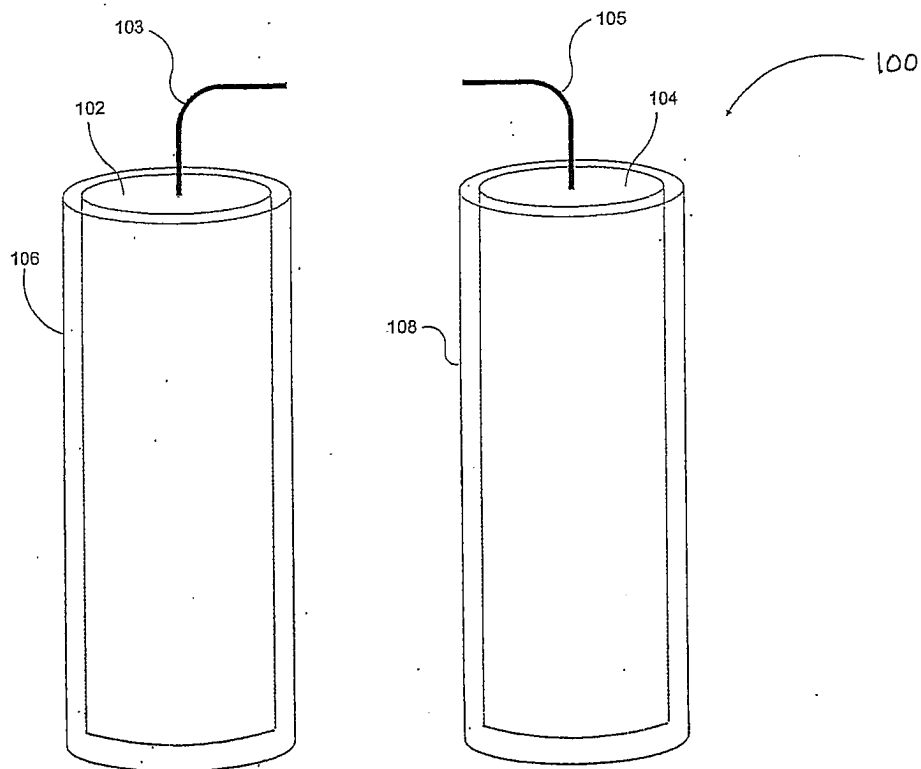


FIG. 1

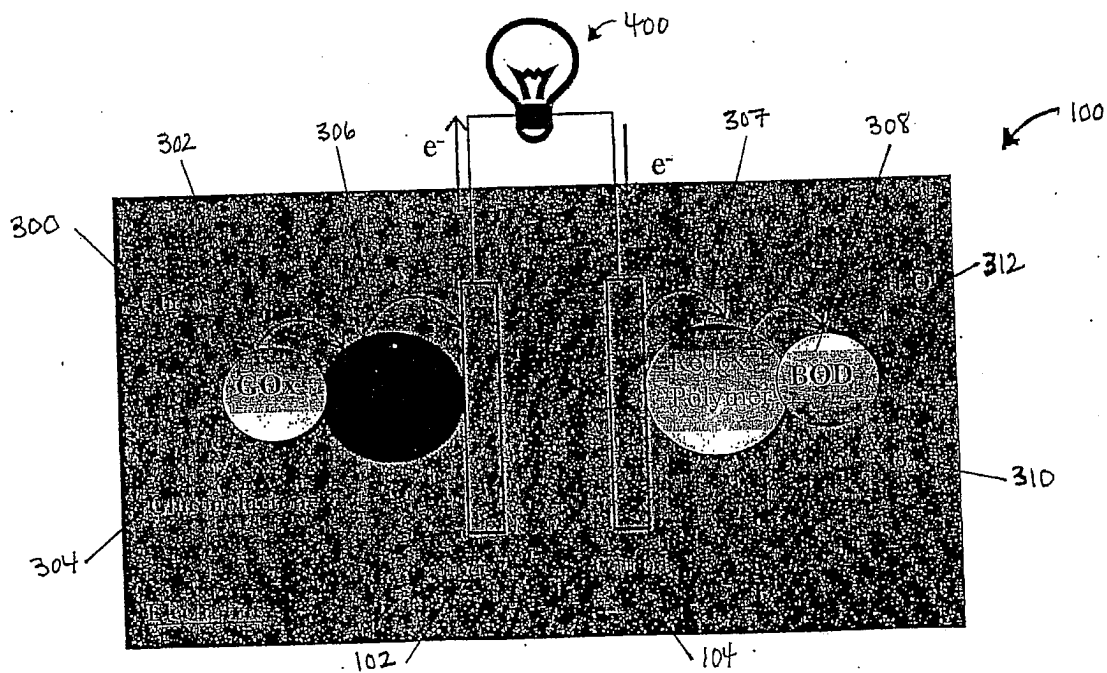


FIG. 2

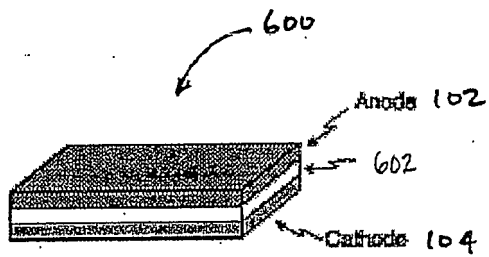


FIG. 3A

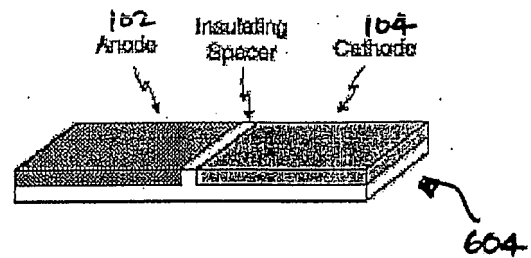


FIG. 3B

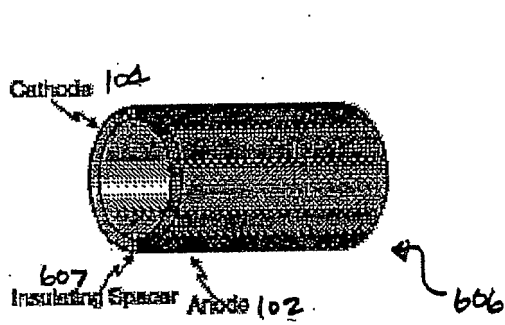


FIG. 3C

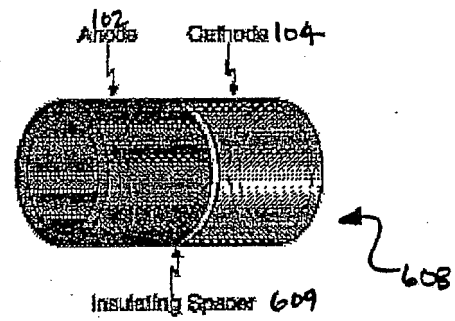


FIG. 3D

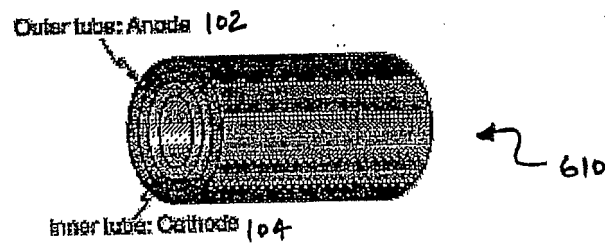


FIG. 3E

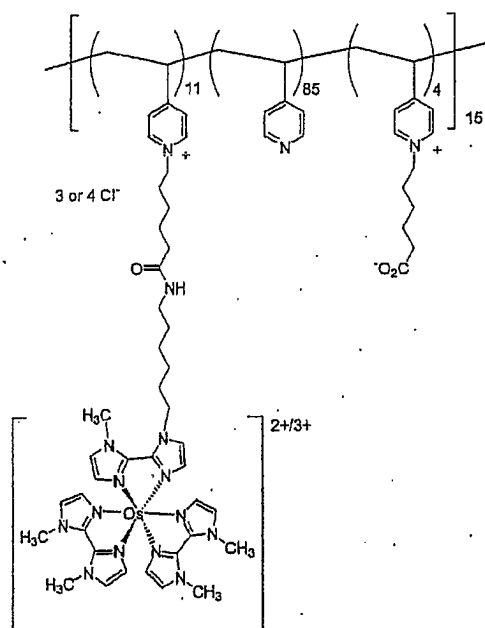


FIG. 4

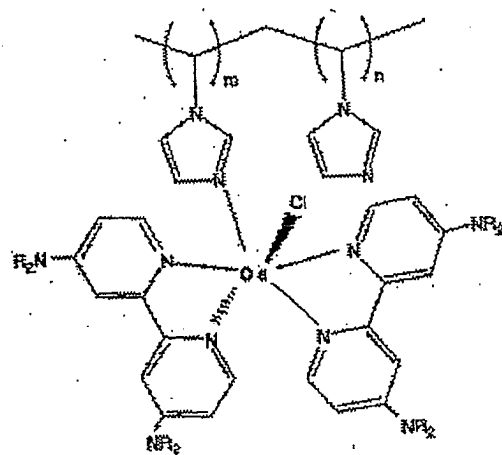


FIG. 5

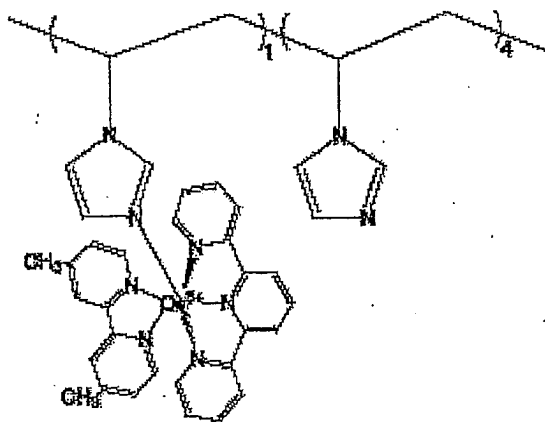


FIG. 6

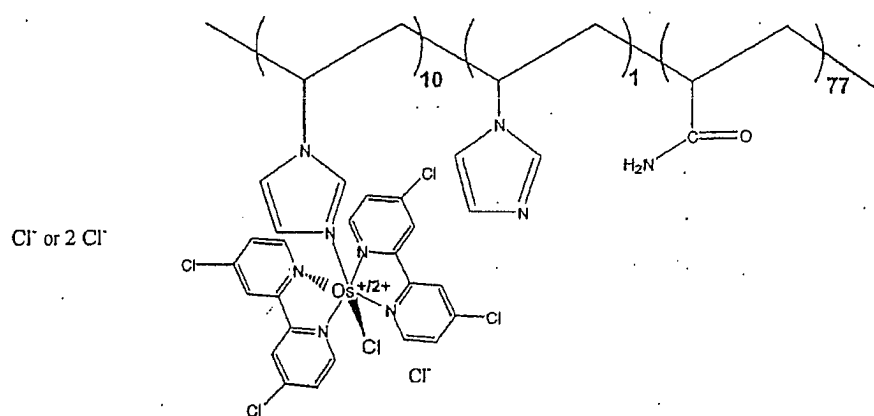


FIG. 7

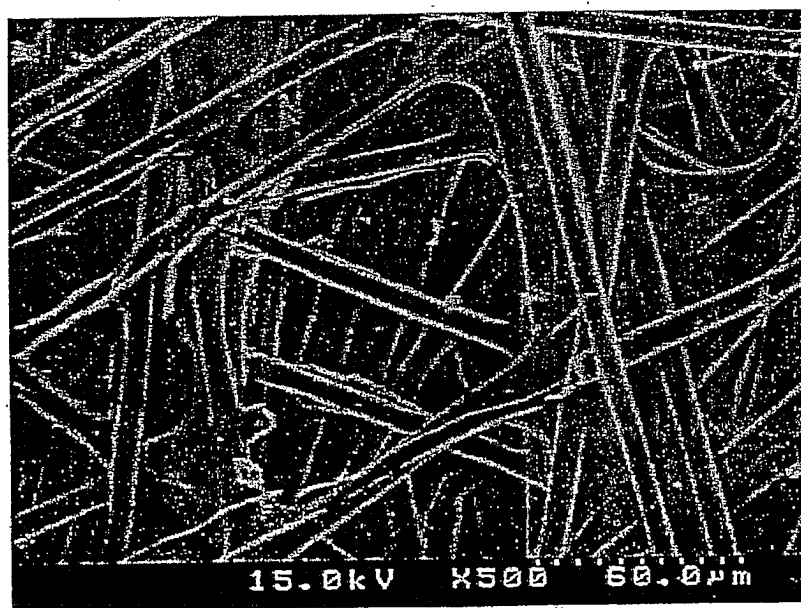


FIG. 8

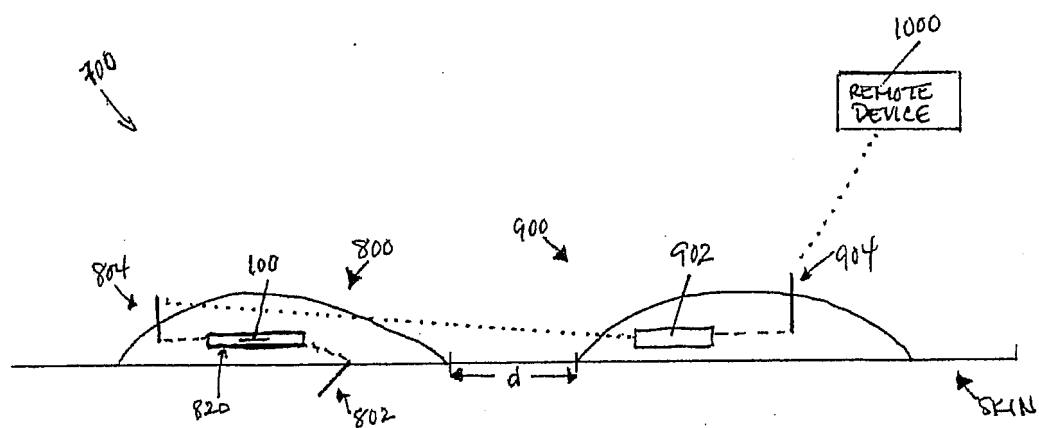


FIG. 9

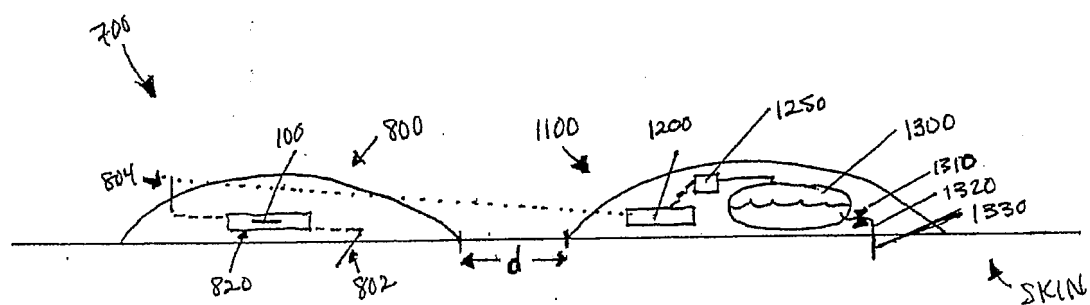
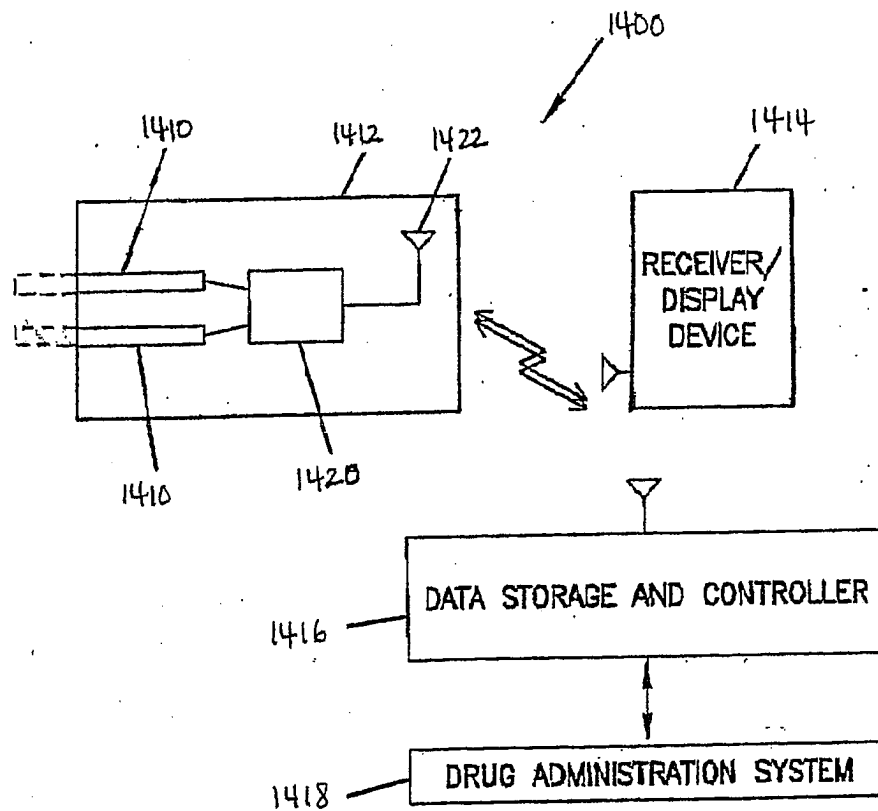


FIG. 10

FIG. 11



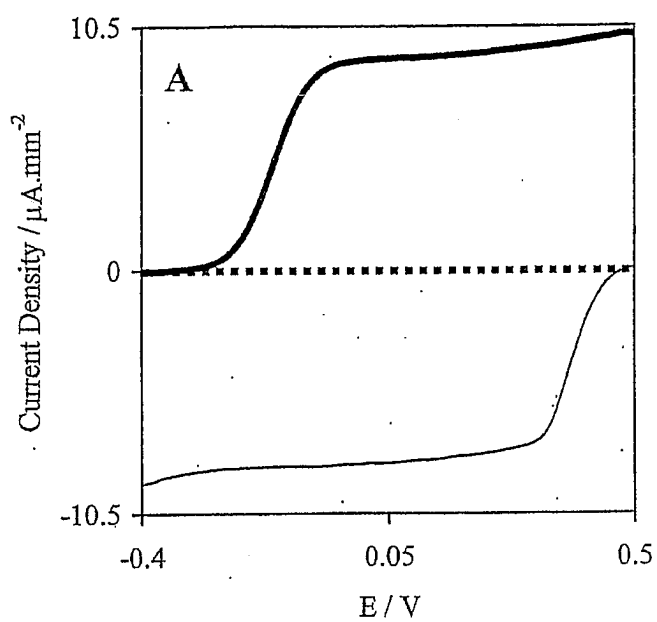


FIG. 12A

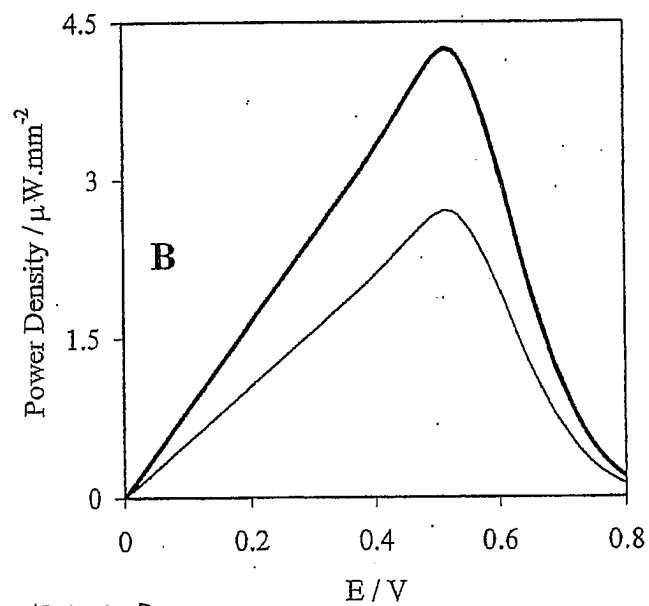


FIG. 12B

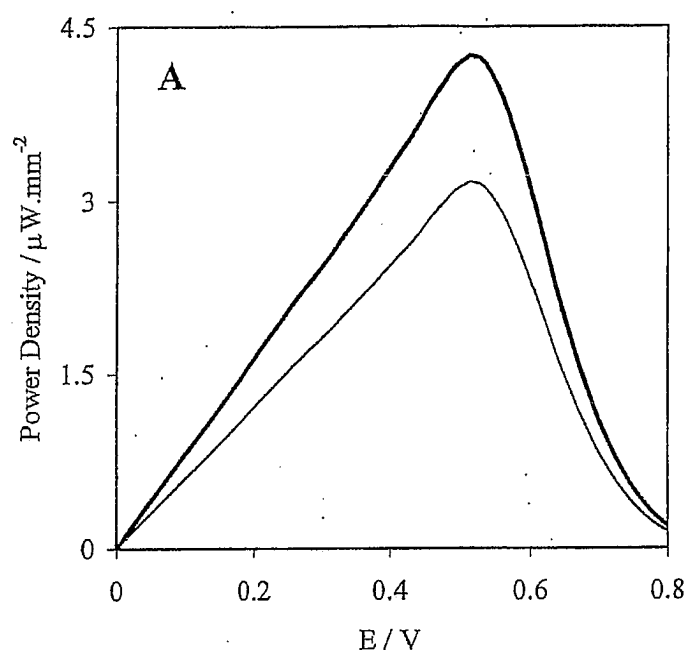


FIG. 13A

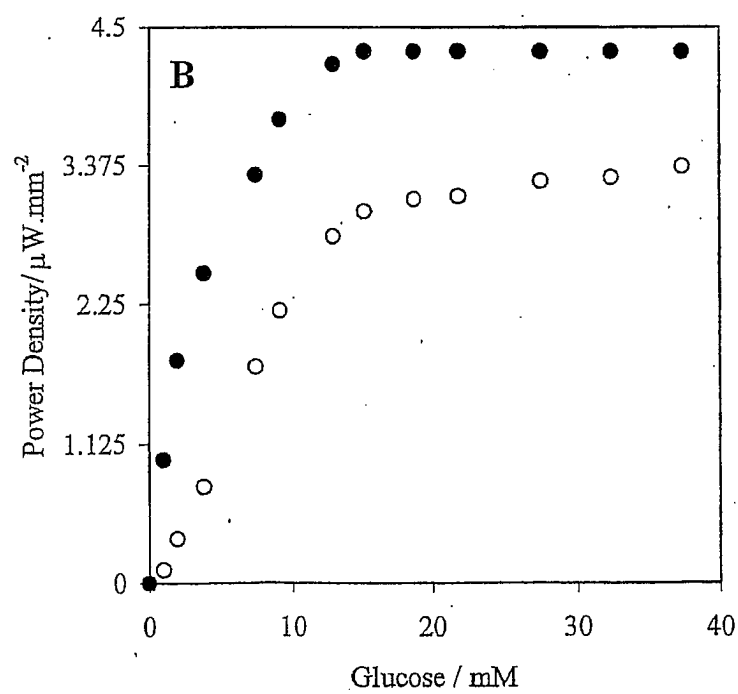


FIG. 13B

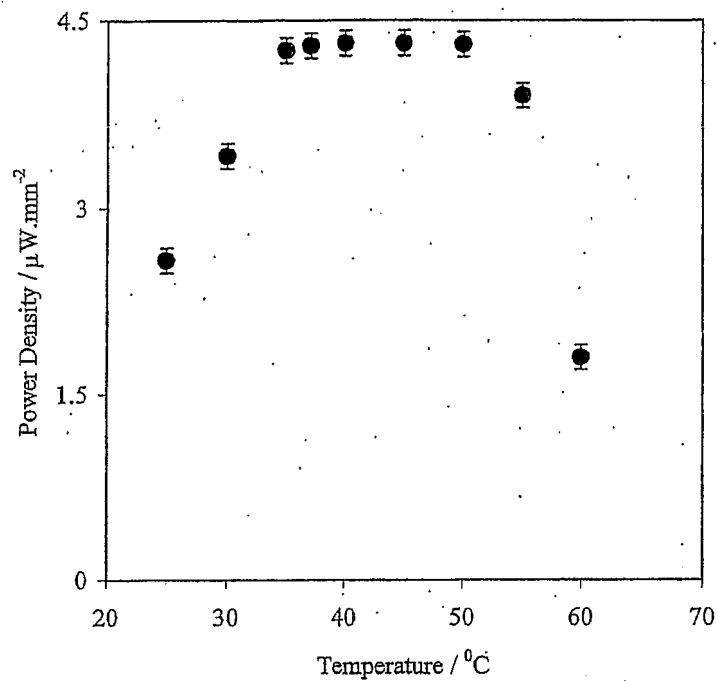


FIG. 14

O_2 / Bilirubin Oxidase : $E = +0.36 \text{ V}$

Cathode Wire : $E = +0.34 \text{ V}$

Anode Wire : $E = -0.19 \text{ V}$

Glucose / Glucose Oxidase
 $E = -0.36 \text{ V}$

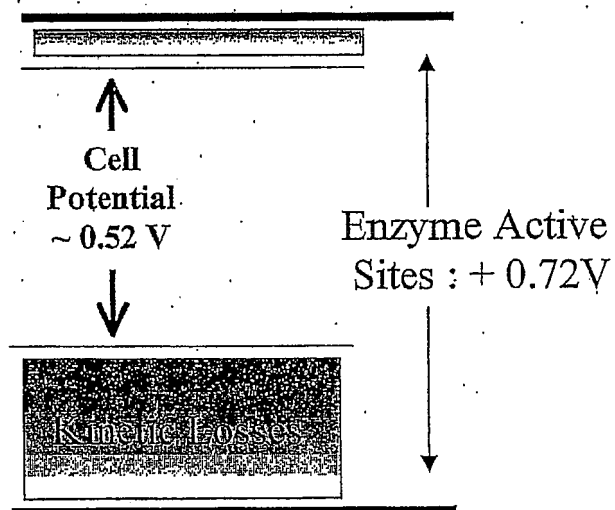


FIG. 17

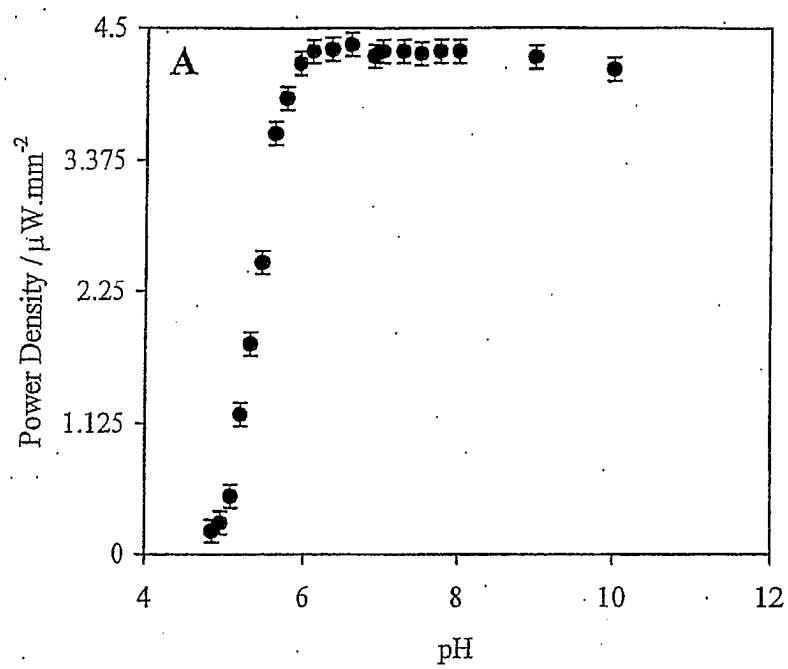


FIG. 15A

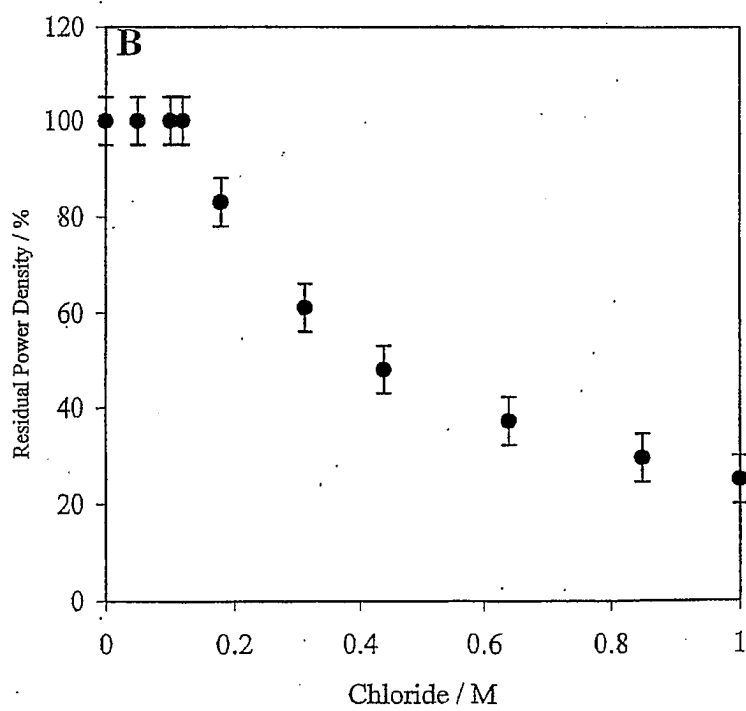


FIG. 15B

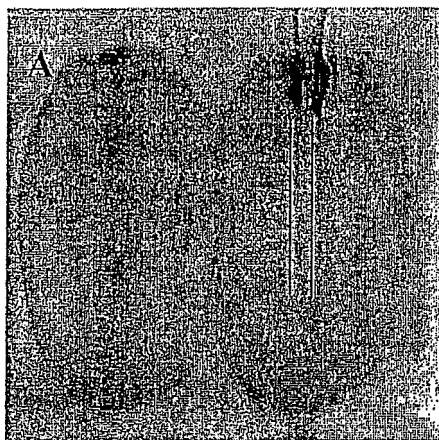


FIG. 16A

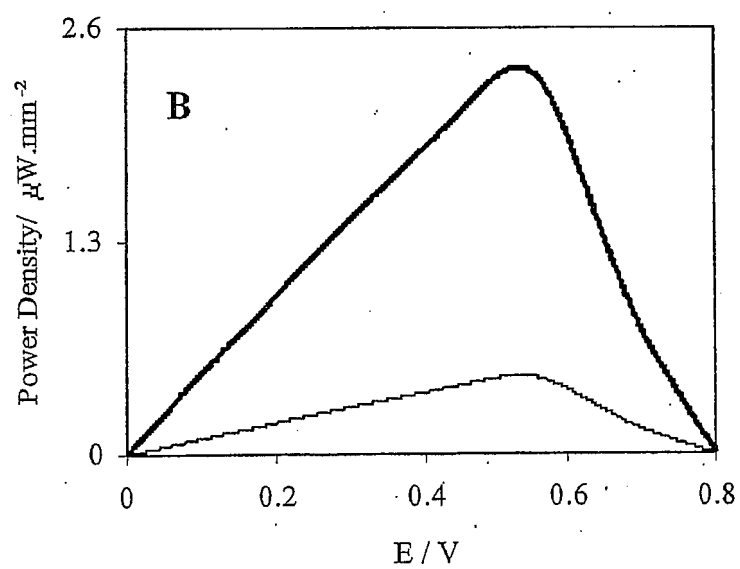


FIG. 16B